CLEITON BARROSO BITTENCOURT

O USO DE ESTRATÉGIAS MULTI-ÔMICAS PARA ESTUDAR AS RESPOSTAS DAS PLANTAS DE DENDÊ (*Elaeis guineensis* Jacq.) A ESTRESSES ABIÓTICOS (SECA E SALINIDADE) E AO AMARELECIMENTO FATAL (AF)

LAVRAS – MG
2023

CLEITON BARROSO BITTENCOURT

O USO DE ESTRATÉGIAS MULTI-ÔMICAS PARA ESTUDAR AS RESPOSTAS DAS PLANTAS DE DENDÊ (*Elaeis guineensis* Jacq.) A ESTRESSES ABIÓTICOS (SECA E SALINIDADE) E AO AMARELECIMENTO FATAL (AF)

Tese apresentada à Universidade Federal de Lavras, como parte das exigências do Programa de Pós-Graduação em Biotecnologia Vegetal, área de concentração em Biotecnologia Vegetal, para a obtenção do título de Doutor.

Dr. Manoel Teixeira Souza Júnior
Orientador

Dra. Betania Ferraz Quirino
Coorientadora

LAVRAS – MG
2023

Ficha catalográfica elaborada pelo Sistema de Geração de Ficha Catalográfica da Biblioteca Universitária da UFLA, com dados informados pelo(a) próprio(a) autor(a).

Bittencourt, Cleiton Barroso.
O uso de estratégias multi-ômicas para estudar as respostas das plantas de dendê (*Elaeis guineensis* Jacq.) a estresses abióticos (seca e salinidade) e ao amarelecimento fatal (AF) / Cleiton Barroso Bittencourt. - 2023.
107 p.

Orientador(a): Manoel Teixeira Souza Júnior.
Coorientador(a): Betania Ferraz Quirino.
Tese (doutorado) - Universidade Federal de Lavras, 2023.
Bibliografia.

1. Estresse abiótico. 2. Estresse biótico. 3. Integração multi-ômica. I. Souza Júnior, Manoel Teixeira. II. Quirino, Betania Ferraz. III. Título.

CLEITON BARROSO BITTENCOURT

O USO DE ESTRATÉGIAS MULTI-ÔMICAS PARA ESTUDAR AS RESPOSTAS DAS PLANTAS DE DENDÊ (*Elaeis guineensis* JACQ.) A ESTRESSES ABIÓTICOS (SECA E SALINIDADE) E AO AMARELECIMENTO FATAL (AF)

THE USE OF MULTI-OMIC STRATEGIES TO STUDY THE RESPONSES OF OIL PALM PLANTS (*Elaeis guineensis* JACQ.) TO ABIOTIC STRESSES (DROUGHT AND SALINITY) AND FATAL YELLOWING (FY)

Tese apresentada à Universidade Federal de Lavras, como parte das exigências do Programa de Pós-Graduação em Biotecnologia Vegetal, área de concentração em Biotecnologia Vegetal, para a obtenção do título de Doutor.

APROVADA em 30 de junho de 2023

Dr. Carlos Antônio Ferreira de Sousa	EMBRAPA Meio-Norte
Dra. Alessandra de Jesus Boari	EMBRAPA Amazônia Oriental
Dr. Wenceslau Geraldes Teixeira	EMBRAPA Solos
Dr. Jorge Cândido Rodrigues Neto	EMBRAPA Agroenergia
Dr. Jaire Alves Ferreira Filho	EMBRAPA Agroenergia

Dr. Manoel Teixeira Souza Júnior
Orientador

Dra. Betania Ferraz Quirino
Coorientadora

LAVRAS – MG
2023

“Penso, logo existo.” – René Descartes

AGRADECIMENTOS

À minha mãe, Eliana Lima Barroso, pelo incentivo, apoio e amor incondicional. Você é um exemplo de vida!

Aos meus irmãos, Clicia Barroso Bittencourt e Clecio Barroso Bittencourt, pelo companheirismo e ensinamentos.

À minha namorada, Inês Marques Veras, por seu amor, compreensão, paciência e apoio durante toda essa jornada.

Ao Sr. Adeládio Batista Vieira pela amizade, receptividade e apoio na minha estadia em Brasília.

Ao meu orientador, Dr. Manoel Teixeira Souza Júnior pela orientação, pela amizade e todas as conversas que foram enriquecedoras para a minha formação.

À minha coorientadora, Dra. Betânia Ferraz Quirino, pela orientação, confiança e apoio para a execução desse trabalho.

Aos meus amigos e colegas de laboratório pelo companheirismo e ajuda na execução de minha pesquisa, a saber; Fernanda Salgado, Ítalo Braga, Thalita Massaro e Thalliton da Silva.

À Dra. Aline de Holanda Nunes Maia, Dr. Carlos Antônio Ferreira de Sousa, Dr. Jorge Cândido, José Antônio e André Leão pelo auxílio e contribuição científica.

Aos funcionários da UFLA e Embrapa Agroenergia. Agradeço imensamente a todos aqueles que contribuíram direta e/ou indiretamente para o desenvolvimento do presente estudo e, especialmente, para a minha formação profissional.

À Denpasa – Dendê do Pará S/A pelo suporte durante as coletadas de dendezeiro para nossas análises.

À Universidade Federal de Lavras – UFLA e ao programa de pós-graduação em Biotecnologia Vegetal pela oportunidade de cursar o doutorado.

À FINEP (01.13.0315.00 DendêPalm Project) pelo suporte financeiro.

O presente trabalho foi realizado com apoio da Coordenação de Aperfeiçoamento de Pessoal de Nível Superior – Brasil (CAPES) – Código de Financiamento 001.

RESUMO GERAL

A palma de óleo africana ou dendezeiro (*Elaeis guineensis*) é uma oleaginosa de grande importância econômica e social. No Brasil, o cultivo da palma de óleo no Cerrado é viável, mas requer irrigação artificial devido à estiagem prolongada nessa região. Nesse contexto, os estresses abióticos, como a seca e a salinidade, representam desafios devido à escassez hídrica e à salinização dos solos irrigados. O Amarelecimento Fatal (AF), uma desordem sem causa conhecida, é uma limitação para a produção da palma de óleo africana no Brasil. Deste forma, o presente estudo teve como objetivo utilizar uma análise abrangente e em larga escala de *single-omics analysis* (SOA) e *multi-omics integration* (MOI) para estudar a resposta da palma de óleo a estresses abióticos (seca e salinidade) e ao Amarelecimento Fatal (AF). Para o estudo, foram coletadas amostras foliares de dendezeiro jovens sob estresse salino (12 dias) e privação hídrica (14 dias) para realizar análises de RNA-seq, UHPLC-MS e LC-MS/MS, para transcriptômica, metabolômica e proteômica, respectivamente. Para o estudo do AF, foram coletados folhas e solo de plantas assintomáticas e sintomáticas no período seco e chuvoso em Santa Bárbara do Pará, Pará, Brasil. Para o material de folha, foram realizadas análises de RNA-seq e metabolômica. Para o solo foi realizada uma análise da estrutura e composição química. Para salinidade, o total de 129 metabólitos, 436 transcritos completos e 74 proteínas que representam enzimas foram diferencialmente expressas. Para seca, 269 metabólitos, 1955 transcritos completos e 131 proteínas foram diferencialmente expressas. Foram encontradas similaridades e dissimilaridades na resposta da palma de óleo ao estresse salino e à seca. A análise de MOI revelou uma lista de vias impactadas, mas destacamos o metabolismo de cisteína e metionina (map00270) como a via mais impactada em ambos os estresses e a análise de correlação revelou 91,55% de semelhanças nos perfis qualitativos. Para o AF, os perfis de metabólitos e físico-químicos do solo e folhas não justificaram as diferenças no fenótipo das plantas. Ao todo, a análise *single-ômics* (SOA) realizada no presente estudo permitiu a identificação de 320 enzimas (a partir da análise do transcriptoma) e 254 metabólitos nas folhas de plantas de dendezeiros submetidas à análise de integração multi-ômica (MOI). Essa análise de MOI produziu uma lista de 27 vias metabólicas afetadas pela mudança da estação seca para chuvosa, tendo pelo menos dez enzimas e metabólitos expressos diferencialmente. Um conjunto de 56 proteínas/genes, regulados negativa ou positivamente em plantas sintomáticas quando comparadas com as assintomáticas, independente da estação do ano, apresenta evidências de interrupções na resistência de não hospedeiro a patógenos não adaptados e na imunidade basal a patógenos adaptados, causada pelas condições anaeróbicas enfrentadas pelas plantas. Por fim, nossos resultados permitem indicar genes candidatos para a engenharia genética de espécies de culturas resistente a ambos os estresses. Para o AF, embora nossos dados não revelem de fato a natureza da doença, os componentes moleculares identificados podem abrir novas portas para produzir materiais resistentes à esta doença e criar um sistema de diagnóstico precoce.

Palavras-chave: Estresse abiótico; Estresse biótico; Integração multi-ômica.

GENERAL ABSTRACT

The African oil palm or oil palm (*Elaeis guineensis*) is an oilseed of great economic and social importance. In Brazil, oil palm cultivation in the Cerrado is feasible, but requires artificial irrigation due to the prolonged drought in this region. In this context, abiotic stresses, such as drought and salinity, pose challenges due to water scarcity and salinization of irrigated soils. Fatal yellowing (FY), a disorder with no known cause, is a limitation for African oil palm production in Brazil. Thus, the present study aimed to use a comprehensive and large-scale analysis of single-omics analysis (SOA) and multi-omics integration (MOI) to study the response of oil palm to abiotic stresses (drought and salinity) and to Fatal Yellowing (FY). For the study, leaf samples of young oil palm under salt stress (12 days) and water deprivation (14 days) were collected to perform RNA-seq, UHPLC-MS and LC-MS/MS analyses, for transcriptomics, metabolomics and proteomics, respectively. For the FY study, leaves and soil of asymptomatic and symptomatic plants were collected in the dry and rainy season in Santa Bárbara do Pará, Pará, Brazil. For leaf material, RNA-seq and metabolomics analyzes were performed. For the soil, an analysis of the structure and chemical composition was carried out. For salinity, a total of 129 metabolites, 436 complete transcripts and 74 proteins representing enzymes were differentially expressed. For drought, 269 metabolites, 1955 complete transcripts and 131 proteins were differentially expressed. Similarities and dissimilarities were found in the response of oil palm to salt stress and drought. MOI analysis revealed a list of impacted pathways, but we highlighted cysteine and methionine metabolism (map00270) as the most impacted pathway in both stresses and correlation analysis revealed 91.55% similarities in qualitative profiles. For FY, the metabolite and physical-chemical profiles of the soil and leaves did not justify the differences in the phenotype of the plants. In all, the single-omics analysis (SOA) performed in the present study allowed the identification of 320 enzymes (from transcriptome analysis) and 254 metabolites in the leaves of oil palm plants subjected to multi-omics integration analysis (MOI). This MOI analysis produced a list of 27 metabolic pathways affected by the change from dry to wet season, having at least ten differentially expressed enzymes and metabolites. A set of 56 proteins/genes, down- or up-regulated in symptomatic versus asymptomatic plants, regardless of season, provide evidence of disruptions in host resistance to non-adapted pathogens and in basal immunity to adapted pathogens, caused by the anaerobic conditions faced by plants. Finally, our results allow us to indicate candidate genes for the genetic engineering of crop species resistant to both stresses. For FY, although our data do not really reveal the nature of the disease, the identified molecular components may open new doors to produce materials resistant to this disease and create an early diagnosis system.

Keywords: Abiotic stress; Biotic stress; Multi-omics integration.

ORGANIZAÇÃO DA TESE

A presente tese foi organizada em quatro capítulos referentes aos artigos publicados e as perspectivas futuras. O **Capítulo 1** refere-se ao capítulo de livro "**Oil Palm Fatal Yellowing (FY), a Disease with an Elusive Causal Agent",** que traz uma revisão bibliográfica dos estudos sobre Amarelecimento Fatal (AF), o impacto da doença para o cultivo da palma de óleo no Brasil e no mundo, além das novas ferramentas introduzidas e as perspectivas para estudos futuros. O **Capítulo 2** refere-se ao artigo **"Molecular Interplay between Non-Host Resistance, Pathogens and Basal Immunity as a Background for Fatal Yellowing in Oil Palm (Elaeis guineensis Jacq.) Plants"**, que apresenta um exercício de integração multi-ômica envolvendo transcriptômica e metabolômica de dendês afetados pelo AF em período seco e chuvoso, além de uma análise da composição físico-química do solo e folhas. **O Capítulo 3** refere-se ao artigo "**Insights from a Multi-Omics Integration (MOI) Study in Oil Palm (*Elaeis guineensis* Jacq.) Response to Abiotic Stresses: Part One—Salinity"**, que descreve um exercício de integração multi-ômica envolvendo transcriptômica, proteômica e metabolômica de dendês jovens submetidos ao cultivo sob estresse salino. **O Capítulo 4** refere-se ao artigo "**Insights from a Multi-Omics Integration (MOI) Study in Oil Palm (*Elaeis guineensis* Jacq.) Response to Abiotic Stresses: Part Two—Drought**", que descreve um exercício de integração multi-ômica envolvendo transcriptômica, proteômica e metabolômica de dendês jovens submetidos ao cultivo sob estresse à seca.

SUMÁRIO

1. APRESENTAÇÃO GERAL

Elaeis guineensis Jacq., conhecido popularmente como palma de óleo africana ou dendezeiro, é uma espécie de palmeira oleaginosa pertencente à família Arecaceae, nativa do continente africano (CORLEY; TINKER, 2015). A palma de óleo é reconhecida como a oleaginosa de maior produtividade, do seu fruto são extraídos o óleo de palma (mesocarpo) e óleo de palmiste (amêndoa) (NORRRAHIM et al., 2022). Com uma produtividade média de 2,94 toneladas por hectare, a palma de óleo supera outras cultivares tradicionais como o girassol (0,74 t), a colza (0,72 t) e soja (0,46) (RITCHIE; ROSER, 2021).

Os óleos vegetais obtidos do fruto do dendezeiro são utilizados na indústria alimentícia (68%), em aplicações industriais, tais como na produção de cosméticos, sabões, detergentes, velas e produtos de limpeza (27%), e na produção de biocombustíveis (5%) (RITCHIE; ROSER, 2021). Desta forma, a palma de óleo desempenha um papel importante na segurança alimentar em várias partes do mundo (ADADE, 2022). Contudo, seu uso ainda varia de país para país, na Alemanha, por exemplo, a bioenergia é o maior uso, respondendo por 41% (RITCHIE; ROSER, 2021).

A palma de óleo é cultivada em regiões de florestas tropicais úmidas, com grande disponibilidade hídrica para crescimento saudável e desenvolvimento adequado dos frutos (CORLEY; TINKER, 2015). A produção é predominantemente concentrada no sudeste asiático, com a Indonésia e a Malásia respondendo por cerca de 84% da oferta global (NORRRAHIM et al., 2022). Na última década, a produção global de palma de óleo quase dobrou, saindo de 43 milhões de toneladas em 2009 para 79 milhões em 2019, motivado pelo crescimento populacional e econômico dos países (RITCHIE; ROSER, 2021).

O Brasil é o país com a maior área com condições edafoclimáticas favoráveis para o cultivo de palma de óleo, no entanto, o país ocupa apenas a 10ª posição no ranking mundial dentre os países produtores (INDEXMUNDI, 2022). Estima-se que existam cerca de 30 milhões de hectares de terras no país que atendem aos critérios adequados para o cultivo do dendezeiro, mas apenas 200 mil hectares estão sendo efetivamente utilizados para essa atividade (RAMALHO FILHO et al., 2010; RITCHIE; ROSER, 2021).

Existem algumas razões que dificultam o melhor aproveitamento do potencial produtivo do Brasil na região amazônica e, dentre elas, destacam-se: desafios relacionados à regularização fundiária, a legislação rigorosa para a utilização de áreas degradadas na Amazônia e, principalmente, questões relativas aos impactos ambientais, como desmatamento e perda da biodiversidade (HOMMA, 2016).

O plantio da palma de óleo fora das florestas tropicais úmidas é visto como uma oportunidade de expandir a zona de produção, promover o desenvolvimento econômico de outras regiões e reduzir a pressão sobre a biodiversidade (ANTONINI; MALAQUIAS, 2019). A região do Cerrado brasileiro corresponde a cerca de 24% da superfície brasileira, estima-se que existam aproximadamente de 25 milhões a 30 milhões de hectares de pastagens degradadas ou em processo de degradação que podem ser aproveitadas para o cultivo do dendezeiro (GALINARI, 2014).

A expansão da indústria da palma de óleo da Amazônia para a região do Cerrado enfrentará desafios, sendo a disponibilidade reduzida de água durante os meses mais secos do ano um dos principais (ANTONINI; MALAQUIAS, 2019). No entanto, é importante notar que a região do Cerrado possui uma considerável rede hidrográfica, que pode fornecer o suporte hídrico necessário para sustentar o cultivo da palma de óleo durante o período de estiagem (TELES, 2014).

Estudos têm demonstrado que a palma de óleo apresenta uma produtividade no Cerrado superior em comparação com o cultivo em regiões úmidas quando é empregado um sistema de irrigação artificial (TELES, 2014). No entanto, é provável que o cultivo da palma de óleo enfrente desafios relacionados à salinidade do solo, uma vez que cerca de 25% a 30% dos solos irrigados são afetados por algum grau de salinização (ZAMAN et al., 2018). Além disso, o estresse hídrico, devido às mudanças climáticas, não deve ser só um problema do cultivo em regiões áridas e semiáridas, como também nas zonas de cultivo tradicional da palma de óleo (MIRANDA, et al., 2009).

Além dos desafios relacionados aos estresses abióticos, o Amarelecimento Fatal (AF), uma doença de causa desconhecida, destaca-se como uma das principais limitações para o cultivo da palma de óleo africana na América e, especialmente, no Brasil (Bittencourt et al., 2022). O primeiro registro do AF foi em 1927 no Panamá, enquanto o primeiro relato no Brasil ocorreu em 1974. Desde então, têm sido conduzidas investigações abrangentes para identificar o agente causal do AF (BITTENCOURT et al., 2022).

Os sintomas do AF iniciam-se com amarelecimento dos folíolos basais das folhas intermediárias seguida de lesão necrótica que aparece nas extremidades dos folíolos que evoluem para a seca total dessas folhas. Em seguida, há a seca da folha flecha, podendo ocorrer a remissão temporária das folhas, com o declínio generalizado e morte da planta de 7 a 10 meses após o aparecimento dos primeiros sintomas. Nas raízes foi observada a redução do número de células meristemáticas e, consequentemente, do crescimento e desenvolvimento, além da lignificação das raízes secundárias e quaternárias. Autores apontam

que os danos nas raízes sejam os primeiros sintomas do AF, antes mesmo do surgimento dos sintomas na parte aérea (VAN SLOBBE, 1991; BITTENCOURT et al., 2022).

Não existem métodos de controle da doença para o AF e a alternativa para a produção de óleo de palma em regiões de elevada incidência do AF no Brasil é a partir do cultivo do híbrido interespecífico, obtido do cruzamento entre *Elaeis guineensis* e *Elaeis oleífera* (origem americana). No entanto, o custo de produção do híbrido aumenta devido a polinização manual, necessária para o desenvolvimento dos frutos e obtenção dos óleos vegetais (CUNHA; LOPES, 2010).

Estudos que buscaram uma origem biótica foram inconclusivos e, utilizando preceitos da fitopatologia clássica, os organismos fitopatógenos isolados de plantas que apresentavam sintomas não foram capazes de atender aos postulados de Koch. Uma possível causa abiótica foi considerada, mas avaliações químicas das folhas e raízes, composição do solo, não forneceram um embasamento concreto para um possível fator primário do ambiente (BITTENCOURT et al., 2022).

Por muitos anos a *Pudricion del Cogollo*, causada pelo oomiceto do gênero *Phytophthora*, foi confundida com o AF na América, no entanto, uma abordagem metagenômica reforçou a distinção entre as duas doenças (COSTA et al., 2018). Um possível fator abiótico ligado a compactação do solo e a uma condição de hipóxia ganhou forças nos últimos anos, e um estudo de proteômica apontou que plantas saudáveis para o AF se encontram sob estresse em solos alagados (NASCIMENTO et al., 2018).

O cultivo da palma de óleo em condições de baixa disponibilidade hídrica e solos salinos requer a disponibilização de cultivares tolerantes a essas condições (MURUGESAN et al., 2017). Da mesma forma, AF é um problema que requer esforços para identificar seu agente causal, fornecer biomarcadores para identificação dos indivíduos doentes em fase inicial e direcionar programas de melhoramento genético (RODRIGUES-NETO et al., 2018). Desta forma, o uso de novas ferramentas biotecnológicas disponíveis pode dar suporte para compreender a resposta da palma de óleo aos estresses abióticos e ao AF (RAY; SATYA et al., 2014).

Ômicas é um termo utilizado para descrever as técnicas e abordagens que envolvem o estudo abrangente dos componentes moleculares de um organismo, como o genoma (genômica), o transcriptoma (transcriptômica), o proteoma (proteômica) e o metaboloma (metabolômica) (GUPTA et al., 2013). Nos últimos anos houve um notável avanço no desenvolvimento das ferramentas ômicas, com maior poder de geração de dados e diminuição dos custos associados a essas técnicas (YANG et al., 2021). Nesse contexto, as análises

singulares de ômicas (*Singular Omics Analysis* – SOA) são largamente utilizadas para estudar a resposta das plantas a diferentes tipos de estresses (GUPTA et al., 2013).

A integração de ômicas (*Multi-Omics Integration* – MOI) é uma abordagem que vem ganhando cada vez mais espaço, uma vez que permite uma avaliação abrangente e holística dos sistemas biológicos (JAMIL et al., 2020). A integração das camadas facilita a identificação de componentes moleculares que desempenham papéis-chave em determinadas vias biológicas, fornecendo *insights* valiosos para a manipulação genética e o desenvolvimento de características desejáveis em plantas e organismos (WANG et al., 2023).

No entanto, a integração exige a utilização de abordagens bioinformática e estatísticas avançadas, que em alguns contextos ainda não estão disponíveis, para extrair informações relevantes e identificar padrões significativos nos dados (HU et al., 2022). Além disso, é necessário desenvolver modelos matemáticos e algoritmos que permitam a integração dos diferentes níveis de dados e a compreensão dos processos biológicos subjacentes (PICARD et al., 2021).

Tendo em vista todo o contexto apresentado sobre a importância da palma de óleo para a segurança alimentar e seus diversos usos, a oportunidade de diversificação da área de cultivo da palma de óleo, e as grandes perdas causadas pelo AF, o presente estudo teve como objetivo aplicar ferramentas ômicas em análise singular (SOA) e de integração (MOI) para estudar a resposta do dendezeiro aos estresses abióticos, seca e salinidade, e ao amarelecimento fatal, a fim de identificar vias e genes afetados por essas condições para servir como subsídio para programas de melhoramento e, na questão do AF, também para a criação de um sistema de diagnose precoce.

REFERÊNCIAS

ANTONINI, Jose Cesar dos Anjos; MALAQUIAS, Juaci Vitoria. Estabelecimento do momento de irrigação da palma de óleo, cultivada sob condições de clima tropical de savana. **Boletim de pesquisa e desenvolvimento – Embrapa**. p.24, 2019

ADADE, Famous Baa. Oil Palm (*Elaeis guineensis*) Cultivation and Food Security in the Tropical World. ***Elaeis guineensis***, 171 p., 2022.

BITTENCOURT, Cleiton Barroso et al. Oil Palm Fatal Yellowing (FY), a Disease with an Elusive Causal Agent. ***Elaeis guineensis***, 2022.

CORLEY, R. Hereward V.; TINKER, Peter BH. **The Oil Palm**, v. 1993, p. 437-459, 2015.

COSTA, Ohana Yonara de Assis et al. Fungal diversity in oil palm leaves showing symptoms of Fatal Yellowing disease. **PloS one**, v. 13, n. 1, p. e0191884, 2018.

CUNHA, Raimundo Nonato Vieira; LOPES, Ricardo. BRS Manicoré: híbrido interespecífico entre o caiaué e o dendezeiro africano recomendado para áreas de incidência de amarelecimento-fatal. **Comunicado Técnico**, p4. setembro, 2010.

INDEXMUNDI. **Agriculture - Palm Oil**. Disponível em: <https://www.indexmundi.com/agriculture/?commodity=palm-oil>. Acesso em: 06 de jun. 2023.

GUPTA, Bhaskar et al. Plant abiotic stress: 'Omics' approach. **Journal of Plant Biochemistry & Physiology**, v. 1, n. 3, p. 10.4172, 2013.

GALINARI, Graziella. **Embrapa mapeia degradação das pastagens do Cerrado. Embrapa. Monitoramento por Satélite**. 2014. Disponível em: https://www.embrapa.br/busca-de-noticias/-/noticia/2361250/embrapa-mapeia-degradacao-das-pastagens-do-cerrado. Acesso em: 05 de junho, 2023.

HOMMA, Alfredo Kingo Oyama. Cronologia do cultivo do dendezeiro na Amazônia. **Documentos – Embrapa**. 52 p. 2016.

JAMIL, Ili Nadhirah et al. Systematic multi-omics integration (MOI) approach in plant systems biology. **Frontiers in plant science**, v. 11, p. 944, 2020.

MURUGESAN, P. et al. Oil palm (*Elaeis guineensis*) genetic resources for abiotic stress tolerance: A review. **Indian Journal of Agricultural Sciences**, v. 87, n. 5, p. 571-579, 2017.

MIRANDA, Juan de Dios et al. Do changes in rainfall patterns affect semiarid annual plant communities? **Journal of Vegetation Science**, v. 20, n. 2, p. 269-276, 2009.

NASCIMENTO, Sidney Vasconcelos do et al. Differential accumulation of proteins in oil palms affected by fatal yellowing disease. **PloS one**, v. 13, n. 4, p. e0195538, 2018.

NORRRAHIM, Mohd Nor Faiz et al. Emerging technologies for value-added use of oil palm biomass. **Environmental Science: Advances**, v. 1, n. 3, p. 259-275, 2022.

PICARD, Milan et al. Integration strategies of multi-omics data for machine learning analysis. **Computational and Structural Biotechnology Journal**, v. 19, p. 3735-3746, 2021.

RAMALHO-FILHO, Antônio et al. Zoneamento agroecológico, produção e manejo para a cultura da palma de óleo na Amazônia. **Embrapa Solos**, 2 16 p. 2010.

RODRIGUES-NETO, Jorge Candido et al. Metabolic fingerprinting analysis of oil palm reveals a set of differentially expressed metabolites in fatal yellowing symptomatic and non-symptomatic plants. **Metabolomics**, v. 14, p. 1-16, 2018.

Ritchie, Hannah; Roser, Max. **Forests and deforestation.** Disponível em: <https://ourworldindata.org/forests-and-deforestation>. Acesso em: 01 de jun. 2023.

RAY, Soham; SATYA, Pratik. Next generation sequencing technologies for next generation plant breeding. **Frontiers in plant science**, v. 5, p. 367, 2014.

TELES, Daniel Aparecida do Amaral. **Características físicas e rendimento mensal em óleo de cachos de duas cultivares de dendezeiro cultivadas, sob irrigação, no Cerrado do Distrito Federal**. 2014. Dissertação (Mestrado em Agronomia). Universidade de Brasília – UNB, Brasília, p. 261. 2009.

WANG, Mingcheng; LI, Rui; ZHAO, Qi. Multi-Omics Techniques in Genetic Studies and Breeding of Forest Plants. **Forests**, v. 14, n. 6, p. 1196, 2023.

YANG, Yaodong et al. Applications of multi-omics technologies for crop improvement. **Frontiers in Plant Science**, v. 12, p. 563953, 2021.

ZAMAN, Mohammad; SHAHID, Shabbir A.; HENG, Lee. Soil salinity: Historical perspectives and a world overview of the problem. **Guideline for salinity assessment, mitigation and adaptation using nuclear and related techniques**, p. 43-53, 2018.

CAPÍTULO I – CAPÍTULO DE LIVRO

“Oil Palm Fatal Yellowing (FY), a Disease with an Elusive Causal Agent”

Autores: Cleiton Barroso Bittencourt, Philippe de Castro Lins, Alessandra de Jesus Boari, Betania Ferraz Quirino, Wenceslau Geraldes Teixeira, Manoel Teixeira Souza Junior

Publicado na IntechOpen
http://dx.doi.org/10.5772/intechopen.98856
Kamyab H, editor. *Elaeis guineensis* [Internet]. IntechOpen; 2022. Disponível em: http://dx.doi.org/10.5772/intechopen.92931

Chapter

Oil Palm Fatal Yellowing (FY), a Disease with an Elusive Causal Agent

Cleiton Barroso Bittencourt, Philippe de Castro Lins, Alessandra de Jesus Boari, Betania Ferraz Quirino, Wenceslau Geraldes Teixeira and Manoel Teixeira Souza Junior

Abstract

Fatal yellowing disease (FY) is a bud rot-type disease that severely affects oil palm plantations in Latin America. Since 1974, when it was first reported in Brazil, this disorder has been responsible for severe economic losses in the oil palm industry; and, for nearly 50 years, several studies have tried to identify its causal agent, without success. The etiological studies regarding FY in oil palm explored either biotic and abiotic stress scenarios, in a single or combined manner. Most recently, the hypothesis in favor of one biotic cause has lost some grounds to the abiotic one, mainly due to new insights regarding deficient aeration in the soil, which reduces the potential for oxy-reduction, causing changes in the ionic composition of the soil solution. This review presents an overview of the history of this disease and the several efforts done to fulfill Koch's postulates over the last 40 years, besides discussing recent studies that revisited this subject using some omics technics. We conclude by discussing further uses of omics via a multi-omics integration (MOI) strategy to help finally find out what is really behind the genesis of FY. Finding this elusive causal agent of FY out will allow either the development of a more efficient diagnostic tool and the advance in studies trying to find out the source of the genetic resistance hidden in the genome of the American oil palm.

Keywords: *Elaeis guineensis*, palm oil, epidemiology, tropical diseases, etiology, abiotic stress, biotic stress

1. Introduction

The African oil palm (*Elaeis guineensis* Jacq.) is a palm tree originally from the West Coast of Africa and currently distributed in three regions of the equatorial tropics; Africa, Southeast Asia, and Central and South America, where it exists in the wild, semi-wild, and cultivated form [1]. Among the oilseeds, it is the one with the highest average yield, producing 4 to 6 tonnes per year of vegetable oil [2]. The fruit palm oil (mesocarp) and the palm kernel oil (almond) are the raw material for several products in the food industry, in the cosmetic and personal hygiene industry, and the biofuels industry [3, 4]. Palm oil provides 36% of the global supply of

vegetable oils with a considerable increase, from crude palm oil (CPO) production from 5.3 million tonnes in 1981 to 71.45 million tonnes in 2018 [2].

The Asian continent concentrates most of the CPO production, led by Indonesia and Malaysia, which together accounts for 85% of the world's CPO production [4]. However, the limited availability of areas for cultivation in Southeast Asia has opened new frontiers for expansion, culminating in the growth of Latin America's share in the global production of oil palm [5]. Latin America has the largest suitable area for oil palm cultivation, notably led by Brazil (2,283,000 km^2), Peru (458,000 km^2), and Colombia (417,000 km^2) [5]. Among Latin countries, Colombia is the world's fourth-largest producer of CPO and the first in the Americas, with an estimated production of 1.67 million tonnes in 2020, followed by Guatemala with 852 thousand tonnes and Honduras with 580 thousand tonnes [4].

Unfortunately, oil palm plantations in this geographical area are affected by a wide variety of pests and diseases that negatively affects productivity and discourage investment in this sector [1]. Notably, "bud-rot type" diseases pose the greatest threat to oil palm plantations in Latin America [6]. Among them, *Pudrición del Cogollo* (PC) and Fatal Yellowing (FY) are the diseases that cause most of the damage, both presenting a common symptom: rotting of the spear leaf that evolves until reaching the apical meristem system leading to the death of individuals [6, 7]. By far, the FY exhibits the most dramatic scenario because, in contrast to PC, its causal agent remains unknown, hindering effective sanitary control practices [8].

Fatal Yellowing was first identified by Reiking in 1928 in oil palm plantations in Panama, with cases reported in Colombia, Ecuador, Peru, Costa Rica, Venezuela, Suriname, Nicaragua, and, reportedly, in Central Africa, after that [6]. In Brazil, it was only in 1974 that the first symptomatic individuals were identified and, from the epidemiological explosion that occurred in the 1980s, FY started to represent the greatest threat to oil palm in the country [9]. As a result, several studies began to search for the possible biotic causal agent behind it and its putative vectors [8]. However, the research efforts made for more than 30 years have not exactly pointed out organisms directly linked to FY's cause [10–16]. Some studies also looked for possible abiotic causes, with inconclusive results so far [17–19]. Recently, techniques such as metabolomics, proteomics, and metagenomics started to be applied to provide insights into the possible FY etiology, initiating a new phase in the process to solve this problem [20–22].

Although Brazil has more than 30 million hectares with an aptitude for oil palm production, it currently has less than 1% of this area destined for this purpose [23]. Fatal Yellowing is the main contributor to hinder the expansion of the oil palm industry in Brazil, and the attempts to control the emergence of sick plants have not been successful, and its nature remains a mystery [10]. This review intends to analyze descriptively the studies carried out to investigate the FY problem in Brazil, besides pointing out new strategies employed for understanding the development of the disease, confirm the real cause behind it, and develop tools for early diagnostics.

2. The oil palm industry: social & economic importance

2.1 In the world

Oil palm is originally from West Africa and adapted to the intertropical areas of Africa, Asia, South and Central America [1]. It is the most profitable oil crop, as it presents a higher yield with a lower production cost [24]. Its oil yield is of the order of 4-6 tonnes per hectare per year of CPO, much higher than that presented by other crops, such as rapeseed (0.69 t), sunflower (0.69 t), and soybeans (0.44 t) [3]. Another positive point is that this crop uses only 6% of the area to produce 36% of

the global oil supply, while soy, for example, occupies 40% of the land to generate 26% [4, 24]. Because of that, oil palm stands out as a player fundamental to help the world meet the growing global demand for vegetable oil in 2050 that will be around 240 million tonnes [25, 26].

The expansion of the oil palm industry has been strongly encouraged by governments and private sectors in Southeast Asia [27]. It is by far the most productive region in the world, supplying 85% of the CPO produced, reflecting the rapid expansion of the cultivated area that started in the middle of the last century [25]. The commercial oil palm plantations in Indonesia, for instance, went from 70 thousand hectares in 1961 to 6.78 million hectares in 2018, with a considerable increase of 9.582% during this period [2]. As a result, Southeast Asia production rose to 63.26 million tonnes in 2018, or a 22,378% increase in the period [2, 3].

Africa has not seen an expansion of the oil palm industry as significant as Southeast Asia in the last 60 years [3, 28]. The area occupied by oil palm increased from 3.55 million hectares in 1961 to 4.55 million hectares in 2018 in the African continent, representing an increase of only 33% (**Figure 2**) [2]. Meanwhile, the Americas now occupy 6% of the international market, producing around 4.89 million tonnes of palm oil in 2018, a 273% increase in the last two decades [2].

The considerable increase in oil palm production was supported mainly by the advances in genetic breeding programs that increased oil productivity more than 2 folds since 1960 [1].

Most of the CPO and its derivatives produced stays in the Asian markets that absorb 51% of the total, led by India, which imports 19.4%, and China 13.0% [29]. The European markets, which import 26%, have the Netherlands (6.1%) and Italy (4.3%) as the leading importers [23]. Africa (12%), the Middle East (4%), and Latin and North America (7%) also have a consumer market for vegetable oils, and palm oil from Southeast Asia helps to supply the demand [29]. The global vegetable oil market allocates 70% of total production to food and 30% to non-food industrial purposes, such as, for example, the production of cosmetics and personal hygiene products (24%) and as a raw material for the production of biofuels (5%) [26].

2.2 In Latin America

The increase in global palm oil production in the 21st century is due mainly to new plantations in producing countries, especially in Malaysia and Indonesia [27]. However, due to a reduction in the areas available for expanding cultivation in Southeast Asia, an opportunity opened up to expand to new frontiers to meet the growing global demand for palm oil [5]. As a result, Latin America became one of the most promising regions for oil palm cultivation, as it has one of the largest areas suitable for cultivation, notably represented by Brazil, Peru, and Colombia [5].

Brazil, Colombia, Costa Rica, Ecuador, Guatemala, Honduras, Mexico, Peru, and Venezuela produce together 4.65 million tonnes of palm oil, representing 6% of world production in 2020 [2]. Colombia is the largest oil palm producer in this region and ranks 4th in the World, with 1.61 million tonnes produced in 2018, or 33% from the annual palm oil of Latin America (**Figure 1**) [2, 30]. Guatemala produced a total of 875 thousand tonnes in 2018 what places the country in the 2nd position in Latin America [2, 31]. Honduras is in the 3rd, followed by Ecuador, Brazil, Costa Rica, and Venezuela [2].

2.3 In Brazil

The first oil palm plants arrived in Brazil in the 16th century, adapting very well to the Northeast region of the country [32]. The oil palm industry in Brazil

Elaeis guineensis

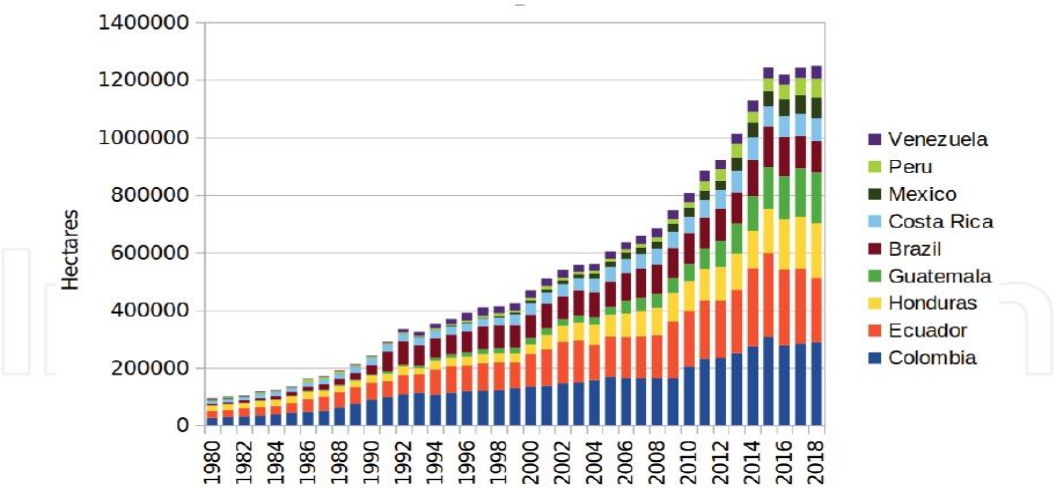

Figure 1.
Land use for oil palm cultivation in central and South America since 1980, in hectares. Source: adapted from our wold in data [2].

Figure 2.
Fatal yellowing (FY) disease in oil palm. (a) Oil palm plantation affected by FY; (b) individual showing signs of yellowing and necrosis of the intermediate leaves; (c, d, e) evolution of yellowing and dryness of the spear leaf with the presence of necrotic tissue, and (f) root section of an individual with signs of rot. Source: by authors.

stayed as a small industry until 1960, when, due to increasing demand for oil for cooling steel sheets in the national steel park, it started to experience significant growth [33]. In 1967, the oil palm cultivation expanded to the Pará State, in the North region of Brazil, with the first commercial-scale plantations comprising about 3.000 hectares [32].

Oil Palm Fatal Yellowing (FY), a Disease with an Elusive Causal Agent
DOI: http://dx.doi.org/10.5772/intechopen.98856

Driven by technical advances and growth in demand for vegetable oils, there was a significant increase in the cultivated area of oil palm in Brazil, which went from 11 thousand hectares in 1980 to more than 236 thousand hectares in 2008 [3]. Brazil has large areas with the aptitude for oil palm production, favored by climatic conditions similar to the most productive regions in the world [1]. However, until 2014, less than 1% of this area was occupied by commercial plantations [34, 35]. Brazil's position as the 13th, and 23rd, in palm oil production and on the productivity scale, respectively, in the world, is due mainly to this under-utilization of available areas [3, 32].

Oil palm production is concentrated in Pará state, which accounts for 97.19% of the cultivated area and 97.99% of the national palm oil production, followed by Bahia (1.98%), Roraima, and Amazonas [36]. The expansion of cultivation to already deforested areas in the Amazon and other regions in Brazil is an opportunity to reduce pressure on forests and supply the palm oil demand from the food and energy sectors [35]. To make the plantations more environmentally sustainable, the Brazilian Government launched the agro-ecological zoning (ZAE) program in 2010, a legal mechanism to delimit the oil palm cultivation area [37]. This area include Acre, Amapá, Amazonas, Mato Grosso, Pará, Rondônia, Roraima and Tocantins, part of Maranhão and five municipalities in Goiás state, comprising about 59% of the Brazilian territory [35].

3. The fatal yellowing (FY) disease

3.1 History in the world

Several fatal syndromes of bud-rot severely affect plantations of oil palm in South and Central America [6, 38]. Bud-rot type disease was reported for the first time on oil palm plantations in Suriname in the 1920s, followed by another incidence in Panama reported by Reinking in 1927 [6]. In general, symptoms of bud-rot type diseases initiate with chlorosis of the youngest leaves and later necrosis that rapidly reach immature tissues of the meristem, causing a collapse of the spear leaf and plant death [9]. Bud rot diseases can take two forms: a lethal form found in Ecuador, Brazil, and in certain zones of Colombia and Suriname, and a non-lethal one, with a high recovery rate, found mainly in the Colombian Llanos [6]. The disease is synonym to a few other names such as "pudrición del cogollo" (PC) in most Spanish speaking countries, "PC típica" (PCt) or "PC diversa" (PCd) in the plantation Palmeras del Ecuador (PDE) in Eastern Ecuador, "amarelecimento fatal" (AF) in Brazil, "spear rot "in Suriname [1, 6, 7].

The first large-scale bud rot damage on oil palm plantations in Latin America was due to the PC disease in northern Colombia, where a field of 2,800 hectares located in the Turbo region was virtually devastated by PC in 1965 [9]. In Suriname, the spear rot was first registered in the Victoria region in 1976 on four-year-old oil palms in a plantation of 1,700 hectares. Despite the phytosanitary practices applied to control the disease, an exponential progression reduced the original area by 85% [39]. In Ecuador, the first PC cases happened in 1976 on four-year-old oil palms on the Pacific slopes of the Ecuadorian cordillera [1], and, like other regions, the plantation was decimated by the disease in a few years [6]. Recently Martinez et al. [7] carried out a study in Colombia to isolate microorganisms and reproduce PC in healthy oil palm plants and, in conclusion, they postulate that the oomycete *Phytophthora palmivora* is associated with the emergence of PC.

Fatal yellowing exhibits, by far, the most dramatic scenario among the bud-rot type diseases of oil palm in the Americas. The factors linked to the emergence of this disease in some countries remain unknown after experiencing more than 50 years of outbreaks in Brazil, Ecuador, Panama, Suriname, Costa Rica, Nicaragua, Honduras, Peru, and Venezuela [6, 9, 10].

3.2 History in Brazil

The FY disease first appeared in Brazil in 1974, with sporadic occurrences in a field established in 1967 near Benevides, a city in the Pará State [8, 12]. The disease progressed slowly in the following years, from 25 symptomatic plants in 1978 to 125 in 1981. In 1984, ten years after the first report, the number of plants diagnosed with FY was 465 [11]. In the first ten years after its first appearance, the disease progressed in a linear model, and the numbers of affected plants remained more or less the same per unit of time. This mode of progress indicated that the contamination did not occur from plant to plant. However, the numbers of affected plants rose to 9,968 in 1986 and 32,673 in 1987, starting a period of exponential increase [11]. In the first two decades after its first occurrence in Brazil, approximately 100 thousand oil palm trees died from this disease, resulting in the loss of entire plantations [11, 40].

Roguing was then put in place to maintain the source of the inoculum of a possible pathogen to a minimum, eliminating all plants showing symptoms up to one month after the discovery [40, 41]. The oil palm industry promoted training on the fast and precise recognition of FY symptoms to guarantee the effectiveness of this phytosanitary measure [42]. Despite it, the disease kept on occurring in plants between the 15th and the 16th year after planting, making FY one of the main problems of this crop in Brazil. Not surprisingly, this discouraged the expansion of oil palm cultivation in the affected regions [11]. As the inability to identify the causal agent and promote effective control of FY persists, the oil palm industry remains in a state of insecurity to expand in the regions affected by FY [42].

3.3 Symptomatology and diagnosis

Proper and early disease diagnosis is vital for applying control practices at the right moment. Without an efficient and effective early diagnosis of the disease and the disease-causing agent, any control measures will be inefficient [43]. Until the FY etiology is known and diagnostic systems developed, the only way to find out that a plant has this disease is by checking for characteristic symptoms and signs. Once a plant is diagnosed with FY, it must undergo roguing. In Brazil, symptoms identification in the field is still the only diagnostic system used for FY [8, 12].

An oil palm plant affected by FY shows necrosis or dryness of the spear leaf that evolves towards the base, then the region of the meristem rots, and a foul odor is felt in some cases (**Figure 2**) [12, 44]. The process of rotting of the meristem region, frequently observed in rainy seasons, motivated the initial designation of the disease as spear leaf rot [8, 40]. After losing the spear leaf, there is a general decline leading to plant death; however, some individuals during this process may temporarily re-issue a new one [12, 18]. In plants affected by FY, chlorosis appears in leaflets at the base of the intermediate leaves, which advances towards the extremity, followed by necroses frequently observed in younger leaves [6]. There is no synchronism between the spear leaf necrosis and the chlorosis of the leaflets. The FY symptoms always begin with leaflets chlorosis, which led to the Fatal

Oil Palm Fatal Yellowing (FY), a Disease with an Elusive Causal Agent
DOI: http://dx.doi.org/10.5772/intechopen.98856

Yellowing disease name [1]. In Brazil, the oil palm tree usually dies 7 to 10 months after the onset of the first symptoms, but it can vary depending on the region [41].

Once the oil palm plant gets affected by FY, the developed bunches can reach the maturation stage and are not affected. However, the immature ones rot, and the inflorescence abort [40, 41]. The root system is visibly affected, and emission of new primary roots reduced, leading to a total cease of roots growth. FY kills the tips of the roots generating new false primary ones. In addition, the root tissue is usually necrotic at the beginning of the appearance of symptoms in the aerial part [45, 46]. On the other hand, no apparent internal symptoms are observed, such as rot or necrosis of the stipe and vascular system, a characteristic that is also seen in PC [41].

4. A genetic source of resistance to FY

The causal agent of FY is still unknown, but a possible genetic solution for this problem exists. This genetic solution resides upon the fact that the American oil palm (*Elaeis oleifera* (Kunth) Cortés) and the interspecific hybrids between this species and the African oil palm are considered resistant to this disease [47].

The genus *Elaeis* (from the Greek *Elaion* that means oil) belongs to the class Liliopsida (Monocotyledones), order Arecales (Palmales), family Arecaceae (Palmae), subfamily Arecoideae, tribe Cocoseae (Cocoinaea) and, subtribe Elaeidinae [48, 49]. This genus consists of two species, *E. guineensis* and *E. oleifera*, with a pantropical distribution and two distinct diversity centers, Nigeria and South America, respectively [50–52]. The former is the African oil palm, the predominant species in commercial plantations Worldwide, and known in Brazil as "Dendê"; and the latter is the American oil palm, which originated from Central and South America, and is known as "Caiaué" [53].

The American oil palm is endemic to Equatorial America, with natural populations distributed from Central America to northern South America, including the countries of Brazil, Colombia, Costa Rica, Ecuador, French Guiana, Honduras, Mexico, Nicaragua, Panama, Peru, Suriname, and Venezuela [1]. In Surinam, there are dense stands on poor, sandy soil, while in Colombia, it can grow in damp or even swampy situations near or on the banks of rivers [1].

The American oil palm also has a history of use as a source of vegetable oils and other products, but its most important value to the oil palm industry is its capacity to hybridize with the African oil palm [1]. The interest in the germplasm of this species is due to valuable characteristics for breeding programs of the African oil palm, such as slow growth, oil quality (mainly unsaturated oil) [54], and disease resistance, including FY [47].

These two species can sexually cross and generate fertile interspecific hybrids with intermediate characteristics to the two parental species [55]. Some interspecific hybrids between these species are already commercially available, and the Brazilian genetic group of *E. oleifera* is parental to most of them — Manicoré (BRS Manicoré from Embrapa, and [Mangenot × Manicoré] × La Mé from PalmElit SAS), Manaus (Amazon from ASD Costa Rica), and Coari (Coari × La Mé, Coari × Yangambi) [47].

Independent whether the origin of FY is biotic or abiotic, or a combination of both, once it is finally known, new studies will be necessary to confirm this genetic resistance and gain insights on possible strategies to transfer this resistance to the African oil palm more efficiently and effectively, besides the use of interspecific crosses followed by backcrosses.

Elaeis guineensis

5. The search for the causal agent

5.1 Biotic stress

5.1.1 Insects

After the epidemiological explosion of FY in 1986, Embrapa (the Brazilian Agricultural Research Corporation) started conducting studies on insects as a possible vector of the FY causal agent [8]. As the spread of the disease followed the direction of the prevailing winds, while natural barriers - such as roads, rivers, and glades - were not sufficient to prevent it supported this hypothesis [8, 56]. This hypothesis on a possible entomological role in the spread of FY also resided in the fact that this disease has similarities with the lethal yellowing-type disease that affects other palms. This disease that affects several other palms is due to insect-transmitted phytoplasmas [57]. Initially, from inventory obtained in plantations affected by FY in the municipalities of Alvaraes, in the Amazonas State, and Benevides, in the Pará State, the main insects suspected of being responsible for the transmission corresponded to *Persis* sp. and *Myndus crudus* because they are commonly found in oil palm plantations and depend on palm oil for nutrition [15].

Initially, an inventory of insects captured directly on the oil palm plantations located inside and outside areas with FY occurrence was generated. Healthy oil palm plants, isolated in cages made of wood and nylon canvas, received populations of the inventoried insects, and the plants monitored for symptoms appearance. After using almost one million insects in the FY transmission test, no symptomatic plant appeared, and there was no relationship between the affected areas with the collected insect fauna [15, 58]. Additional studies have attempted to establish a link between the insects *Contigucephalus* sp., *Omolicna* sp., and *Myndus crudus* and this disease, but they all gave negative results. Consequently, the authors discarded a Homoptera as the FY vector and suggested new studies on possible very active and rare insect species [8, 56].

Another study attempted to investigate the relationship between the presence of homopterans in the vegetation cover in oil palm plantations and the occurrence of FY [12]. No relation between the vegetation cover and FY occurrence appeared as the disease manifested itself either in an area covered with *Pueraria* spp. as in areas where there were grasses, especially *Brachiaria* spp. [25]. Studies using a series of chemicals in areas where FY occurs - such as insecticides, fungicides, and bactericides - did not reduce the appearance and development of FY [40].

5.1.2 Phytoplasmas

Phytoplasmas are prokaryotes of the Class Mollicutes that cause diseases in several plant species, including several economically important ones [59]. As biotrophic parasites, they colonize the elements riddled with the phloem and can also be found inside the vectors [60]. These organisms are responsible for Lethal Yellowing (LF), a fatal disease that affects the coconut (*Cocos nucifera* L.) and at least 36 other palm species in the Americas [61, 62].

Insects from the Homoptera order, popularly known as leafhoppers, are the vectors for most phytoplasmas causing disease in plants [63]. Biological characteristics, symptoms, and specificity of the insect vector were the focus of the first studies aiming to associate phytoplasmas with plant diseases [64, 65]. Later, new and more accurate DNA-based techniques started to dominate these studies, leading to the production of specific oligonucleotides for diagnosis [65].

Oil Palm Fatal Yellowing (FY), a Disease with an Elusive Causal Agent
DOI: http://dx.doi.org/10.5772/intechopen.98856

Transmission electron microscopy was, for many years, the tool used for the detection and study of the cytological interaction between phytoplasmas and the hosts [66]. Studies using this tool were not successful in associating phytoplasma with FY, been replaced by new molecular techniques for the same purpose [8]. Studies carried out by Brioso et al. [67, 68] using nested-PCR in oil palm plants symptomatic for FY found just a very few samples positives for the presence of phytoplasmas from the SrI and 16SrI groups, which do not allow to associate these phytoplasmas to FY. An attempt to reproduce the disease was carried out by grafting intermediate leaf tips with FY into healthy seedling petioles and, during the period of two years, healthy individuals did not show symptoms characteristic of FY and, thus, the hypothesis proposing phytoplasma as the causal agent was discarded [12].

5.1.3 Fungi, bacteria, and nematodes

In the attempt to establish a causal relationship between plant pathogenic fungi, bacteria, and nematodes with FY, some studies tried to reproduce the symptoms in healthy young and adult oil palm plants inoculated with some of these microorganisms previously isolated from symptomatic plants [69, 70].

A pathogenicity test focused on studying the growth, reproductive and developmental habits of microorganisms, included one-year-old nursery plants with individual inoculations and a mixture of three fungi (*Fusarium* sp., *Pythium* sp., and *Coprinus* sp.) isolated from symptomatic plants; and again, the inoculum was unable to reproduce the disease in healthy oil palm trees [69]. The possibility of mechanical transmission between symptomatic and asymptomatic individuals by some microorganisms was also tested, with no success [69]. The chemical control attempts using fungicides or antibiotics failed to link fungi and bacteria to FY in oil palm [11].

Interestingly, some authors have observed similarities between the disease PC in Colombia and FY in Brazil. Furthermore, the oomycete *Phythophtora palmivora* was reported to be the PC causal agent [7]. The strategy used by Martinez et al. [7] was to remove tissue from oil palm plants exhibiting early symptoms of PC disease to inoculate fruit traps. Once microbial growth was observed in the fruits, tissue was transferred to culture media and pure cultures were obtained. Using the DNA isolated from the pure culture, amplification of the ITS region was performed and sequence analysis showed 99.9% homology to *P. palmivora*. The same study reported pathogenicity tests where sporangia were inoculated into the base of the spear of 150 oil palm nursery plants. After 3 to 4 days, the first symptoms of PC were observed in 85% of the plants [7]. However, full PC symptom development occurred in 15% of inoculated oil palm plants, and depended on environmental conditions. In another experiment, 20 immature spear leaves were inoculated with *P. palmivora,* and 3 days later all tissues were disintegrated, displaying a characteristic odor. Microscopy experiments showed the presence of *P. palmivora* in these tissues, and it was re-isolated using the fruit trap technique.

Nematodes are typically wormlike invertebrates able to live in the soil or inside plant structures such as roots, stems, leaves, and flowers and can cause morphological and developmental changes in their hosts [71]. The hypothesis of a nematode as a causative agent of FY came from observations of FY and the red ring disease - caused by the nematode *Bursaphelenchus cocophilus* - in the same area. Ferraz [72] did not observe this nematode in necrotic tissues or young leaves. Some studies found nematodes in the spear leaf rake and young leaves of symptomatic plants and the soil of oil palm plantations with a history of FY but were unable to link it to the appearance of this disease [24, 72].

5.1.4 Viruses and viroids

Other plant pathogens studied as potential causal agents of FY in oil palm were viruses and viroids. Several methods, including mechanical transmission, grafting, pollen-mediated dispersion, transmission electron microscopy, nested RT-PCR, RCA - rolling circle amplification, and electrophoresis, were used to test the hypothesis of a virus or a viroid as the causal agent of FY, without success [8, 10].

Lin et al. [73] evaluated extracts from plants with and without FY using the polyacrylamide gel electrophoresis technique, and the band patterns generated in both samples did not reveal any apparent difference. The same author also carried out a study to purify virus particles via separation with a fractional density gradient with no success [74]. Kitajima [75] evaluated ultrafine tissues from roots, leaves, and spear leaf of symptomatic and asymptomatic individuals by transmission electron microscopy, but no pathogen could be associated with FY.

Other studies have directed their efforts towards viroids, which are the smallest known phytopathogens, consisting basically of a single-stranded, circular RNA molecule not encapsulated [76, 77]. Beuther et al. [13] searched for viroids and viroid-like RNAs in oil palm plants using two-dimensional gel electrophoresis and return gel electrophoresis of nucleic acid extracts, with no success in showing a link between this type of pathogen and FY.

5.2 Abiotic stress

The initial pieces of evidence of a possible abiotic cause for FY came from observations made about the indefinite dissemination pattern in affected areas, with an exponential growth form not observed in the case of biotic stresses [78, 79]. Among the possible abiotic causes linked to the appearance of FY, there are lower and higher amounts of water, high or low temperature, high content of soluble salts in the soil, soil pH unsuitable for oil palm, nutritional deficiencies or excesses, presence of toxic organic compounds and intensity and balance of nutrients [78].

The regions with oil palm plantations and FY occurrence located in the North region of Brazil have soils with patches of quartz sand interspersed with patches of lateritic concretions and are subject to prolonged floodings, 5 to 6 months per year [41]. Thus, studies started aiming to understand the composition of the soil and its influence on FY emergence.

The concentrations of Cu, Fe, Mn, and Zn in the leaves of healthy and symptomatic oil palm plants and resistant interspecific hybrids were determined and found out that their concentrations were below the ideal range, suggesting their involvement in the appearance of FY [80]. Compact soils that stay temporarily saturated by rainfall suffer oxidation by anoxia, making it impossible for plants to absorb Fe [80]. Based on these observations, applications of ferrous sulfate were carried out on plants under different stages of FY, but after 120 days of the experiment, there was no regression of the disease in the evaluated oil palms [80].

The physical properties of the soil from areas with the occurrence of FY revealed that they were naturally well-drained and deep but had a thickening or compacting between the depths of 30 cm and 60 cm, as well as the occurrence of speckles in this depth, which results in soil saturation in the superficial layer during the rainfall season [81]. Bernardes [82] carried out chemical analysis on roots of symptomatic plants, and the results did not allow to pinpoint any element imbalance that could be responsible for FY. Another fact that needs consideration as possibly linked to a potential cause for the disease is the fact that at the moment when the first symptoms appear in the aerial part, the root system is severely impaired, which explains the plants' lack of response to fertilization and other interventions [82].

Oil Palm Fatal Yellowing (FY), a Disease with an Elusive Causal Agent
DOI: http://dx.doi.org/10.5772/intechopen.98856

A series of field observations made in the heart of the oil palm production area in Brazil led to new hypotheses for a possible abiotic cause for FY [83]. The main field observations taken into consideration were: a higher occurrence of flooding in oil palm plantations, in comparison to the previous level, observed under native vegetation cover; the layers close to the soil surface without vegetation cover or with oil palm tend to stay close to water saturation for periods much longer than in the native forest; the presence of mottled-iron reduction in the profile of the oil palm plantations, and the redox-potential values (Eh) below −200 mV; and the presence of reduced iron ions on the soil surface in oil palm plantations during periods of intense rain [83].

The new hypotheses were brought together and summarized as: Deficient aeration reduces the potential for oxy-reduction in the soil, causing changes in the ionic composition of the soil solution (reduction of Fe^{3+} ions; NO^{3+}; Mn^{3+}). The soil solution with a high concentration of reduced ions initially causes damage to the root system (**Figure 3**) predisposing the oil palm plant to physiological disturbances (passive poisoning and attacks of secondary pathogens) whose symptoms are known as FY [84].

To gain insights into the idea of oxygen deficiency (hypoxia) in the origin of FY, a study by Encinas [85] evaluate the influence of land use and temporal variations on the dynamics of nutrients in the solution of soil and water at an oil palm plantation and a nearby area still with primary forest. Another by Muniz [83] compared the changes in water flow at an oil palm plantation and a nearby area still with native vegetation cover and evaluated its effects on iron dynamics and the structure of the soil. These two studies gathered additional shreds of evidence to further support this hypothesis, such as the electrical conductivity increased during a long flooding period (95 days), indicating that ions from the aggregates migrate to the solution; the soil pH increases after the initial flooding period, reaching values close to neutrality, with a subsequent reduction, but above the values found in aerated soil; the soil redox potential decreases during the flooding period, forming a highly reducing environment; the total carbon contained in the macroaggregates reduced

Figure 3.
Oil palm plant showing reduction of the root system in hypoxia conditions (A), and soil clouds showing the typical reductimorphic or oximorphic color mottles caused by stagnating soil environment (B). Source: Wenceslau Teixeira.

after flooding for a period of 11 days; the iron contained in the aggregates of Yellow Latosols with medium texture migrates to the soil solution under flooding conditions; there is a high negative correlation between the iron in the flooding solution and the DMG of the aggregates in the Yellow Latosols, and flooding for a period of 11 days promotes the destabilization of aggregates of Yellow Latosols with medium goethite texture.

6. New technologies to gain insights on the FY causal agent

The so-called 'omics' techniques (**Figure 4**) provide new opportunities to study oil palm FY. To get insights on FY possible causal agent, different research groups in Brazil have used metagenomics, metabolomics, and proteomics analysis [20–22]. To our knowledge, no work focusing on transcriptomics and FY has been published yet. The most commonly used approach in these studies is to compare healthy plants (without symptoms of FY) to those showing disease symptoms at different stages of progression. In contrast to more traditional non-molecular studies of FY, these techniques provide a global glimpse of the organism by looking at the associated microbiota (metagenomics), the complete protein content (proteomics), or metabolite content (metabolomics) of cells.

6.1 Metagenomics

Koch's postulate was fundamental to the identification of disease-causing microorganisms [86]. In short, the strategy of isolating and cultivating the potential pathogen, and inoculating it into a healthy organism to confirm the symptoms of the disease, brought many advances to the study of infectious diseases [87]. More recently, due mainly to the advent of next-generation sequencing (NGS) technologies, the frontiers of microbiology expanded to those microorganisms that we cannot cultivate by classical microbiology techniques. That has opened the possibility to test the hypothesis that a microorganism not grown in vitro easily is the cause of FY [88]. If this is the case, metagenomics would be the technique to study FY.

Metagenomics is a culture-independent approach to study microbial communities. A metagenomics strategy allows one to skip the step of isolation and cultivation of microbial species. Metagenomics studies can contribute to elucidate the identity

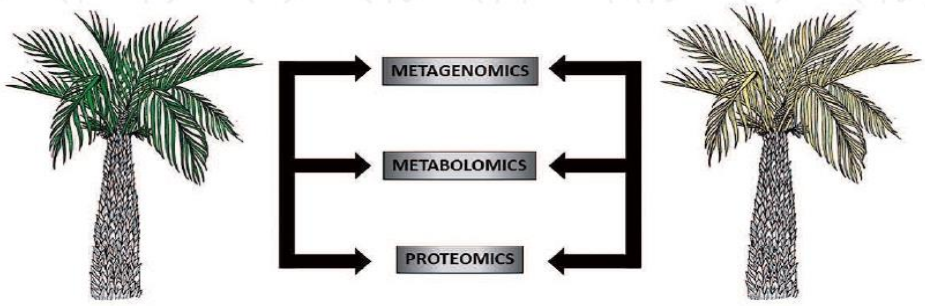

Figure 4.
Schematic showing a healthy oil palm tree (green leaves) and another one (yellow leaves) showing fatal yellowing (FY) symptoms. Different molecular techniques such as metagenomics, metabolomics and proteomics can be used to compare these contrasting biological situations. Metagenomics is a culture-independent technique that can be used to identify the microorganisms present. Metabolomics can used to identify and quantify cellular metabolites. Proteomics allows the identification of differentially expressed proteins. These 'omics' techniques are important high throughput tools that have been used to understand the biology of oil palm when challenged by FY disease. (credit: Clarissa Kruger).

metabolic capabilities as well as the interactions between the organisms of the community [97]. One limitation to this method, however, is that the plant host genome sequence needs to be available and subtracted *in silico* from microbial community sequences. If possible, it is useful to find a way to selectively extract microbial DNA from the samples before sequencing to avoid or reduce the presence of the plant host DNA [98]. It should be noted that if the complexity of the microbial community is high or if a lot of host DNA is present in the sequenced samples, inadequate sequencing depth might be an important limitation to this method. To our knowledge this approach has not been used yet to search for the causal agent of FY.

6.2 Proteomics and metabolomics

Proteome designates the set of proteins expressed by a cell, tissue, or organism at any given time [99]. Proteomic tools make it possible to obtain a protein profile with precision and sensitivity with the aid of electrophoresis, chromatography, mass spectrometry, and bioinformatics [99]. Proteomics is more and more used nowadays to understand plant responses to different biotic and abiotic stress conditions [100, 101].

In this context, and based on the hypothesis that the primary stress behind FY was abiotic and present in the soil, proteomics was applied to study this disease [21]. This hypothesis is based on observations regarding symptoms seen in the root system before they appeared in the aerial part [83]. Soil compaction, which hinders drainage and subject the roots to long periods of flooding in a hypoxia condition, would be in the origin of the stress [83].

Nascimento et al. [21] carried out a proteomic analysis to compare the protein profiles from symptomatic and asymptomatic oil palm plants, employing the mass spectrometry technique. The study looked for proteins linked to tolerance induction to relate the different areas collected and the distinct stages of the disease, analyzing the roots of symptomatic plants in early, intermediate, and final stages.

Proteins involved in the metabolism of phenylpropanoids and lignins, with a recognized role in reducing the effects of biotic and abiotic stress, were negatively regulated in symptomatic individuals, aggravating FY symptoms. In asymptomatic plants, enzymes such as S-adenosylmethionine - with a crucial role in methionine's biosynthetic metabolism - showed a recognized action in response to the stress. Plants with FY symptoms showed some pathogen-related proteins positively regulated, implying a progression of infection by biotic agents [21].

The hypothesis of a possible physiological dysfunction caused by factors present in the soil was reinforced by the large accumulation of antioxidant proteins in asymptomatic individuals [21]. The participation of the antioxidant system may indicate some level of resistance, considering that this system is vital for plants in conditions of soil flooding [102]. In addition, the accumulation of aldehyde dehydrogenase may indicate that the root system is under an anaerobic condition as it converts the acetaldehyde, promoting plant survival in this condition [21, 103]. Thus, these results indicate that plants affected by FY are in abiotic stress conditions and, with the damages done to the roots, it becomes a gateway for several opportunistic organisms [21].

In contrast to proteomics, metabolomics refers to a comprehensive analysis to identify the set of metabolites present in a sample with the aid of analytical techniques, such as liquid chromatographies or liquid–gas, associated or not with mass spectrometry, among others [104].

Rodrigues-Neto et al. [20] performed the first metabolomics work to study FY in Brazil using an untargeted metabolomics strategy to prospect metabolites differentially expressed in the leaves of FY symptomatic and asymptomatic plants. A high

and/or the genetic and metabolic capabilities of the microorganisms present in a sample, including any that are potentially pathogenic [89].

In this sense, metagenomics complements the classic techniques of isolation and cultivation of microorganisms, and one can apply it to study different classes of microorganisms (e.g., viruses, bacteria, fungi, archaea) [22, 90–92]. Metagenomics protocols begin with the extraction of total DNA from the sample of interest, which contains microorganisms. Samples can be many different ones, such as soil or plant parts with FY disease symptoms. There are distinct ways to study the microbial community from this DNA. Many studies in different plants use the ribosomal RNA (rRNA) gene or ITS amplification approach (i.e., PCR amplification with specific primers) to identify the microorganisms present, including a potential pathogen [93–95].

16S rRNA gene-specific primers amplify bacterial and archaeal sequences (16S rDNA). Similarly, the 18S rRNA gene and the ITS-specific primers amplify fungal sequences. The ITS refers to the internal transcribed spacer, the DNA situated between the small-subunit ribosomal RNA and large-subunit rRNA genes. The 16S rDNA, 18S rDNA, and the ITS regions are highly polymorphic, thus allowing taxonomical identification of the microorganisms present in a sample. The PCR-amplified DNA is then sequenced and submitted to bioinformatics analysis to compare the obtained sequences with sequence databanks, leading to a putative microorganism. In summary, this metagenomics approach that combines PCR amplification with NGS allows identifying microorganisms present in the community [96].

The first metagenomics work to use ITS amplification and high throughput NGS to study FY in Brazil was performed by Costa et al. [22], who evaluated fungal communities associated with leaves of oil palm plants, with and without symptoms of FY. Leaves from health plants and from plants showing FY symptoms in three different disease stages (stages 2, 5, and 8) were obtained. Because of the similarities between PC and FY, using primers specific to the genus *Phythophtora*, the authors attempted PCR-amplification of oil palm leaf samples showing symptoms of FY. Weak amplification was obtained in only one sample. Thus, this study provided preliminary evidence that DNA of the genus *Phytophtora* may not be commonly present in Brazilian FY, contrary to what has been reported in Colombia [7]. However, further experiments with more samples, and additional controls are needed to clarify the validity of this initial observation.

The Costa et al. [22] study reported the analyses of fungal diversity using the ITS region. Results showed that the fungal community in different healthy asymptomatic oil palm leaves are more similar to each other than those presenting FY disease symptoms. The fungal communities were not the same among all the symptomatic samples, and were not consistent even between samples at the same stage of FY disease. Importantly, no fungal taxon had its relative proportion increased in leaves across all the FY diseased oil palm plants. It was hypothesized that the changes observed in the fungal community composition could be a secondary effect of FY disease. Similar metagenomic studies to analyze the viral, bacterial and archaeal communities associated with FY are needed.

A less common metagenomic approach that can also be used to study plant disease is to assemble genomes from the metagenome obtained from plants showing symptoms of disease. In this case, instead of using PCR to amplify a specific gene, one can completely sequence the DNA extracted from the samples of interest, and use bioinformatics tools to assemble genomes (metagenome-assembled genomes) of the microorganisms present. This type of methodology allows, in addition to identifying microorganisms present, access to their genomes. This creates the possibility of studying the genetic relationship among the species present, and predicting

throughput method based on metabolic fingerprinting MS, using UHPLC coupled to high-resolution mass spectrometry (HRMS), was employed, and chemometric analysis, PCA and PLS-DA, were used to evaluate metabolic differences. This study aimed at prospecting a biomarker for FY early diagnosis, besides gaining insights on pathways responsive to this disease valuable for future improvement studies.

Nine secondary metabolites were detected in a higher concentration in the healthy plants in comparison to the FY affected ones: Glycerophosphorylcholine, arginine, asparagine, paniculatin or apigenin 6,8-di-C-hexose, tyramine, Chlorophyllide, 1,2-dihexanoyl-sn-glycero-3-phosphoethanolamine, proline, malvidin 3-glucoside-5-(6″-malonylglucoside) or kaempferol 7-methyl ether 3-[3-hydroxy-3-methylglutaryl-(1–> 6)]-[apiosyl-(1–> 2)-galactoside]. These metabolites made possible to identify different metabolic pathways that have been affected by the FY, such as the glycerophospholipid metabolism, the isoquinoline alkaloid biosynthesis, the flavonoid biosynthesis, the tetrapyrrole biosynthesis and citrate cycle derivatives pathways.

Unfortunately, due to the fact that these metabolites are already described in the literature as linked to other types of stress, they are not good candidate for biomarkers; except for two of them, glycerophosphorylcholine and 1,2-dihexanoyl-sn-glycero-3-phosphoethanolamine [20].

7. Final considerations

Fatal yellowing disease represents a threat of great magnitude to the Brazilian oil palm industry. For decades, several studies attempted to identify its causal agent without success. As a result, no measures used today can effectively reduce the economic loss for the oil palm industry due to this disease. The only glimpse of hope in solving this problem still resides in the genetic resistance found in the American oil palm. However, the road to transfer this resistance through interspecific crosses and backcrosses is very long and has many uncertainties.

The search for the primary stress leading to FY must go on, whether it is of biotic or abiotic origin - or the combination of both. Only then might be able to block its occurrence, or, if not possible to do that, develop early diagnostic tools to reduce its spread to a minimum.

Recent studies using single omics analysis have shown that these new technics can take the etiological studies regarding FY in oil palm to another level. We postulate that transcriptomics should be the next step in using omics to gain further insights regarding this disease. Even more, we believe that it should be done under the scope of a multi-omics integration (MOI) strategy, together with metabolomics, proteomics, and ionomics, at least.

Acknowledgements

The author(s) disclosed receipt of the following financial support for the research, authorship, and/or publication of this article: The grant (01.13.0315.00 - DendêPalm Project) for this study was awarded by the Brazilian Innovation Agency - FINEP.

Conflict of interest

The authors declare no conflict of interest.

Elaeis guineensis

Author details

Cleiton Barroso Bittencourt[1], Philippe de Castro Lins[2], Alessandra de Jesus Boari[3], Betania Ferraz Quirino[4], Wenceslau Geraldes Teixeira[5] and Manoel Teixeira Souza Junior[4*]

1 Universidade Federal de Lavras (UFLA), Lavras, MG, Brazil

2 Universidade de Brasília (UnB), Brasília, DF, Brazil

3 Embrapa Amazônia Oriental, Belém, PA, Brazil

4 Embrapa Agroenergia, Brasília, DF, Brazil

5 Embrapa Solos, Rio de Janeiro, RJ, Brazil

*Address all correspondence to: manoel.souza@embrapa.br

References

[1] Corley RHV, Tinker PB. The oil palm. 5th ed. Chichester: Wiley Blacwell; 2016. 1299 p. DOI: 10.1002/9781118953297

[2] Our World in Data. Oil palm. [Internet]. 2020. Available from: https://ourworldindata.org/palm-oil [Accessed: 2021-03-02]

[3] FAOSTAT. Food and agriculture organization of the United Nations. 2018. [Accessed: 2021-03-01]

[4] IndexMundi. 2020. Palm Oil Production by Country in 1000 MT. 2020. Available from: https://www.indexmundi.com/agriculture/?commodity=palm-oil. [Accessed: 2021-03-01]

[5] Furumo PR, Aide TM. Characterizing commercial oil palm expansion in Latin America: land use change and trade. Environmental Research Letters. 2017; 12(2):024008. DOI: 10.1088/1748-9326/aa5892

[6] Franqueville H. Oil palm bud rot in Latin America. Experimental Agriculture. 2003; 39(3): 225-240. DOI: 10.1017/S0014479703001315

[7] Martínez G, Sarria GA, Torres GA, Aya HA, Ariza JG, Rodríguez J. *Phytophthora* sp. es el responsable de las lesiones iniciales de la Pudrición del cogollo (PC) de la Palma de aceite en Colombia. Revista Palma. 2008; 29(3):31-41

[8] Boari ADJ. Estudos realizados sobre o amarelecimento fatal do dendezeiro (*Elaeis guineensis* Jacq.) no Brasil. Embrapa Amazônia Oriental-Documentos (INFOTECA-E). 2008

[9] Benítez É, García C. The history of research on oil palm bud rot (*Elaeis guineensis* Jacq.) in Colombia. Agronomía Colombiana. 2014; 32(3):390-398. DOI: 10.15446/agron.colomb.v32n3.46240

[10] Boari AJ, Teixeira WG, Venturieri A, Martorano L, Tremacoldi CR, Carvalho KB. Avanços nos estudos sobre o amarelecimento fatal da palma de óleo (*Elaeis guinnensis* Jacq.). In Embrapa Solos-Artigo em anais de congresso (ALICE). Tropical Plant Pathology, Brasília, DF, v. 37, ago. 2012. Suplemento. Edição dos Resumos do 45 Congresso Brasileiro de Fitopatologia, Manaus, 2012

[11] Van Slobbe WG. Amarelecimento Fatal (A.F.) at the oil palm estate Denpasa, Brazil. In: International Seminar on the Identification and Control of the Organism(s) and/or Other Factor(s) Causing the Spear Rot Syndrome in Oil Palm, Paramaribo (Suriname) 8-12 Mar 1988; Paramaribo (Suriname). Ministry of Agriculture; 1991. p. 75-80

[12] Trindade DR, Poltronieri LS, Furlan Júnior J. Abordagem sobre o estado atual das pesquisas para a identificação do agente causal do amarelecimento fatal do dendezeiro. In: Poltronieri LS, Trindade DR, Santos IP. (Ed.). Pragas e doenças de cultivos amazônicos. Belém, PA: Embrapa Amazônia Oriental; 2005. p. 439-450

[13] Beuther E, Wiese U, Lukáacs N, Van Slobbe WG, Riesner D. Fatal Yellowing of Oil Palms: Search for Viroids and Double-Stranded RNA. Journal of Phytopathology. 1992;136(4);297-311. DOI: 10.1111/j.1439-0434.1992.tb01312.x

[14] Brioso PST, Montano HG, Figueiredo DV, Poltronieri LS, Furlan Junior J. Amarelecimento fatal do dendezeiro: sequenciamento parcial do fitoplasma associado. Summa Phytopathologica. 2006; 32;50

[15] Celestino FP, Louise C, Lucchini F. Estudos de transmissão do amarelecimento fatal do dendezeiro (*Elaeis guineensis*, Jacq), com insetos suspeitos. In: Congresso Brasileiro de Entomologia, 14., 1993, Piracicaba, SP. Resumos. Piracicaba: SEB; 1993. 807 p.. p.194

[16] Louise C. Inventory of Homoptera and Heteroptera in relation to the amarelecimento fatal disease. Spear rot of oil palm in tropical America. Proceedings.1990; 36-46

[17] Viégas I, Frazão D, Furlan Júnior J, Trindade D, Thomaz M. Teores de micronutrientes em folhas de dendenzeiros sadios e com sintomas de amarelecimento fatal. In: Embrapa Amazônia Oriental-Artigo em anais de congresso (ALICE). In: XXV Reunião brasileira de fertilidade do solo e nutrição de plantas; VIII Reunião Brasileira Sobre Micorrizas; VI Simpósio Brasileiro De Microbiologia Do Solo; III Reunião Brasileira De Biologia Do Solo. 24-26, october 2000; Santa Maria, RS. Fertbio; 2000.

[18] Silveira RI, Veiga AS, Ramos EJA, Parente JR. Evolução da sintomatologia do amarelecimento fatal a adubações com omissão de macro e micronutrientes. Belém, PA: Denpasa; 2000

[19] Baena ARC. Propriedades físicas do solo em áreas de ocorrência do amarelecimento fatal do dendezeiro. Embrapa Amazônia Oriental-Séries anteriores (INFOTECA-E). 1999; 1-3

[20] Rodrigues-Neto JC, Correia MV, Souto AL, Ribeiro JAA, Vieira LR, Souza MT, Abdelnur PV. Metabolic fingerprinting analysis of oil palm reveals a set of differentially expressed metabolites in fatal yellowing symptomatic and non-symptomatic plants. Metabolomics. 2018;14(10):1-16. DOI: https://doi.org/10.1007/s11306-018-1436-7

[21] Nascimento SVD, Magalhães MM, Cunha RL, Costa PHDO, Alves RCDO, Oliveira GCD, Valadares RBDS. Differential accumulation of proteins in oil palms affected by fatal yellowing disease. PloS one. 2018;13(4):e0195538. DOI: 10.1371/journal.pone.0195538

[22] Costa OYA, Tupinambá DD, Bergmann JC, Barreto CC, Quirino BF. Fungal diversity in oil palm leaves showing symptoms of Fatal Yellowing disease. PloS one. 2018;13(1):e0191884. DOI: 10.1371/journal.pone.0191884

[23] Kuss VV, Kuss AV, Rosa RG, Aranda DA, Cruz YR. Potential of biodiesel production from palm oil at Brazilian Amazon. Renewable and Sustainable Energy Reviews. 2015; 50:1013-1020. DOI: 10.1016/j.rser.2015.05.055

[24] Carter C, Finley W, Fry J, Jackson D, Willis L. Palm oil markets and future supply. European Journal of Lipid Science and Technology. 2007;109(4):307-3014. DOI: 10.1002/ejlt.200600256

[25] Barcelos E, Rios SDA, Cunha RN, Lopes R, Motoike SY, Babiychuk E, Skirycz A, Kushnir S. Oil palm natural diversity and the potential for yield improvement. Frontiers in plant Science. 1990;6. DOI: 10.3389/fpls.2015.00190

[26] Corley RHV. How much palm oil do we need? Environmental Science & Policy. 2009;12(2):134-139. DOI: 10.1016/j.envsci.2008.10.011

[27] Sheil D, Casson A, Meijaard E, Van Noordwijk M, Gaskell J, Sunderland-Groves J, Wertz K, Kanninen M. The impacts and opportunities of oil palm in Southeast Asia: What do we know and what do we need to know? Center for International Forestry Research. 2009; 51:1-80. DOI: 10.17528/cifor/002792

[28] Carrere, R. Oil palm in Africa: Past, present and future scenarios. WRM series on tree plantations. 2010. 5:111

[29] Pacheco P, Gnych S, Dermawan A, Komarudin H, Okarda B. The palm oil global value chain: Implications for economic growth and socialand environmental sustainability. Working Paper 220. Bogor, Indonésia. CIFOR; 2017. 55 p. DOI: 10.17528/cifor/006405

[30] Castiblanco C, Etter A, Aide TM. Oil palm plantations in Colombia: a model of future expansion. Environmental science & policy. 2013;27:172-83. DOI: 10.1016/j.envsci.2013.01.003

[31] GREPALMA. Palma of Guatemala. Available from: https://www.grepalma.org/en/development-for-guatemala/ [Accessed: 2021-03-02]

[32] Silva FL, Homma AK, Pena HWA. O cultivo do dendezeiro na Amazônia: promessa de um novo ciclo econômico na região. Embrapa Amazônia Oriental-Artigo em periódico indexado (ALICE). 2011; 158: 1-24

[33] Homma AKO, Furlan-Júnior J, Carvalho RAD, Ferreira CAP. Bases para uma Política de Desenvolvimento da Cultura do Dendezeiro na Amazônia. In: Viegas, I., Muller, A. (eds), A Cultura do Dendezeiro na Amazônia Brasileira, 1 ed., cap. 1. Belém, Pará, 2000

[34] Bentes EDS, Homma AKO. Importação e exportação de óleo e palmiste de dendezeiro no Brasil (2010-2015). In Embrapa Amazônia Oriental-Artigo em anais de congresso (ALICE). In: Congresso da Sociedade Brasileira de Economia, Administração e Sociologia Rural (SOBER); 14-17 Agosto 2016; Universidade Federal de Alagoas – UFAL. Maceió. 2016. p. 1-16

[35] Ramalho Filho A, Da Motta P, Freitas P, Teixeira W. Zoneamento agroecológico, produção e manejo para a cultura da palma de óleo na Amazônia. 1st ed. Embrapa Solos; 2010. 216 p

[36] Sistema IBGE de Recuperação Automática – SIDRA. Produção agrícola. Available from: https://sidra.ibge.gov.br/pesquisa/pam/tabelas/. 2019. [Accessed: 2021-03-02]

[37] Motta PEF, Naime UJ, Goncalves A, Baca J. Zoneamento agroecológico do dendezeiro para as áreas desmatadas do Estado de Rondônia. In Embrapa Solos-Artigo em anais de congresso (ALICE). In: XXXII CONGRESSO BRASILEIRO DE CIÊNCIA DO SOLO; 2-7 agosto 2009; Fortaleza: SBCS. 2009.

[38] Brazilio M, Bistachio NJ, Cillos Silva V, Nascimento DD. O Dendezeiro (*Elaeis guineensis* Jacq.) - Revisão. Bioenergia em Revista: Diálogos. 2012; 2(1): 27-45.

[39] Van de Lande HL. Studies on the Epidemiology of Spear Rot in Oil Palm (*Elaeis guineensis* Jacq.) in Suriname. Proefschrift Landbouwuniversiteit, Wageningen, the Netherlands. 1993

[40] Trindade DR, Furlan Júnior J. Amarelecimento fatal do dendezeiro. In: Muller AA; Furlan Júnior J. (Ed.). Agronegócio do dendê: uma alternativa social, econômica e ambiental para o desenvolvimento sustentável da Amazônia. Belém, PA: Embrapa Amazônia Oriental; 2001. p. 145-152

[41] Van Slobbe WG. Amarelecimento fatal: final report. Belém, PA: Denpasa, 1991. 100 p

[42] DENPASA. Amarelecimento Fatal. 2021. Available from: http://denpasa.com.br/pt-br/amarelecimento-fatal-af/ [Accessed: 2021-02-15]

[43] Riley MB, Williamson MR, Maloy O. Plant disease diagnosis. The Plant Health Instructor. 2002; 3. DOI: 10.1094/PHI-I-2002-1021-01

[44] Kastelein P, Van Slobbe WG, De Leeuw GTN. Symptomatological and histopathological observations on oil palms from Brazil and Ecuador affected by fatal yellowing. Netherlands Journal of Plant Pathology. 1990;96(2):113-117. DOI: 10.1007/BF02005135

[45] Ayala LS. Relatório de visita à Denpasa. In: DENPASA. Pesquisa sobre amarelecimento fatal do dendezeiro. Belém, PA. 2001. 319 p.

[46] Bernardes MSR. Relatório de visitas à plantação de Paricatuba, na Denpasa, visando à identificação das causas do AF (1999). In: DENPASA. Pesquisa sobre amarelecimento fatal. Belém, PA, 2001

[47] Rios SDA, da Cunha RNV, Lopes R, da Silva EB. Recursos genéticos de palma de óleo (*Elaeis guineensis* Jacq.) e caiuaé (*Elaeis oleifera* (HBK) Cortes). Embrapa Amazônia Ocidental-Documentos (INFOTECA-E);2012

[48] Dransfield J, Uhl NW, Asmussen CB, Baker WJ, Harley MM, Lewis CE. A new phylogenetic classification of the palm family, Arecaceae. Kew Bulletin. 2005;559-569

[49] Eiserhardt WL, Pintaud JC, Asmussen-Lange C, Hahn WJ; Bernal R; Balslev H; Borchsenius F. Phylogeny and divergence times of *Bactridinae* (Arecaceae, Palmae) based on plastid and nuclear DNA sequences. Taxon. 2011; 60(2):485-498. DOI:10.1002/tax.602016

[50] Bakoumé C, Wickneswari R, Siju S, Rajanaidu N, Kushairi A, Billotte N. Genetic diversity of the world's largest oil palm (*Elaeis guineensis* Jacq.) field genebank accessions using microsatellite markers. Genetic Resources and Crop Evolution. 2015;62(3):349-360. DOI:10.1007/s10722-014-0156-8

[51] Maizura I, Rajanaidu N, Zakri AH, Cheah SC. Assessment of Genetic Diversity in Oil Palm (*Elaeis guineensis* Jacq.) using Restriction Fragment Length Polymorphism (RFLP). 2006;53(1):187-195. DOI:10.1007/s10722-004-4004-0

[52] Ithnin M, The CK, Ratnam W. Genetic diversity of *Elaeis oleifera* (HBK) Cortes populations using cross species SSRs: implication's for germplasm utilization and conservation. BMC Genetics. 2017; 18(1):18-37. DOI:10.1186/s12863-017-0505-7

[53] Junior RAG, Lopes R, Cunha RNV, Abreu-Pina AJ, Quaresma CE, Campelo RD, Resende MDV. Ganhos de seleção para produção de cachos em híbridos interespecíficos entre caiaué e dendê. Pesquisa Agropecuária Brasileira. 2019;54(X): e00819-x. DOI: 10.1590/S1678-3921.pab2019.v54.00819

[54] España MD, Mendonça S, Carmona PAO, Guimarães MB, da Cunha RNV, Souza, M. T. Chemical characterization of the American oil palm from the Brazilian Amazon forest. Crop Science. 2018;58(5): 1982-1990. DOI: https://doi.org/10.2135/cropsci2018.04.0231

[55] Hormaza P, Fuquen EM, Romero HM. Phenology of the oil palm interspecific hybrid *Elaeis oleifera*×*Elaeis guineensis*. Scientia Agricola. 2012;69(4), 275-280. https://doi. org/10.1590/S0103-90162012000400007

[56] Trindade DR. Ações de pesquisas, objetivando a identificação do agente causal do amarelecimento fatal-AF do dendezeiro. Embrapa Amazônia Oriental-Outras publicações científicas (ALICE), 1995

[57] Harrison NA, Helmick, E. E., & Elliott, M. L. Lethal yellowing-type diseases of palms associated with phytoplasmas newly identified in Florida, USA. Annals of Applied Biology. 2008;153(1), 85-94 DOI: https://doi.org/10.1111/j.1744-7348.2008.00240.x

[58] Santos AF, Valois AC, Hartz JL. Workshop sobre a cultura do dendê. In: Workshop sobre a cultura do dendê; 24-27 october 1995. Manaus, Amazona. 1995

[59] Bertaccini A. Phytoplasmas: diversity, taxonomy, and epidemiology. Front Biosci. 2007;12(2):673-689. 10.2741/2092

[60] Bertaccini A, Duduk B. Phytoplasma and phytoplasma diseases: a review of recent research. Phytopathologia mediterranea. 2009;48(3):355-378. DOI: 10.14601/ Phytopathol_Mediterr-3300

[61] Harrison NA, Helmick EE, Elliott ML. Lethal yellowing-type diseases of palms associated with phytoplasmas newly identified in Florida, USA. Annals of Applied Biology. 2008;153(1):85-94. DOI: 10.1111/j.1744-7348.2008.00240.x

[62] Bertaccini A, Duduk B, Paltrinieri S, Contaldo N. Phytoplasmas and phytoplasma diseases: a severe threat to agriculture. American Journal of Plant Sciences. 2014;5, 1763-1788: DOI: 10.4236/ajps.2014.512191

[63] Trivellone V. An online global database of Hemiptera-Phytoplasma-Plant biological interactions. Biodiversity data jornal. 2019;7:e32910. DOI: 10.3897/BDJ.7.e32910

[64] Montano HG, Brioso PS, Pimentel JP. List of phytoplasma hosts in Brazil. Bulletin of Insectology. 2007; 60:129-130

[65] Montano HG. Fitoplasmas e fitoplasmoses no Brasil. Revisão Anual de Patologia de Plantas (RAPP). 2013;21:034-095

[66] Musetti R, Favali MA. Microscopy techniques applied to the study of phytoplasma diseases: traditional and innovative methods. Multidisciplinary Microscopy Research and Education. 2004. 2:72-80

[67] Brioso PST, Montano HG, Trindade DR, Poltronieri LS, Barcelos E, Veiga AS, Furlan-Júnior J. Fitoplasma do grupo 16S rRNA I associado ao amarelecimento fatal de Elaeis guineensis. In Congresso Paulista de Fitopatologia (Vol. 26); 2003

[68] Brioso PST, Montano HG, Figueiredo DV, Poltronieri LS, Furlan Junior J. Amarelecimento fatal do dendezeiro: sequenciamento parcial do fitoplasma associado. Summa Phytopathologica. 2006;32-35

[69] Silva HM. Relatório de atividades junto ao consultor em nematologia; 1995.

[70] Silva HM. Relatório de avaliação dos trabalhos com amarelecimento fatal. Belém, PA; 1989. 5 p

[71] Mendonça, 2016

[72] Ferraz LCCB. Relatório final - Apoio técnico na especialidade de nematologia de plantas. In: DENPASA. 2021

[73] Lin MT. Study on fatal yellowing of oil palms: two technical reports research contract Denpasa-Bioplanta.1990; 24 p.Typescripts (unpublisshed).

[74] Lin MT. Comparative analysis of oil palm tissues with and without fatal yellowing symptoms by centrifugation: technical report-research contract Denpasa-Bioplanta. 1989; 5 p. Typescripts (unpublisshed)

[75] Kitajima EW. Report to Uepae de Belém about E. M. observations on tissues of healthy and by AF affected palms from Denpasa. Brasilia, DF: Universidade de Brasília – Departamento de Biologia Celular. 1991. 2 p. Typescript (unpblished).

[76] Singh RPAG, Avila AC, Dusi AN. Boucher A, Trindade DR, Van

Slobbe WG, Ribeiro SG, Fonseca MEN, Association of viroid-like nucleic acids with the fatal yellowing diseases of oil palm. Fitopatologia Brasileira.1988; 13(4):392-394.

[77] Dollet M, Mazzolini L, Bernard V. Research on viroid-like molecules in oil palm. In: ACIAR PROCEEDINGS. Australian Centre for International Agricultural Research, 1993. p. 62-62.

[78] Bergamin-Filho A, Amorim L, Laranjeira FF, Berger RD, Hau B. Análise temporal do amarelecimento fatal, do dendezeiro como ferramenta para elucidar sua etiologia. Fitopatologia Brasileira. 1998; 23(3): 391-396.

[79] Laranjeira FF, Bergamin-Filho A, Amorim L, Berger RD, Hau B. Análise espacial do amarelecimento fatal do dendezeiro como ferramenta para elucidar sua etiologia. Fitopatologia Brasileira. 1998; 23(3): 397-403.

[80] Viégas IJM, Frazão DAC, Furlan-Júnior J, Trindade DR, Thomaz MAA. Teores de micronutrientes em folhas de dendezeiros sadios e com sintomas de amarelecimento fatal. In: XXV Reunião Brasileira de Fertilidade do Solo e Nutricão de Plantas, VIII Reunião Brasileira Sobra Micorrizas, VI Simpósio Brasileiro de Microbiologia do Solo, III Reunião Brasileira de Biologia do Solo. 22-26 October 2000; Santa Maria. Rio Grande do Sul. 2000. p. 1-4.

[81] Silveira RI, Veiga AS, Ramos EJA, Parente JR. Evolução da sintomatologia do amarelecimento fatal a adubações com omissão de macro e micronutrientes. Belém, PA: Denpasa, 2000. 35 p.

[82] Bernardes MSR. Relatório de visitas à plantação de Paricatuba, na Denpasa, visando à identificação das causas do AF (1999). In: DENPASA. Pesquisa sobre amarelecimento fatal. Belém, PA, 2001.

[83] Muniz RS. Alterações do fluxo hídrico e seus efeitos na dinâmica do ferro e na estrutura de um Latossolo Amarelo na Amazônia [thesis]. Rio de Janeiro: Universidade Federal do Rio de Janeiro. 2017.

[84] Teixeira W, Pina ADA, Boari ADJ, Martins GC, Lima WAA, Muniz RS, Gonçalves AO, Encinas OC, Araújo AC. A hipótese abiótica como agente causal do amarelecimento fatal (AF) da palma de óleo (*Elaeis guineensis* Jacq.) no Brasil. In XXXVI Congresso Brasileiro de Ciência do Solo. 30-04 august 2017; Belém. Pará; 2017.

[85] Encinas OC. Dinâmica da água e nutrientes na solução do solo em um dendezal (*Elaeis guineensis* Jacq.) na Amazônia Central [thesis]. Manaus: Universidade Federal do Amazonas; 2016.

[86] Hosainzadegan H, Khalilov R, Gholizadeh P. The necessity to revise Koch's postulates and its application to infectious and non-infectious diseases: a mini-review. European Journal of Clinical Microbiology & Infectious Diseases. 2020 Feb;39(2):215-218. DOI: 10.1007/s10096-019-03681-1

[87] Antonelli G, Cutler S. Evolution of the Koch postulates: towards a 21st-century understanding of microbial infection. Clinical Microbiology and Infection. 2016 Jul;22(7):583-584. DOI: 10.1016/j.cmi.2016.03.030

[88] Boolchandani M, D'Souza AW, Dantas G. Sequencing-based methods and resources to study antimicrobial resistance. Nature Reviews Genetics. 2019;20(6):356-370. DOI: 10.1038/s41576-019-0108-4

[89] Giwa AS, Ali N, Athar MA, Wang K. Dissecting microbial community structure in sewage treatment plant for pathogens' detection using metagenomic sequencing technology.

Archives of Microbiology. 2020 May;202(4):825-833. DOI: 10.1007/s00203-019-01793-y

[90] Garmaeva S, Sinha T, Kurilshikov A, Fu J, Wijmenga C, Zhernakova A. Studying the gut virome in the metagenomic era: challenges and perspectives. BMC Biology. 2019 Oct 28;17(1):84. DOI: 10.1186/s12915-019-0704-y

[91] Li X. Metagenomic screening of microbiomes identifies pathogen-enriched environments. Environmental Sciences Europe. 2019 Dec;31(1):37. DOI: 10.1186/s12302-019-0217-x

[92] Tupinambá DD, Cantão ME, Costa OYA, Bergmann JC, Kruger RH, Kyaw CM, et al. Archaeal Community Changes Associated with Cultivation of Amazon Forest Soil with Oil Palm. Archaea. 2016 Feb 24;2016:3762159. DOI: 10.1155/2016/3762159

[93] Alteio LV, Schulz F, Seshadri R, Varghese N, Rodriguez-Reillo W, Ryan E, et al. Complementary metagenomic approaches improve reconstruction of microbial diversity in a forest soil. mSystems. 2020 Mar 10;5(2). DOI: 10.1128/mSystems.00768-19

[94] Liu X-F, Liu C-J, Zeng X-Q, Zhang H-Y, Luo Y-Y, Li X-R. Metagenomic and metatranscriptomic analysis of the microbial community structure and metabolic potential of fermented soybean in Yunnan Province. fst. 2020 Mar;40(1):18-25. DOI: 10.1590/fst.01718

[95] Prodan A, Tremaroli V, Brolin H, Zwinderman AH, Nieuwdorp M, Levin E. Comparing bioinformatic pipelines for microbial 16S rRNA amplicon sequencing. PLoS One. 2020 Jan 16;15(1):e0227434. DOI: 10.1371/journal.pone.0227434

[96] Fadiji AE, Babalola OO. Metagenomics methods for the study of plant-associated microbial communities: A review. J Microbiol Methods. 2020 Mar;170:105860. DOI: 10.1016/j.mimet.2020.105860

[97] Bandla A, Pavagadhi S, Sridhar Sudarshan A, Poh MCH, Swarup S. 910 metagenome-assembled genomes from the phytobiomes of three urban-farmed leafy Asian greens. Scientific Data - Nature. 2020 Aug 25;7(1):278. DOI: 10.1038/s41597-020-00617-9

[98] Pascale A, Proietti S, Pantelides IS, Stringlis IA. Modulation of the root microbiome by plant molecules: the basis for targeted disease suppression and plant growth promotion. Frontiers in Plant Science. 2019;10:1741. DOI: 10.3389/fpls.2019.01741

[99] Chen S, Harmon A.C. Advances in plant proteomics. Proteomics. 2006; 6(20), 5504-5516. DOI:10.1002/pmic.200600143

[100] Kosová K, Vítámvás P, Prášil IT, Renaut J. Plant proteome changes under abiotic stress—contribution of proteomics studies to understanding plant stress response. Journal of proteomics. 2011;74(8), 1301-1322. DOI: 10.1016/j.jprot.2011.02.006

[101] Quirino BF, Candido ES, Campos PF, Franco OL, Krüger RH. Proteomic approaches to study plant–pathogen interactions. Phytochemistry. 2010;71(4), 351-362. DOI: https://doi.org/10.1016/j.phytochem.2009.11.005

[102] Alam I, Lee DG, Kim KH, Park CH, Sharmin SA, Lee H, ... & Lee, B. H. (2010). Proteome analysis of soybean roots under waterlogging stress at an early vegetative stage. Journal of Biosciences, 35(1), 49-62. DOI: 10.1007/s12038-010-0007-5

[103] Nakazono M, Tsuji H, Li Y, Saisho D, Arimura SI, Tsutsumi N, Hirai A. Expression of a gene encoding mitochondrial aldehyde dehydrogenase in rice increases under submerged

conditions. Plant Physiology. 2000;124(2), 587-598. DOI: 10.1104/pp.124.2.587

[104] Nakabayashi R, Saito K. Metabolomics for unknown plant metabolites. Analytical and bioanalytical chemistry. 2013;405(15), 5005-5011. DOI: 10.1007/s00216-013-6869-2

CAPÍTULO II – ARTIGO 1

"Molecular Interplay between Non-Host Resistance, Pathogens and Basal Immunity as a Background for Fatal Yellowing in Oil Palm (Elaeis guineensis Jacq.) Plants"

Autores: Cleiton Barroso Bittencourt, Thalliton Luiz Carvalho da Silva, Jorge Cândido Rodrigues Neto, André Pereira Leão, José Antônio de Aquino Ribeiro, Aline de Holanda Nunes Maia, Carlos Antônio Ferreira de Sousa, Betania Ferraz Quirino e Manoel Teixeira Souza Júnior.

Publicado no Periódico *International Journal of Molecular Sciences*
https://doi.org/10.3390/ijms241612918
Volume 24(16): 12918. doi: 10.3390/ijms241612918, Agosto, 2023.

International Journal of
Molecular Sciences

MDPI

Article

Molecular Interplay between Non-Host Resistance, Pathogens and Basal Immunity as a Background for Fatal Yellowing in Oil Palm (*Elaeis guineensis* Jacq.) Plants

Cleiton Barroso Bittencourt [1], Thalliton Luiz Carvalho da Silva [1], Jorge Cândido Rodrigues Neto [2], André Pereira Leão [2], José Antônio de Aquino Ribeiro [2], Aline de Holanda Nunes Maia [3], Carlos Antônio Ferreira de Sousa [4], Betania Ferraz Quirino [2] and Manoel Teixeira Souza Júnior [1,2,*]

[1] Graduate Program of Plant Biotechnology, Federal University of Lavras, Lavras 37203-202, MG, Brazil; cleiton_court@hotmail.com (C.B.B.); thallitons@gmail.com (T.L.C.d.S.)
[2] The Brazilian Agricultural Research Corporation, Embrapa Agroenergy, Brasília 70770-901, DF, Brazil; jorgecrn@hotmail.com (J.C.R.N.); andre.leao@embrapa.br (A.P.L.); jose.ribeiro@embrapa.br (J.A.d.A.R.); betania.quirino@embrapa.br (B.F.Q.)
[3] The Brazilian Agricultural Research Corporation, Embrapa Environment, Jaguarina 13918-110, SP, Brazil; aline.maia@embrapa.br
[4] The Brazilian Agricultural Research Corporation, Embrapa Mid-North, Teresina 64008-780, PI, Brazil; carlos.antonio@embrapa.br
* Correspondence: manoel.souza@embrapa.br

Abstract: An oil palm (*Elaeis guineensis* Jacq.) bud rod disorder of unknown etiology, named Fatal Yellowing (FY) disease, is regarded as one of the top constraints with respect to the growth of the palm oil industry in Brazil. FY etiology has been a challenge embraced by several research groups in plant pathology throughout the last 50 years in Brazil, with no success in completing Koch's postulates. Most recently, the hypothesis of having an abiotic stressor as the initial cause of FY has gained ground, and oxygen deficiency (hypoxia) damaging the root system has become a candidate for stress. Here, a comprehensive, large-scale, single- and multi-omics integration analysis of the metabolome and transcriptome profiles on the leaves of oil palm plants contrasting in terms of FY symptomatology—asymptomatic and symptomatic—and collected in two distinct seasons—dry and rainy—is reported. The changes observed in the physicochemical attributes of the soil and the chemical attributes and metabolome profiles of the leaves did not allow the discrimination of plants which were asymptomatic or symptomatic for this disease, not even in the rainy season, when the soil became waterlogged. However, the multi-omics integration analysis of enzymes and metabolites differentially expressed in asymptomatic and/or symptomatic plants in the rainy season compared to the dry season allowed the identification of the metabolic pathways most affected by the changes in the environment, opening an opportunity for additional characterization of the role of hypoxia in FY symptom intensification. Finally, the initial analysis of a set of 56 proteins/genes differentially expressed in symptomatic plants compared to the asymptomatic ones, independent of the season, has presented pieces of evidence suggesting that breaks in the non-host resistance to non-adapted pathogens and the basal immunity to adapted pathogens, caused by the anaerobic conditions experienced by the plants, might be linked to the onset of this disease. This set of genes might offer the opportunity to develop biomarkers for selecting oil palm plants resistant to this disease and to help pave the way to employing strategies to keep the safety barriers raised and strong.

Keywords: bud rot; hypoxia; molecular plant biology; pathogen; palm oil; fatal yellowing; molecular mechanisms; transcriptomics; metabolomics; multi-omics; non-host resistance; immunity

Citation: Bittencourt, C.B.; Carvalho da Silva, T.L.; Rodrigues Neto, J.C.; Leão, A.P.; de Aquino Ribeiro, J.A.; Maia, A.d.H.N.; de Sousa, C.A.F.; Quirino, B.F.; Souza Júnior, M.T. Molecular Interplay between Non-Host Resistance, Pathogens and Basal Immunity as a Background for Fatal Yellowing in Oil Palm (*Elaeis guineensis* Jacq.) Plants. *Int. J. Mol. Sci.* **2023**, *24*, 12918. https://doi.org/10.3390/ijms241612918

Academic Editor: Jozef Kovacik

Received: 18 July 2023
Revised: 8 August 2023
Accepted: 13 August 2023
Published: 18 August 2023

1. Introduction

Throughout the last decade, oil palm (*Elaeis guineensis* Jacq.) has been the source of the most consumable vegetal oils on the planet [1]. Palm oil and palm kernel oil increased

in consumption from 64 to approximately 85 million metric tons between the 2013/14 and 2022/23 seasons. In the top oil palm production countries, the palm oils yield an average of four metric tons per hectare, far better than soybean, canola, peanuts, and other known oilseed crops in terms of oil yield [2,3]. Indonesia, Malaysia, Nigeria, Thailand, and Colombia are the top five countries in the world in terms of oil palm harvested area [3].

Brazil has about 200,000 hectares harvested with oil palm nowadays, even though there are over seven million hectares of preferential area for oil palm cultivation in the so-called Legal Amazon Area, an area of more than five million square kilometers comprising nine states, and larger than the Amazon biome itself [4]. In 2010, a Sustainable Palm Oil Production Program was launched that aimed to strengthen the palm oil industry in the country. Such program had as guidelines: (a) the protection of the environment, the conservation of biodiversity, and the rational use of natural resources; (b) the respect for the social function of property; (c) the expansion of oil palm cultivation exclusively in areas already occupied by man; (d) encouraging cultivation to recover degraded areas; (e) social inclusion; and (f) the environmental regularization of rural properties [5]. More than a decade after launching that program, the problem of FY study is very real, especially in Brazil.

A closer look at the reasons behind the failure to succeed in this endeavor will reveal a complex and multi-factor scenario where the Fatal Yellowing (FY) disease, a bud rod disorder of unknown etiology, is one of the top constraints affecting the growth of the oil palm industry in the country [6]. FY symptoms initiate with the yellowing of the leaflets at the base of the intermediate leaves and progress to necrosis of the edges, which spreads to the other leaves. Subsequently, necrosis and dryness of the spear leaf occur, which evolves towards the meristem region, causing decay and culminating in the death of the oil palm plant. Generally, symptoms progress to oil palm death in a few months (acute form) to three years (chronic) [7,8].

The etiology of FY has been a challenge embraced by several research groups in plant pathology throughout the last 50 years, with no success in completing Koch's third postulate—inoculation of a healthy plant with the cultured microorganism must recapitulated the disease [6]. Furthermore, the exponential growth of cases and the undefined pattern of spread of the disease weaken a possible biotic primary cause [9]. Most recently, the hypothesis of having an abiotic stressor as the initial cause of FY has gained ground [6]. Silveira et al. [10] showed surface compaction of the soils in the area where FY occurs. This condition can lead to soil saturation with water where oxygen deficiency (hypoxia) possibly damages the root system. An imbalance of nutrients such as Copper, Iron, Manganese, and Zinc has been suggested as a possible cause [11]. Silveira et al. [10] found that the evolution of FY symptoms was more pronounced when there was a reduction in Boron and Copper in the soil. On the other hand, the application of iron sulfate in the study conducted by Viégas et al. [11] ruled out Fe deficiency being involved. Muniz [12] reaffirms the same, and also observed that poor aeration reduces the redox potential of the soil, increasing the concentration of reduced ions, such as Fe^{3+}, NO^{3+}; Mn^{3+}, predisposing oil palm to toxicity (abiotic effect) and leaving it vulnerable to opportunistic pathogen attacks (biotic effect).

Recent studies using single omics analysis (SOA), such as genomics/meta-genomics, transcriptomics/meta-transcriptomics, proteomics/meta-proteomics, metabolomics, epigenomics, ionomics, and phenomics, have shown that these new techniques can take the etiological studies regarding FY in oil palm to another level [13–15]. Costa et al. [13] used a metagenomics approach to rule out the hypothesis that *Phytophthora palmivora* could be the causal agent of FY in Brazil, as has been shown to be the case for Pudricion del Cogollo in Colombia, a disease characterized by the rotting of all the new tissues, preserving the leaves that were formed before infection. This oomycetes is responsible for the first symptoms, and opens doors for several opportunistic pathogens that promote the intensification of the rotting [16,17]. Rodrigues-Neto et al. [14] applied untargeted metabolomics analysis to characterize the leaves of FY asymptomatic and symptomatic oil palm plants, and identified two metabolites (glycerophosphorylcholine and 1,2-dihexanoyl-

sn-glycero-3-phosphoethanolamine) with no known direct relation to plant stress, and which are presented as potential biomarkers. Nascimento et al. [15], used a proteomics approach to describe protein alterations associated with FY in oil palm roots, and found enzymes that suggested an anaerobic condition before or during FY. According to [15], their finding suggests that changes in abiotic factors may precede the occurrence of FY, paving the way for opportunistic pathogens.

In the present study, we carried out a comprehensive, large-scale, single- (SOA) and multi-omics integration (MOI) analysis of the metabolome and transcriptome profiles on the leaves of oil palm plants contrasting in terms of FY symptomatology—asymptomatic and symptomatic—and collected in two distinct seasons—dry and rainy. We also performed an analysis of leaf chemical and soil physicochemical composition. The initial goals of such a study were to obtain insights into the possible occurrence and role of oxygen deficiency (hypoxia) in the onset of FY and to search for molecular symptoms (gene- and metabolic pathway-based) that could reveal opportunities for genetic control of this disease of unknown etiology.

2. Results

2.1. Soil Physicochemical and Leaf Chemical Analysis

In Figure 1, to facilitate the understanding, a design of this study is presented. Figure 2 and Table S2 summarize the results of the ionomics analysis of the soil and oil palm leaves collected in the dry period (DP) and wet period (WP). Asymptomatic and symptomatic plants were compared within each period and between periods.

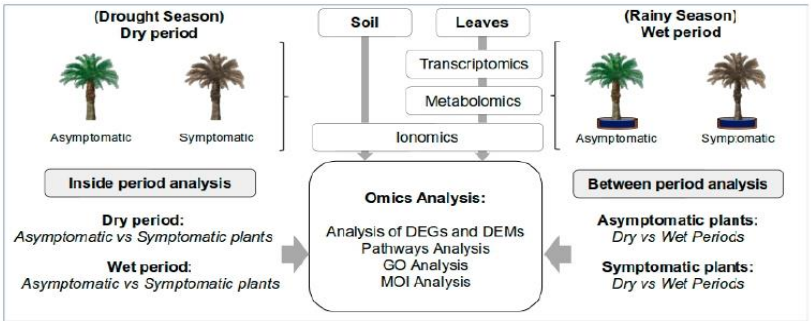

Figure 1. Experimental design for sample collection, and the general work-flow of the strategy of the analysis carried out in four scenarios—symptomatic vs. asymptomatic in the dry period; symptomatic vs. asymptomatic in the wet period; wet vs. dry period in symptomatic plants; and wet vs. dry in asymptomatic ones.

In the soil, Carbon, Chlorine, Sodium, Phosphorus, and Zinc showed significant differences ($p \leq 0.05$) between FY asymptomatic and symptomatic plants in the DP, with all showing reduced values in the DP. In soils sampled in the WP, only Calcium and Zinc showed significant differences $p \leq 0.05$), with increased amounts in the symptomatic plants. Soil organic matter and pH showed significant ($p \leq 0.05$) lower values in samples from symptomatic plants in the DP but not in the WP. On the other hand, cationic exchange capacity, acidity, and clay showed significant ($p \leq 0.05$) lower values in soil samples from symptomatic plants. Finally, Ca/CEC (cation-exchange capacity) and K/CEC showed higher values in soil samples from symptomatic plants.

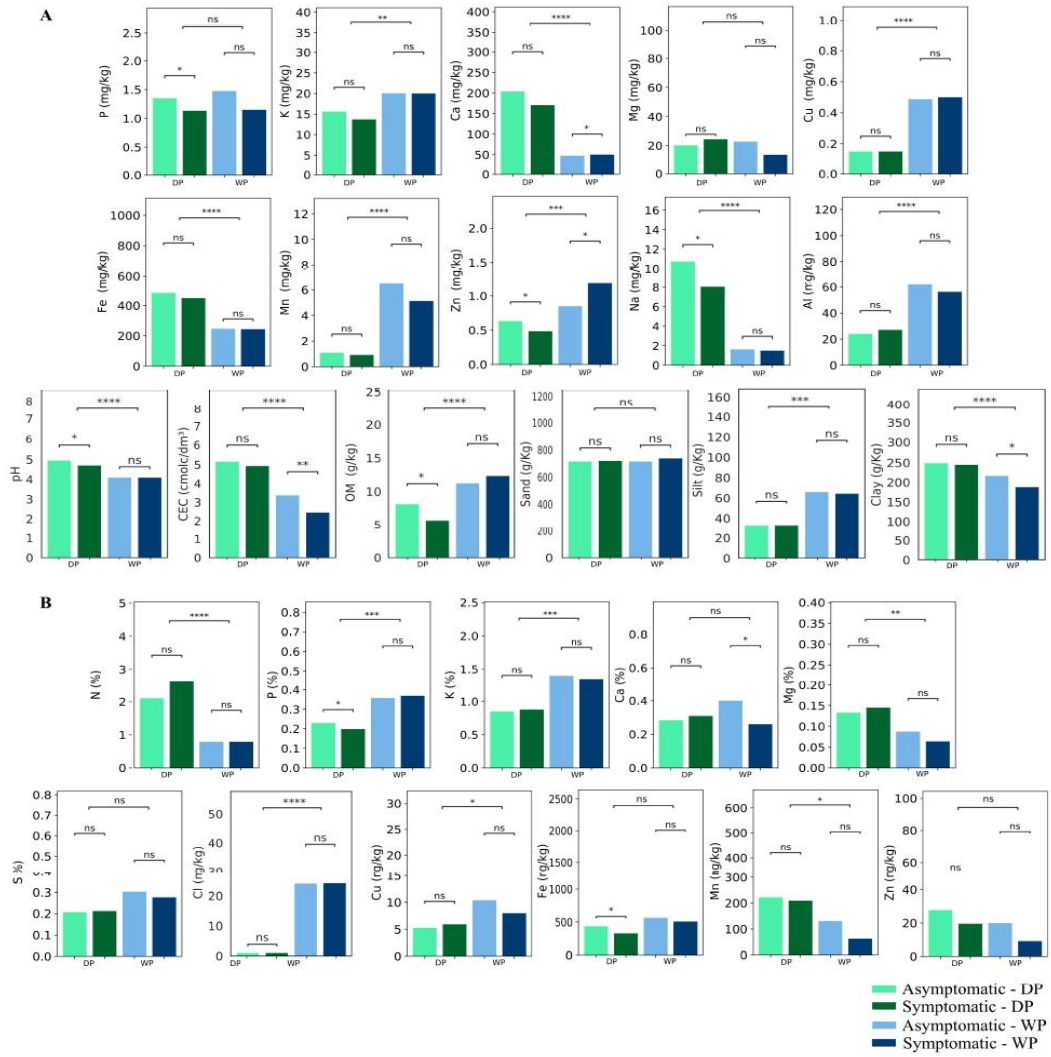

Figure 2. Physical–chemical characteristics of the soil (**A**) and chemical from the leaves (**B**) of FY asymptomatic and symptomatic oil palm plants sampled in two time-points: Dry period—DP and Wet period—WP. The ns means non-significant. The asterisks indicate a significant difference between the two groups (*t*-test). * $p \leq 0.05$; ** $p \leq 0.01$; *** $p \leq 0.001$; **** $p \leq 0.0001$.

When comparing the soil samples collected in DP and WP conditions, K, Ca, Cu, Fe, Mn, Zn, Na, Al, pH, CEC, OM, silt, and clay showed significantly distinct values ($p \leq 0.05$). K, Cu, Mn, Zn, Al, OM, and silt showed higher values in WP conditions, while Ca, Fe, Na, pH, CEC, and clay showed lower values in that condition (Figure 2 and Table S2).

In the case of the leaves from FY asymptomatic and symptomatic oil palm plants in the DP, only Phosphorus and Iron showed significantly distinct values ($p \leq 0.05$), lower in the latter plants. Meanwhile, Calcium was the only element showing a different (and lower)

value in the symptomatic plants in the WP. When comparing the leaf samples collected in DP and WP conditions, N, P, K, Mg, Cl, Cu, and Mn showed significantly distinct values ($p \leq 0.05$), with N, Mg, and Mn being lower in WP, and P, K, Cl, and Cu higher (Figure 2 and Table S2).

A principal component analysis (PCA) was performed, revealing the clustering of micro- and macro-nutrients from soil and leaf samples, as well as soil complex and granulometry, accordingly to the collection period (Figure 3). When performing PCA within each period, no clustering of FY asymptomatic and symptomatic plant groups appeared (Figure S1).

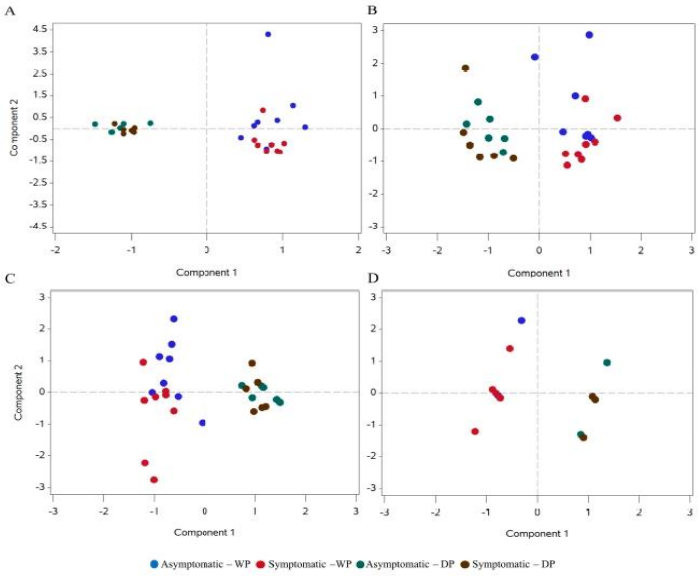

Figure 3. Principal component analysis (PCA) of the micro− and macro−nutrients from soil (**A**) and leaves (**B**), assorted complex (**C**) and granulometry (**D**) including all samples of FY asymptomatic and symptomatic oil palm plants sampled in Dry and Wet period.

2.2. Metabolomics Analysis

The Statistical Analysis module of the MetaboAnalyst 5.0 returned 1924, 576, 2469, and 272 peaks for the positive and negative polar and lipidic fractions, respectively, when using the dry period (DP) samples. There were 29 peaks differentially expressed in the positive polar fraction, and 22 in the negative polar fraction. Regarding the lipidic fractions, 29 and 9 were differentially expressed in the positive and negative ones, respectively. Accordingly to the Functional Analysis module of the MetaboAnalyst 5.0, 89 differentially expressed peaks are below the minimal number for functional interpretation using the combined meta-analysis of the mummichog and GSEA pathways. However, when using false discovery rate (FDR) ≤ 0.06, the number of differentially expressed peaks rose to 121, above the minimal number necessary for the functional interpretation analysis. In this case, it was possible to identify 15 differentially expressed metabolites (DEMs) with FDR ≤ 0.05 (Table 1).

Table 1. List of metabolites identified in the leaves of oil palm affected by fatal yellowing in the dry period, after submitting the differentially expressed (DE) peaks to the pathway topology analysis module in MetaboAnalyst 5.0. FDR: False Discovery Rate; FC: Fold Change.

Query Mass	Matched Compound	Matched Form	Mass Diff	Compound Name	Log_2(FC)	FDR	Profile
792.12440	C00024	M-H_2O+H[1+]	1.95×10^{-3}	Acetyl-CoA	−5.37	0.0004	Down
742.22112	C03541	M+K[1+]	2.18×10^{-3}	THF-polyglutamate	−5.17	0.0012	Down
293.21349	C06427	M-H+O[-]	1.28×10^{-3}	alpha-Linolenic acid	−1.11	0.0026	Down
312.16523	C16448	M-$C_3H_4O_2$+H[1+]	1.43×10^{-3}	Dihydrozeatin-O-glucoside	1.93	0.0111	Up
836.28348	C05275	M-HCOOK+H[1+]	2.18×10^{-3}	trans-Dec-2-enoyl-CoA	−2.53	0.0220	Down
409.38261	C01054	M-H_2O+H[1+]	2.33×10^{-4}	(S)-2,3-Epoxysqualene	−4.13	0.0305	Down
425.37851	C22116	M-HCOOH+H[1+]	6.34×10^{-4}	3beta-Hydroxy-4beta	−2.62	0.0305	Down
309.20812	C04785	M-H[-]	9.86×10^{-4}	(9Z,11E,15Z)-(13S)-Hydroperoxyoctadeca-9,11,15-trienoate	−1.33	0.0346	Down
361.20077	C18016	M+HCOO[-]	7.15×10^{-4}	3beta-Hydroxy-9beta-pimara-7,15-diene-19,6beta-olide	−1.20	0.0346	Down
426.38263	C22121	M(C13)+H[1+]	1.45×10^{-3}	Cycloeucalenone	−2.26	0.0359	Down
407.36819	C03313	M-HCOOH+H[1+]	8.83×10^{-4}	Phylloquinol	−1.90	0.0372	Down
87.00852	C00258	M-H_2O-H[-]	2.12×10^{-4}	D-Glycerate	0.75	0.0384	Up
446.16191	C00101	M(Cl37)-H[-]	1.00×10^{-3}	Tetrahydrofolate	−0.64	0.0398	Down
129.01926	C06032	M-H_2O-H[-]	3.35×10^{-5}	D-erythro-3-Methylmalate	1.00	0.0401	Up
173.00911	C00311	M-H_2O-H[-]	1.61×10^{-5}	Isocitrate	1.00	0.0447	Up

In the case of the wet period (WP) samples, the ultra-high performance liquid chromatography and tandem mass spectrometry (UHPLC–MS/MS) statistical analysis returned 1976, 771, 2824, and 461 chromatography peaks for the positive and negative polar and lipidic fractions, respectively. None of them presented differentially expressed peaks using the statistical analysis criteria (FDR ≤ 0.05). When applying the principal component analysis (PCA) to detect any inherent patterns within the data in the DP and WP samples, one could not completely separate the groups between the asymptomatic and the symptomatic plants in all fractions analyzed (Figure S2).

When looking for DEMs between FY asymptomatic oil palm plants from DP and WP, the statistical analysis returned 2267, 836, 2675, and 487 chromatography peaks for the positive and negative polar and lipidic fractions, respectively. Altogether, 2749 differentially expressed chromatography peaks were identified among the asymptomatic plants and subjected to functional interpretation via analysis in the Functional Analysis module of MetaboAnalyst 5.0 (see Section 4), and the combined meta-analysis of the mummichog and GSEA pathways resulted in a list of 303 DEMs (Supplementary Table S3). Likewise, for the FY symptomatic plants from DP and WP, the statistical analysis returned 2259, 789, 2549, and 487 peaks for the positive and negative polar and lipidic fractions, respectively. Altogether, 2446 differentially expressed peaks were identified among the symptomatic plants, and subjected to functional interpretation as before, resulting in a list of 259 DEMs (Table S4). These two groups of DEMs had 179 metabolites in common (Table S5), while their behavior in the asymptomatic and symptomatic oil palm plants showed a very weak positive correlation (Figure 4).

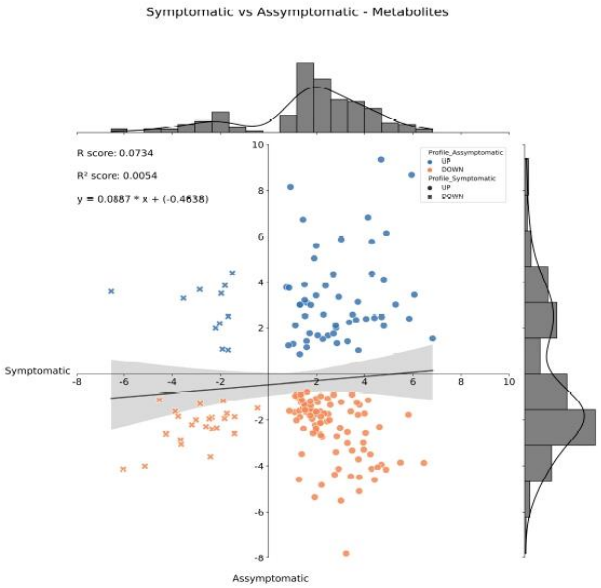

Figure 4. Histogram and correlation analysis of the Log_2(FC) of common differentially expressed metabolites from Dry vs. Wet periods of FY asymptomatic and symptomatic plants by pairwise comparison. Dots represent metabolites positively regulated in FY symptomatic plants; x's represent metabolites negatively regulated in FY asymptomatic plants. Blue dots and x's represent metabolites positively regulated in FY symptomatic plants, and orange dots and x's represent metabolites negatively regulated under FY asymptomatic plants. FC = Fold Change.

2.3. Transcriptomics Analysis

When comparing the leaf transcriptome of asymptomatic and symptomatic plants collected in the dry period, 274 proteins were differentially expressed (DEPs) when using an FDR ≤ 0.05, and an FC $\neq 1$, with 103 upregulated and 171 downregulated. In the wet period, the number of DEPs increased to 1087, with 456 upregulated and 631 downregulated. That amount of differentially expressed proteins—274 and 1087—correspond, respectively, to just 0.63% and 2.50% of all 43,551 proteins present in the reference genome of E. guineensis (Singh et al., 2013). A group of 70 DEPs appeared in both DP and WP, and a correlation analysis was performed to compare their expression profiles under two scenarios, allowing the visualization of 56 proteins with similar expression profiles in the leaves of oil palm plants due to the FY disease, independently of whether it was the dry or wet period (Figure 5).

On the other hand, when comparing the leaf transcriptome of asymptomatic plants in both periods, 6058 proteins were differentially expressed when using an FDR ≤ 0.05, and an FC $\neq 1$, with 3071 upregulated and 2987 downregulated. Likewise, when comparing the leaf transcriptome of symptomatic plants in both periods, the number of DEPs was 5426, 2781 upregulated, and 2645 downregulated. A group of 3806 DEPs appeared in both the asymptomatic and symptomatic plants, and a correlation analysis was performed to compare their expression profiles under the two scenarios studied, showing a strong positive correlation (Figure 6). Such transcriptomics results show that the leaf transcriptome of oil palm plants becomes more affected by the change in the environment—from the dry to rainy seasons—than by the presence of the FY disease. Meanwhile, the disease effects were more prevalent in the WP compared to the DP.

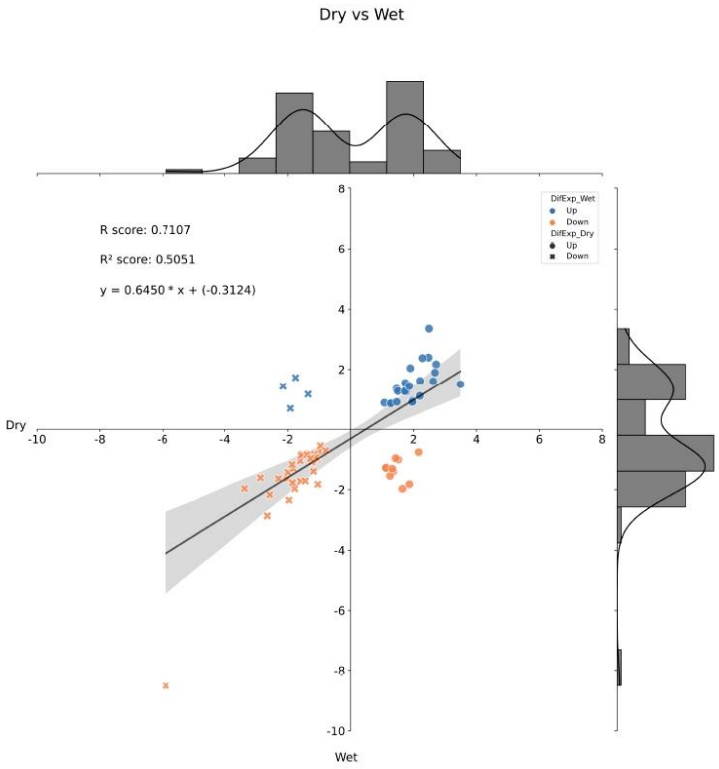

Figure 5. Histogram and correlation analysis of the Log_2(FC) of common differentially expressed metabolites by pairwise comparison from Dry and Wet periods of FY asymptomatic vs. symptomatic analysis. Dots represent metabolites positively regulated in the Dry period; x's represent metabolites negatively regulated in the Wet period. Blue dots and x's represent metabolites positively regulated under the Dry period, and orange dots and x's represent metabolites negatively regulated in the Wet period. FC = Fold Change.

After removing the 3806 DEPs that appeared in both the asymptomatic and symptomatic plants from the above-mentioned group of 5426 ones, a set of 1620 that appeared only in the symptomatic plants underwent gene ontology analyses. This set represents those genes/proteins affected by the change from the dry to rainy season, but only in the FY symptomatic plants; there was a direct link between the disease and the environment. In terms of enzyme category, the two most prevalent groups of enzymes were transferases and hydrolases, followed by translocases and oxidoreductases (Figure 7A). In the case of biological process (BP), protein phosphorylation and regulation of transcription, both had approximately 80 positive hits. Protein, ATP, and RNA binding were the most prevalent molecular functions (MF), in that order. Finally, in terms of cellular component (CC), membrane had almost 700 positive hits all together (Figure 7B).

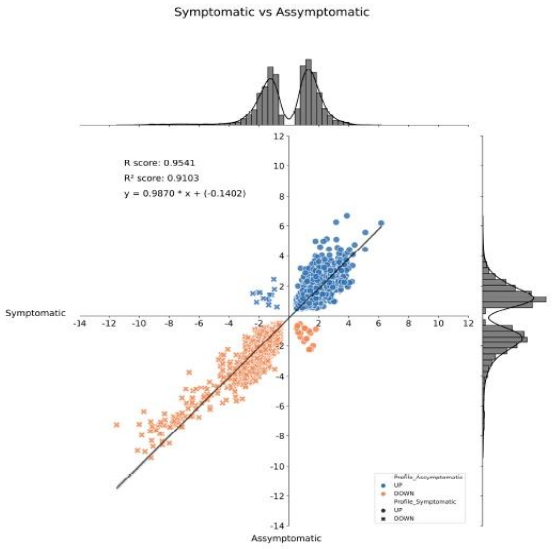

Figure 6. Histogram and correlation analysis of the Log_2(FC) of common differentially expressed genes by pairwise comparison from Dry vs. Wet periods of FY asymptomatic and symptomatic analysis. Dots represent genes positively regulated in FY symptomatic plants; x's represent genes negatively regulated in FY asymptomatic plants. Blue dots and x's represent metabolites positively regulated in FY symptomatic plants, and orange dots and x's represent metabolites negatively regulated in FY asymptomatic plants. FC = Fold Change.

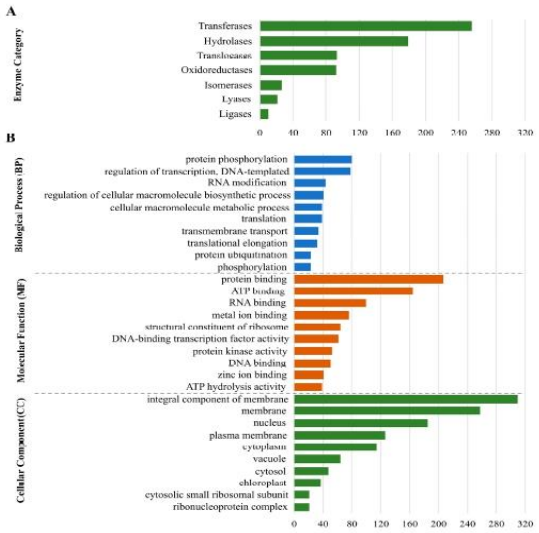

Figure 7. Amount of full-length transcripts present only in FY-affected oil palm based on Gene Ontology (GO) annotation from 1602 differential expresses genes/proteins that appear only in FY symptomatic oil palm plants; enzyme classification (**A**) and biological process, molecular function, and cellular component (**B**). Only the ten most populated groups per GO term are shown.

2.4. Multi-Omics Integration Analysis

The MOI analysis was employed three times in this study. First, it integrated DEMs and DEPs identified when comparing symptomatic and asymptomatic plants within an specific scenario—dry period or wet period. Here, 15 DEMs and 30 differentially expressed enzymes (out of the 274 DEPs identified when evaluating the differences between symptomatic and asymptomatic plants in the dry period) underwent integration using the Omics Fusion platform. The results revealed that two pathways had five or more of those enzymes differentially expressed; they were Carbon fixation pathways in prokaryotes (p00720) and Methane metabolism (map00680), both with two DEPs and three DEMs. On the other hand, as there were no DEMs identified in the wet period, only the 51 differentially expressed enzymes (out of the 1.087 DEPs identified when evaluating the differences between symptomatic and asymptomatic plants in the wet period) were analyzed using the above-cited platform. The results revealed Glycolysis/Gluconeogenesis (map00010) as the only pathway with five differentially expressed enzymes.

Then, in a second moment, MOI was employed to integrate 96 enzymes—found among the 1620 DEPs that appeared only in the symptomatic plants and underwent gene ontology analyses—and the 80 DEMs present only in symptomatic plants when comparing WP and DP. The results revealed three pathways with ten or more enzymes and metabolites differentially expressed; they were Glycolysis/Gluconeogenesis (map00010), Methane metabolism (map00680), and Cysteine and methionine metabolism (map00270), respectively, with 12, 10, and 10 features (Table 2).

Table 2. List of the pathways most affected in symptomatic plants, or in both symptomatic and asymptomatic plant at once, obtained via Multi-Omics Integration (MOI) using Omics Fusion, and with 10 or more enzymes and metabolites common to both phenotypes.

Pathway	Pathway ID	Common (Symptomatic and Asymptomatic)			Only in Symptomatic		
		Enzymes & Metabolites	Enzymes	Metabolites	Enzymes & Metabolites	Enzymes	Metabolites
Purine metabolism	230	32	15	17	9	4	5
Porphyrin and chlorophyll metabolism	860	29	10	19	4	3	1
Phenylpropanoid biosynthesis	940	20	4	16	4	2	2
Starch and sucrose metabolism	500	19	17	2	5	4	1
Glycolysis/Gluconeogenesis	10	17	14	3	12	9	3
Carbon fixation pathways in prokaryotes	720	17	5	12	8	2	6
Cysteine and methionine metabolism	270	16	8	8	10	7	3
Ubiquinone and other terpenoid-quinone biosynthesis	130	16	2	14	5	1	4
Pentose phosphate pathway	30	15	9	6	8	5	3
Aminoacyl-tRNA biosynthesis	970	14	12	2	3	3	0
Methane metabolism	680	14	8	6	10	7	3
Glyoxylate and dicarboxylate metabolism	630	14	7	7	5	3	2
Pyruvate metabolism	620	13	8	5	7	5	2
Glycerophospholipid metabolism	564	12	10	2	5	4	1
Glutathione metabolism	480	12	7	5	7	5	2
Citrate cycle (TCA cycle)	20	12	7	5	4	3	1
Glycine, serine and threonine metabolism	260	12	7	5	4	3	1
Galactose metabolism	52	11	6	5	5	4	1
Pyrimidine metabolism	240	11	4	7	4	1	3
Carotenoid biosynthesis	906	11	0	11	6	0	6
Flavonoid biosynthesis	941	11	0	11	4	0	4
Amino sugar and nucleotide sugar metabolism	520	10	9	1	5	4	1
Carbon fixation in photosynthetic organisms	710	10	7	3	7	5	2

Table 2. *Cont.*

Pathway	Pathway ID	Common (Symptomatic and Asymptomatic)			Only in Symptomatic		
		Enzymes & Metabolites	Enzymes	Metabolites	Enzymes & Metabolites	Enzymes	Metabolites
Sulfur metabolism	920	10	6	4	4	1	3
Terpenoid backbone biosynthesis	900	10	5	5	4	2	2
Steroid biosynthesis	100	10	1	9	8	1	7
Biosynthesis of various secondary metabolites—part 2	998	10	0	10	2	0	2

Finally, the group of 5426 DEPs present in the symptomatic plants, and that also including the 3806 DEPs present in the asymptomatic ones, underwent analysis for enzyme selection—there were 320 enzymes—and subsequent integration with the 259 above-mentioned DEMs. In Table 2, a list of 27 metabolic pathways affected only in symptomatic plants, or in both the asymptomatic and symptomatic plants at once, by the change of season—from dry to rainy—is presented. Three pathways had 20 or more enzymes and metabolites differentially expressed; they were Purine metabolism (map00230), Porphyrin and chlorophyll metabolism (map00860), and Phenylpropanoid biosynthesis (map00940), respectively, with 32, 29, and 20 enzymes and metabolites.

3. Discussion

Throughout the 50 years since this disease first appeared in Brazil, several initiatives in Brazil and abroad tried to elucidate the etiology of this disease. Not a single one was able to fulfill Koch's third postulate. With no knowledge about the causal agent(s), nothing was done to develop a diagnostic system or a control measure. For those interested in knowing more about this disease, we encourage you to read [6].

The initial goal of this study was to obtain insights into the possible occurrence and role of oxygen deficiency (hypoxia) in the onset of FY. In that sense, the results showed that the soil underwent much more profound changes in its physicochemical attributes as a function of the season—the change from the dry to rainy season—than as a function of the cultivation of oil palm plants symptomatic or asymptomatic for FY. In the rainy season, the wet soil increased the availability of K, Cu, Mn, Zn, and Al, while decreasing the availability of Ca, Fe, and Na. Concomitantly, it caused a reduction in the pH, clay contents, and cation-exchange capacity, in addition to an increase in the organic matter.

The increase in the availability of cationic micronutrients (Cu, Mn, Zn) and Al in the wet soil, in general, may be related to the decrease in pH. It is known that the lower the soil pH, the greater the availability of cationic micronutrients. Soil pH dropped from a value close to 5.0 (dry period) to 4.1 (wet period). With excess water in the soil, in addition to K, an increase in the availability of other bases, such as Ca and Mg, was expected. However, we saw a decrease in Ca, Fe, and Na, while Mg did not change. The drop in pH may have affected the availability of Ca, Mg, and Na. It is also necessary to consider the changes that occur with the alternation between aerobic and anaerobic conditions, which is reflected in the oxide reduction potential of the soil. For example, organic matter breakdown is slower under anaerobic conditions than under aerobic conditions [18]. And effectively, organic matter increased in the wet period in the oil palm field that supplied the samples for the present study. Additionally, much of the Fe^{2+} formed during reductive dissolution is likely to have been chelated with soil organic matter and, possibly, eluted from the soil; some will have been held by cation exchange in the constituent clay minerals [19].

In summary, the differences in physicochemical attributes of the soil where the sampled oil palm plants grew did not justify the difference in phenotypes—symptomatic and asymptomatic regarding FY—and the same was true for the chemical attributes of the leaves from such plants. So, independently of whether the plants were under hypoxia due to excessive rain and soil waterlogging, no differences regarding leaves and soil attributes

justified the distinct FY phenotypes seen among the plants sampled for this study. Would that be different in the leaf metabolome?

Surprisingly, only 15 differentially expressed metabolites (DEM) appeared between symptomatic and asymptomatic plants in the dry period. In the wet period, it was even worst, with no DEM found when using FDR ≤ 0.05 as the statistical analysis criteria. In synthesis, the metabolomes from the leaves of oil palm plants did not present pathways highly affected by the disease. The same was not true for those cases where the metabolomes were from plants with the same phenotype but at different seasons. Here, it was possible to select 80 metabolites that only differentially expressed in the symptomatic plants, not in the asymptomatic; and those metabolites allowed the identification of four pathways affected in sick plants by the rainy season; they were Steroid biosynthesis (map00100), Carbon fixation pathways in prokaryotes (p00720), Carotenoid biosynthesis (map00906), and Purine metabolism (map00230). Such pathways represent a direct link between the disease and the environment and might help to understand, at the molecular level, the intensification of the FY symptoms seen in the leaves in the rainy season. It is common sense that in the rainy season, the visual FY symptoms intensify (Denpasa's staff—Dendê do Pará S/A company—www.denpasa.com.br (accessed on 30 June 2023), personal communication).

As mentioned in Bittencourt et al. [20], untargeted metabolomics allows the search for novel metabolic perturbations in various biological systems. However, as seen in the present study, when using the profile of hundreds or thousands of peaks with varying chemical properties, just a few dozen metabolites are identified. The reasons behind this are the still limited capacity to identify novel compounds of interest and the need for advanced and more robust databases [21]. Would that be different in the leaf transcriptome?

RNA-Seq uses deep-sequencing technologies to characterize the transcriptome profiling of a cell, a tissue, an organ, or even the entire organism, and provides a far more precise measurement of levels of transcripts and their isoforms than any other methods [22]. Accordingly to Wang et al. [22], characterizing the transcriptome allows us to catalog all types of transcripts present in that cell/tissue/organ/organism at a specific moment, and to quantify the changes in expression levels of each transcript under distinct scenarios; moreover, it allows us to determine the transcriptional structure of genes, in terms of their start sites, 5′ and 3′ ends, splicing patterns and other post-transcriptional modifications.

RNA-seq became a powerful tool to study host–pathogen interactions, enlarging the horizon of opportunities for the development of early diagnosis tools, as well as for the identification of candidate genes to be employed in the development of improved genotypes resistant to a specific disease [23–26]. In the present study, RNA-Seq allowed not only the identification of genes/proteins differentially expressed in the leaves of FY symptomatic oil palm plants in comparison to the asymptomatic ones—either in the dry or rainy seasons— but also the identification of those differentially expressed in plants with similar FY-based phenotypes between seasons.

A set of 56 genes/proteins differentially expressed in the leaves of oil palm plants symptomatic for FY compared to asymptomatic ones, either in the dry or rainy seasons, was selected after transcriptomics analysis. They are molecular symptoms in the plant directly linked to the disease, which are positively (33 proteins) or negatively (23 proteins) expressed in the symptomatic plants—in comparison with the asymptomatic ones—independently of the season. Here, three of them underwent discussion, and the remaining 53 genes/proteins will undergo further analysis, and the results will be reported in the future. The protein most negatively regulated among those 56 selected (Figure 7) codes for a ribosomal protein large (RPL) subunit. RPLs are the components of the ribosome machinery and, to a certain extent, are required for protein synthesis. The ribosomal proteins names follow the subunit of the ribosome to which they belong—the small (S1 to S31) and the large (L1 to L44) [27].

This oil palm RPL belonged to the Ribosomal protein L19 protein family (IPR001857) and the Ribosomal protein L19 homologous superfamily type (IPR038657). In symptomatic plants, the expression level of that gene was reduced to 1.7% and 0.27% of the initial level seen in the asymptomatic plants in the dry and rainy seasons, respectively.

Nagaraj et al. [28] showed that when NbRPL19 was silenced in *Nicotiana benthamiana*, the non-host resistance became compromised, and the same was true in *Arabidopsis* mutants for AtRPL19. More recently, Ramu et al. [29] reported that RPL10-silenced *N. benthamiana* plants showed compromised disease resistance against the non-host pathogen *Pseudomonas syringae* pv. *tomato* T1.

Non-host resistance (NHR) is a safety barrier that protects plants from a large and diverse array of potential phytopathogens. Non-host species present an innate immunity that cannot be overcome by potential pathogenic microbes, resulting from a series of physical, chemical, and inducible defenses. NHR is a very durable type of resistance, which has raised great interest everywhere regarding its genetic basis and functionally transferring it to plant species of commercial interest [30–32].

Besides being linked to resistance against non-host pathogens, RPL19 also showed high RNA-chaperone activity in a trans-splicing assay where the pre-mRNA of the thymidylate synthase (td) gene containing a group I intron was spliced into two halves [33]. Kovacs et al. [34] showed that RPL19 from *E. coli* is partially unstructured and/or has molten globule-like characteristics once without the support of rRNA, and exhibited potent chaperone activity with the substrates alcohol dehydrogenase (ADH) and lysozyme in three different chaperone assays. Finally, Gorelova et al. [35] demonstrated that one of the bifunctional dihydrofolate reductase/thymidylate synthase (DHFR-TS) isoforms of *A. thaliana* (*At2g21550*) operates as an inhibitor of its homologs, regulating DHFR and TS activities. Such regulation affects folate abundance. Gorelova and colleagues also proposed a novel function of folate metabolism in plants, which is the maintenance of the redox balance by contributing to NADPH production through the reaction catalyzed by methylenetetrahydrofolate dehydrogenase, thus allowing plants to cope with oxidative stress [35].

At2g21550 codes for NP_001324557.1, and using that protein sequence once to Blastp against the reference genome of oil palm [36], six positive hits appeared. Five were from a gene (LOC105048636) in chromosome seven. The former did not differentially express in the transcriptome of oil palm plants, but the latter did. There, the latter showed reduced expression in the rainy season, compared with the dry season, in both the asymptomatic and symptomatic plants, but was not differentially expressed in symptomatic plants compared with asymptomatic plants in the dry or rainy seasons. According to InterPro [37], XP_029121477.1 (coded by LOC105048636) is a representative of the bifunctional dihydrofolate reductase/thymidylate synthase (IPR012262) family, is positive for the dTMP biosynthetic process (GO:0006231), the one-carbon metabolic process (GO:0006730), the tetrahydrofolate biosynthetic process (GO:0046654), the biological process, and for thymidylate synthase activity (GO:0004799), dihydrofolate reductase activity (GO:0004146), and transferase activity, for transferring one-carbon groups (GO:0016741), and for molecular function. Altogether, the results in the present study show that the negative regulation of XP_029121477.1 is due to the changes in the environment—from dry to rainy season— and is not linked to the change in phenotype from asymptomatic to symptomatic.

This specific oil palm RPL is under the regulation of twelve genes, according to a gene regulatory network available in our lab [38] featuring epigenetic regulators and transcription factors from the oil palm genome and built based on the strategy reported by McCoy et al. [39]. Such analysis was performed by applying GENIE3 to mine 306 public oil palm transcriptome datasets. Such a study used 1333 unique regulators and 27,642 target genes from the oil palm reference genome [36]. The expression profiles of the twelve genes showed seven of them not present or not differentially expressed in the four scenarios evaluated in the present study. The scenarios are: (a) symptomatic vs. asymptomatic in the dry period; (b) symptomatic vs. asymptomatic in the wet period; (c) wet vs. dry period in symptomatic plants; and (d) wet vs. dry in asymptomatic ones. Among the remaining five, three were not differentially expressed in the two first scenarios but were positively regulated in the two last. Finally, two were only differentially expressed in the third scenario; one positive and one negative. In summary, such results do not allow us to

point out any direct effect of any of those 12 regulatory genes in the changes of expression observed in *EgRPL19-2* in the two first scenarios.

The whole genome sequence of the American oil palm (*E. oleifera*) [40] revealed four positive hits for ribosomal protein L19-2. A Blastp analysis of those four positive hits against the oil palm reference genome [36] allowed the identification of two proteins in the African oil palm with expression profiles highly different from each other in the four above-mentioned scenarios. The *E. guineensis* RPL19-2 protein, whose expression level was highly reduced in FY-symptomatic plants in the dry and rainy seasons, compared to the asymptomatic ones, has very high identification with three of the above-mentioned positive hits for ribosomal protein L19-2 protein in *E. oleifera*, a species known to be resistant to FY [6].

Among those 33 proteins down-regulated there were two WAK-like proteins (WAKLs). Wall-associated kinases (WAKs) and WAKs-like proteins (WAKLs) belong to a plant-specific subfamily of the receptor-like kinase family (IPR045274), and some of them have been implicated in resistance to bacterial and fungal diseases [41,42]. When investigating the defense role of a pathogen-induced WAK gene from wheat chromosome 7D, designed as *TaWAK7D*, Qi et al. [41] suggested that such a gene positively participates in the defense against infection by the soilborne and necrotrophic fungus *Rhizoctonia cerealis*, through activating the expression of several pathogenesis-related (PR) genes, including *Chitinase3*, *Chitinase4*, *PR1*, *PR17* and *β-1,3-Glucanase*.

Plants have either plasma membrane-localized receptor kinases (RKs) or receptor-like proteins that perceive pathogen- or microbe-associated molecular patterns (PAMPs/MAMPs), as well as damage-associated molecular patterns (DAMPs). Recognizing such patterns triggers immunity, which contributes to basal immunity to adapted pathogens and NHR to non-adapted pathogens by the induction of both local and systemic immune responses [43].

The expression levels of the two WAKLs proteins—differentially expressed in the leaves of FY-symptomatic oil palm plants in the present study—were reduced to 25–45% of the initial level seen in the asymptomatic plants. The genes that code XP_010934766.2 (LOC105054847), a wall-associated receptor kinase 2-like protein, and XP_010934767.1 (LOC105054848), a putative wall-associated receptor kinase-like 16, are located side by side in chromosome 12 of the oil palm reference genome [36]. According to InterPro [37], they are representative of the Receptor-like kinase WAK-like (IPR045274) family, positive for protein phosphorylation (GO:0006468) and for cell surface receptor signaling (GO:0007166), for biological process, and ATP binding (GO:0005524), protein kinase activity (GO:0004672), calcium ion binding (GO:0005509), polysaccharide binding (GO:0030247), and molecular function. Moreover, they showed 85% of identity measured across approximately their entire amino acid sequence.

Again, the gene regulatory network in our lab [38] showed that no unique regulator regulates the LOC105054848 (XP_010934767.1) gene/protein, and the LOC105054847 (XP_010934766.2) might be under the regulation of 16 genes. The transcriptome generated in the present study revealed that 13 genes out of the 16 were not present in the transcriptome or did not differentially express in any of the four scenarios evaluated. Among the remaining three, two were negatively and one positively regulated in the last scenario. Finally, two were differentially expressed only in the third scenario; one positively and one negatively. In summary, such results also do not allow to us to point out any direct effect of any of those 16 regulatory genes in the changes of expression observed in LOC105054847 in the first two scenarios.

The pathway-based MOI analysis performed in this study using the Omics Fusion platform brought together enzymes (from transcriptomics studies) and metabolites that expressed differentially in the leaves of oil palm plants under distinct conditions (dry and wet periods or dry and rainy seasons). First, the analysis integrated differentially expressed metabolites and enzymes found only in symptomatic plants and then those found in both asymptomatic and symptomatic plants. By doing that, our results revealed those pathways affected by the environment—independently of the FY phenotype—but also allowed us to

map those enzymes and metabolites that play a role only in the symptomatic plants. For instance, in the case of Purine metabolism (map00230), five metabolites (out of seventeen) appeared only in the symptomatic plant, and the same was true for four enzymes (out of fifteen). Moreover, two of the remaining twelve metabolites had distinct qualitative expression profiles, while all remaining proteins had similar qualitative expression profiles in asymptomatic and symptomatic plants. At the same time, this allowed the identification of metabolites and enzymes with similar qualitative expression profiles but with differences in the quantitative one. For instance, Inosine monophosphate (IMP—C00130) was positively regulated 113 times in the symptomatic plants and only 3 times in the asymptomatic ones; meanwhile, Inosine diphosphate (IDP—C00104) was positively regulated 88 times in the symptomatic plants, and negatively in only 7% of the asymptomatic ones (Tables 2–4).

Table 3. List of genes/proteins integrated in the purine metabolism (map00230), the top most affected pathway, and their behavior in FY asymptomatic and symptomatic oil palm plants, obtained via Multi-Omics Integration (MOI) using Omics Fusion.

Protein ID	UniProt Accession	EC Number	FC Symptomatic	Profile Symptomatic	FC Asymptomatic	Profile Asymptomatic
XP_010912022.1	A0A6I9QPT3	1.17.4.1	−4.0	DOWN	−2.3	DOWN
XP_010938967.1	A0A6I9S8I9	2.7.1.25	−2.5	DOWN	−3.0	DOWN
XP_010911123.2	A0A6I9QKC5	2.7.1.40	−5.9	DOWN	−3.6	DOWN
XP_010930617.1	A0A6I9RQ67	2.7.1.40	−1.8	DOWN	−2.8	DOWN
XP_010919863.2	A0A6I9R3I3	2.7.1.40	−2.9	DOWN	−2.2	DOWN
XP_010924524.1	A0A6I9RE71	2.7.4.6	−2.5	DOWN	−2.7	DOWN
XP_010937073.1	A0A6I9S4K9	2.7.4.8	−4.2	DOWN	−3.3	DOWN
XP_010910297.1	A0A6I9QJ47	2.7.6.5	−4.0	DOWN	−3.6	DOWN
XP_010933384.1	A0A6I9RX86	2.7.6.5	−2.6	DOWN	−2.9	DOWN
XP_010932410.1	A0A6I9RU27	2.7.6.5	−2.8	DOWN	−2.7	DOWN
XP_010921622.1	A0A6I9R798	2.7.6.5	−4.9	DOWN	−5.4	DOWN
XP_029119510.1	A0A8N4F2W4	2.7.7.4	−3.6	DOWN	−4.7	DOWN
XP_010932834.1	A0A6I9RV40	2.7.7.4	−2.2	DOWN	−2.4	DOWN
XP_010920819.1	A0A6I9R728	3.5.4.6	−3.3	DOWN	−3.7	DOWN
XP_010937877.2	A0A6I9S697	3.5.4.6	−4.6	DOWN	−2.2	DOWN
XP_029116569.1	A0A8N4EWM4	5.4.2.2	−2.0	DOWN	−3.0	DOWN
XP_010934074.1	A0A6I9RXY5	5.4.2.2	−1.9	DOWN	−2.1	DOWN
XP_010911922.1	A0A6I9QMW6	2.4.2.7	1.8	UP	−1.3	NDE
XP_010920467.1	A0A6I9R4T4	2.7.1.20	1.9	UP	1.2	NDE
XP_029117373.1	A0A8N4ID85	2.7.4.6	1.5	UP	−1.2	NDE
XP_010933513.1	A0A6I9RXJ3	2.7.1.40	−6.4	DOWN	No	No
XP_010905734.1	A0A6I9QAR4	1.7.3.3	2.1	UP	1.6	UP
XP_010907802.1	A0A6I9QFG8	1.7.3.3	3.2	UP	2.8	UP
XP_010941354.1	A0A6I9SCA5	2.7.4.3	1.7	UP	1.7	UP
XP_010908713.1	A0A6I9QHG6	2.7.4.3	1.8	UP	1.9	UP
XP_010935173.1	A0A6I9RZH1	2.7.4.3	4.6	UP	3.9	UP
XP_010919758.1	A0A6I9R9M7	2.7.4.6	2.4	UP	1.5	UP
XP_010933580.1	A0A6I9RXP4	2.7.4.6	3.6	UP	2.6	UP
XP_010943858.1	A0A6I9SHJ3	2.7.6.5	3.9	UP	2.8	UP
XP_010914531.2	A0A6I9QT08	6.3.3.1	1.7	UP	1.8	UP
XP_010910143.1	A0A6I9QKR6	6.3.4.13	2.2	UP	1.9	UP

The groundwater at the oil palm field where the plants sampled in the present study were growing was almost on the soil surface during the rainy season (Figure 8E), indicating that those plants were growing in waterlogged soil and likely experiencing oxygen deficiency (hypoxia), which was possibly affecting their root system. The soil physical–chemical and leaf chemical analyses pointed out differences due to changes in the environment but not due to the FY phenotype. It is common sense that in the rainy season, the visual symptoms of this disease intensify, and the results of the present study show that the number of differentially expressed genes/proteins and metabolites is much higher when one

compares plants with the same phenotype in different seasons than between symptomatic and asymptomatic plants in a specific season.

Table 4. List of metabolites integrated in the purine metabolism (map00230), the top most affected pathway, and their behavior in FY asymptomatic and symptomatic oil palm plants, obtained via Multi-Omics Integration (MOI) using Omics Fusion.

KEGG ID	Compound	Matched Form Symptomatic	Fold Change Asymptomatic	Profile Asymptomatic	Fold Change Symptomatic	Profile Symptomatic
C00104	IDP	M-HCOOK+H[1+]	0.07	DOWN	87.59	UP
C06197	P1,P3-Bis(5′-adenosyl) triphosphate	M+NaCl[1+]	0.16	DOWN	0.05	DOWN
C00212	Adenosine	M+Cl[-]	0.30	DOWN	4.97	UP
C00387	Guanosine	M+Na[1+]	0.52	DOWN	2.54	UP
C04640	2-(Formamido)-N1-(5′-phosphoribosyl) acetamidine	M+HCOONa[1+]	0.27	DOWN	0.20	DOWN
C12248	5-Hydroxy-2-oxo-4-ureido-2,5-dihydro 1H-imidazole-5-carboxylate	M[1+]	0.42	DOWN	2.88	UP
C00242	Guanine	M+Na[1+]	0.12	DOWN	9.74	UP
C00224	Adenylyl sulfate	M-NH_3+H[1+]	0.19	DOWN	2.74	UP
C00655	Xanthosine 5′-phosphate	M+NaCl[1+]	0.37	DOWN	2.98	UP
C04823	1-(5′-Phosphoribosyl)-5-amino-4 (N-succinocarboxamide)-imidazole	M-HCOOH+H[1+]	0.20	DOWN	7.89	UP
C00301	ADP-ribose	M-H_2O-H[-]	No	No	0.22	DOWN
C00385	Xanthine	M+Na-2H[-]	No	No	7.90	UP
C00206	dADP	M+3H[3+]	No	No	14.49	UP
C02091	(S)-Ureidoglycine	M[1+]	No	No	2.51	UP
C00059	Sulfate	M(S34)-H[-]	No	No	2.27	UP
C04677	1-(5′-Phosphoribosyl)-5-amino-4 imidazolecarboxamide	M-H[-]	10.95	UP	66.60	UP
C00130	IMP	M-H_4O_2+H[1+]	2.93	UP	112.58	UP

Oxygen deficiency in plants affects several metabolic pathways, and under such conditions substantial changes in the expression levels of transcripts, proteins, and metabolites have been observed [44,45]. However, the initial cellular response to a decrease in O_2 availability, regardless of whether the species is tolerant or not, is the promotion of the anaerobic metabolism of pyruvate, which is highly conserved in plants and animals [46,47]. Perhaps for this reason, glycolysis and the Krebs cycle are the most-studied metabolic pathways under conditions of hypoxia/anoxia, as pyruvate is the end product of the first and the initial substrate of the second.

The MOI results from this present study showed that all three metabolites identified in the Glycolysis/Gluconeogenesis (map00010) pathway were differentially expressed only in the symptomatic plants, and all were positively regulated in the rainy season. Beta-D-Fructose 6-phosphate (C05345) was the metabolite with the top increase in expression level, 12×, followed by beta-D-Fructose 1,6-bisphosphate (C05378), with 5×, and Acetaldehyde (C00084), with 3×. In the case of the TCA Cycle (map00020) pathway, just one (S)-Malate (C00149) was differentially expressed only in symptomatic plants, with a 6× increase in expression level. Isocitrate (C00311), cis-Aconitate (C00417), and 2-Oxoglutarate (C00026) are negatively regulated in asymptomatic plants and positively regulated in symptomatic. In terms of proteins, Malate dehydrogenase and Succinate--CoA ligase [ADP-forming] subunit beta (mitochondrial) experienced a 50% increase in expression, and phosphoenolpyruvate carboxykinase (ATP) expression level was reduced to 25% of the level in symptomatic plants during the rainy season, without any change in expression level in the asymptomatic plants.

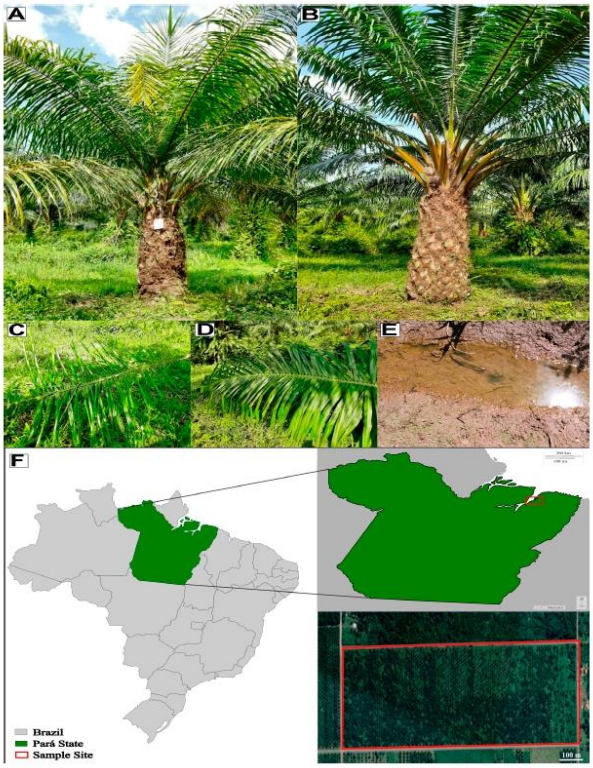

Figure 8. Overview of the sample site, soil condition and FY general phenotype; oil palm symptomatic (**A**) and asymptomatic (**B**) for FY; second leaf after spear leaf collected from a symptomatic (**C**) and asymptomatic (**D**) oil palm individual; waterlogged soil in the sample site from Dry period (**E**); sample site in Santa Bárbara do Pará, Pará, Brazil (**F**).

4. Materials and Methods

4.1. Soil and Leaf Samples—Collection and Chemical and Physicochemical Analysis

The soil and plant material used in this study came from a commercial oil palm plantation belonging to Denpasa—Dendê do Pará S/A company (www.denpasa.com.br, accessed on 30 June 2023) located in Santa Bárbara do Pará, state of Pará, northern Brazil (1°13′25″ S and 48°17′40″ W, 21 m above sea level). This oil palm field started in 2011 and has shown a high incidence of FY, with about 19% of plants affected in 2021, according to Denpasa's staff (personal communication) (Figure 8).

Soil and leaf samples were collected from asymptomatic and symptomatic plants in the intermediate stages of the disease [48] in two distinct periods: in October 2021—the dry period (DP)—and in June 2022—the wet period (WP). The selected asymptomatic individuals had never shown symptoms of AF, according to Denpasa's staff (personal communication). The same individuals were sampled in the DP and WP, with only one symptomatic plant replaced (Table S1).

Soil samples collected from three equidistant points around the plant stem—one meter from it and at 10 cm in diameter and 30 cm deep holes—were homogenized and stored in a plastic bag. Six asymptomatic and six symptomatic plants were sampled in DP, totaling twelve samples, and eight in WP, per treatment, totaling sixteen. Before being sent for analysis, all soil samples were dried at room temperature. Leaves from six asymptomatic

and six symptomatic plants were sampled in DP and WP, totaling 24 samples. Leaf samples were dried in an oven at 65 °C, ground using a Wiley mill (Model TE 680, Tecnal, Piracicaba, SP, Brazil), and passed through a 1 mm (20-mesh) sieve. Soil and leaf samples underwent analysis at Soloquímica (www.soloquimica.com.br)—DP samples—and at Terra Análises para Agropecuária (www.laboratorioterra.com.br)—WP samples.

4.2. Experimental Design and Statistical Analysis

A completely randomized design was adopted to investigate the influence of two factors and their interaction on the selected soil and leaf variables. The four groups ('treatments') were then constituted of combinations of the state of the soil of the experimental area (DP and WP) and the status of plants regarding the FY disorder (symptomatic or asymptomatic). Analyses considered two methods: (a) a separate analysis for each period state, and (b) a conjoint analysis using data from both periods.

We investigated the influence of plant state (symptomatic or asymptomatic) on each of the response variables classified into four groups: soil/leaf macro and micronutrient, soil sorption complex, and soil granulometry. The one-way analysis of variance (ANOVA) was used in this study. Because the factor plant status has only two levels, the ANOVA F-test was applied to compare the factor means. Then we also performed a principal component analysis (PCA) for each of the four groups of variables, as a graphical complementary way of investigating whether plant status was a factor for separating plant groups.

The two-way repeated measures ANOVA quantified the influence of period status and plant status, and their interaction on each response variable. The means corresponding to each period status within plant status were compared via the F-test for contrasts and the means for each plant status were determined by ANOVA F-tests. The PCA was also performed for each of the four groups of variables, but using measurements made during the wet and dry periods and including all samples. We used those measurements that were present in both periods.

In both situations, the statistical software SAS/STAT® was employed; PCA was carried out using the PRINCOMP Procedure for PCA analyses, and the GLM (General Linear Model) Procedure for the ANOVAs (SAS Institute Inc., 2020, Tokyo, Japan). Data were standardized before running PCAs to avoid conflicts due to the different magnitudes of the response variables within each group. The significance level adopted for ANOVAs was 0.05.

4.3. Transcriptomics Analysis

The second apical leaf, counted after the arrow leaf, was collected for transcriptomic analysis, and a total of six leaflets from each side of the intermediate portion of the leaf were harvested and sectioned into 10 cm portions from their base. The leaflet sections were stored in RNA later™ solution (Invitrogen, Waltham, MA, USA) on ice, transported to the laboratory, removed from the RNA later™ solution, and kept at −80 °C until extraction. Six biological replicates were collected from symptomatic and six from asymptomatic plants in DP and WP, totaling 24 samples.

Total RNA was isolated from oil palm leaves using the Qiagen RNeasy® Plant Mini kit (QIAGEN, Redwood City, CA, USA), following the manufacturer's protocol. The quantity and quality of RNA were measured using a Nanodrop Qubit 2.0 fluorometer (Life Technologies, Carlsbad, CA, USA). Library preparation and RNA-Seq were performed by the GenOne Company (Rio de Janeiro, RJ, Brazil) using an Illumina platform and the paired-end strategy.

All RNA-Seq analyses were performed using the OmicsBox platform, version 2.2.4 [49]. We used FastQC [50] and Trimmomatic [51] for quality control, read filtering, and removal of low-quality bases. The oil palm reference genome [36]—files downloaded from NCBI (BioProject PRJNA192219; BioSample SAMN02981535) in October 2020—was used to align the RNA-Seq data using standard OmicsBox version 2.2.4 parameters, through the STAR software [52].

HTSeq version 0.9.0 was used to quantify gene or transcript expression [53], applying the standard parameters of OmicsBox version 2.2.4. Paired differential expression analysis between experimental conditions (symptomatic vs. asymptomatic) was performed using edgeR version 3.28.0 [54], applying a simple design and exact statistical test without filtering for low-count genes.

4.4. Metabolomics Analysis

The leaf samples for metabolomics analysis were collected simultaneously and using the same criteria as for the transcriptomics samples, following the "split-sample data" strategy. Six biological replicates were collected for both symptomatic and asymptomatic individuals in DP and WP, resulting in a total of 24 samples.

Before solvent extraction, all samples underwent grounding in liquid nitrogen. We employed a well-established protocol [55,56] to extract the metabolites in three phases (polar, non-polar, and protein pellet) from aliquots of 50 mg of ground tissue. The solvents used were methanol grade UHPLC, acetonitrile grade LC-MS, formic acid grade LC-MS, and sodium hydroxide ACS grade LC-MS, all from Sigma-Aldrich, with water treated in a Milli-Q system from Millipore.

The analytical method ultra-high performance liquid chromatography and tandem mass spectrometry (UHPLC–MS/MS) was used in this study, with the UHPLC system (Nexera X2, Shimadzu Corporation, Kyoto City, Japan) equipped with a C8 reverse-phase column from Waters Technologies (Acquity UPLC HSS T3, 1.8 µm, 2.1 by 150 mm at 35 °C). Solvent A was 0.1% (v/v) formic acid in water and solvent B was 0.1% (v/v) formic acid in acetonitrile/methanol (70:30, v/v). The gradient elution used, with a flow rate of 0.4 mL min^{-1}, was as follows: 0–1 min isocratic, 0% B; 1–3 min, 5% B; 3–10 min, 50% B; 10–13 min, 100% B; 13–15 min isocratic, 100% B; then five minutes re-balancing to the initial conditions. The column temperature was set at 40 °C.

High-resolution mass spectrometry was used for detection (MaXis 4G Q-TOF MS, Bruker Daltonics), equipped with an electrospray source in positive (ESI-(+)-MS) and negative (ESI-(−)-MS) modes. The settings of the mass spectrometer were as follows: capillary voltage, 3800 V; dry gas flow, 9 L min^{-1}; dry temperature, 200 °C; nebulizer pressure, 4 bar; and final plate offset, 500 V. The rate of acquisition spectra was 3.00 Hz, mass range m/z 70–1200 for the polar fraction analysis and m/z 300–1600 for the lipidic fraction. For external calibration of the equipment, we used a sodium formate solution (10 mM HCOONa solution in 50:50 v/v isopropanol and water containing 0.2% formic acid), injected through a six-way valve at the beginning of each chromatographic run. Ampicillin ([M + H] + m/z 350.1186729 and $[M - H]^-$ m/z 348.1028826) was the internal standard for later peak normalization of data analysis.

The DataAnalysis 4.2 software (Bruker Daltonics, Bremen, Germany) was the first used to analyze the raw data from UHPLC-MS, as mzMXL files. Pre-processing of data was performed using XCMS Online [57,58], including peak detection, retention time correction, and alignment of the metabolites. CentWave was used for peak detection (maximum peak width, 20 s; $\Delta m/z = 10$ ppm; minimum peak width, 5 s). For the alignment of retention times, the parameters were mzwid = 0.015, minfrac = 0.5 and bw = 5. The unpaired parametric *t*-test (Welch *t*-test) was used for the statistical analysis at the pre-processing stage.

Initially, the pre-processed data (csv file) underwent analysis in the Statistical Analysis module of the MetaboAnalyst 5.0 [59], using the Pareto method as scaling [60]. Then, the differentially expressed peaks (DEPs)—those passing the criteria of false rate discovery (FDR) ≤ 0.05 and Log_2(fold change [FC]) $\neq 1$—were selected and submitted to the Functional Analysis module, applying the following parameters: molecular weight tolerance of 5 ppm; mixed ion mode; joint analysis using both the mummichog [61] and Gene Set Enrichment Analysis (GSEA) [62] algorithms, and the latest KEGG version of the *Oryza sativa* pathway library. The *p*-value cutoff from the mummichog algorithm was at 1.0×10^{-5}.

DEPs with two or more matched forms were observed. In those cases, the mass error was the criteria for the feature selection, keeping the smallest. Then, KEGG IDs with two or

more features (m.z) were also observed; and, again, the smallest mass error was the criteria for the feature selection. Finally, the KEGG IDs of the matched compounds—one KEGG ID per m.z—were submitted to the pathway analysis module for visualization through integrating enrichment and pathway topology analysis [63]. The parameter sets were the hypergeometric test and the latest KEGG version of the *O. sativa* pathway library.

4.5. Correlation and Integratomics Analysis

DEPs and DEMs underwent correlation analysis under two distinct scenarios, symptomatic × asymptomatic plants and dry × wet periods. First, to check for the data distribution, the Data Overview module of Omics Fusion [64], the web platform for integrative analysis of omics data, was used, and then the Scatter Plot one for the correlation analysis between the sets of data—a pairwise combination of the different scenarios evaluated. The input data was the Log_2(FC) from the DE molecules obtained from the single-omics analysis.

The DEPs and DEMs identified underwent a pathway-mapping approach of integration using the Omics Fusion platform [64]. Before the integration, the NCBI accession of enzymes was converted to UniProt ID. Thus, the input data used were the UniProt accession ids for transcriptomics and KEGG ids for metabolomics. The data underwent enrichment through several databases (EMBL—www.embl.org (accessed on 30 June 2023), KEGG—www.genome.jp/kegg (accessed on 30 June 2023), NCBI—www.ncbi.nlm.nih.gov (accessed on 30 June 2023), and UniProt—www.uniprot.org (accessed on 30 June 2023), and then the module "KEGG feature distribution" was used to map these omics data in known pathways—www.genome.jp/kegg/annotation (accessed on 30 June 2023)).

5. Conclusions

This study aimed to obtain insights into the possible occurrence and role of oxygen deficiency (hypoxia) in the onset of Fatal Yellowing (FY), a disease of unknown etiology that limits the oil palm industry in Brazil. Soil and leaf samples from asymptomatic and symptomatic plants in the intermediate stages of the disease were collected in two distinct periods: in October 2021—the dry season—and in June 2022—the rainy season. The changes observed in the physicochemical attributes did not allow for the discrimination of plants asymptomatic or symptomatic for this disease, not even in the rainy season, when the soil became waterlogged. The same was true for the chemical attributes and the metabolome profiles of the leaves. Only transcriptome profiles of the leaves allowed the identification of molecular symptoms able to distinguish symptomatic from asymptomatic plants, independently of the season—dry or rainy. A set of 56 proteins/genes, negatively or positively regulated in symptomatic plants compared to the asymptomatic ones, resulting from this study, is undergoing additional analysis, aiming at a broad in silico functional annotation and the validation of the RNA-Seq expression profile employing qPCR analysis.

Altogether, the single-omics analysis (SOA) performed in the present study allowed the identification of 320 enzymes (from the transcriptome analysis) and 254 metabolites on the leaves of oil palm plants that underwent multi-omics integration (MOI) analysis. Such a set was composed of enzymes and metabolites differentially expressed in asymptomatic and symptomatic plants in the rainy season—waterlogged soil—compared to the dry season, plus those differentially expressed only in the symptomatic ones. Such an MOI analysis produced a list of 27 metabolic pathways affected by the change from dry to rainy season, with at least ten enzymes and metabolites differentially expressed. Starting from the premise that the visual FY symptoms intensify in the rainy season, we postulate that a closer look at such pathways might reveal insights into the role of hypoxia in the symptom intensification of FY.

Finally, the closer analysis of three out of the fifty-six proteins/genes selected employing transcriptomics analysis under four distinct scenarios strongly points to the following postulate: the oxygen deficiency (hypoxia) experienced by the oil palm plants for long periods of the year promotes stress in the roots of those plants and triggers, directly or indirectly, a cascade of events that breaks some of the safety barriers that protect plants from

a large and diverse array of potential phytopathogens. Breaks in the non-host resistance to non-adapted pathogens—as suggested by the strong negative regulation of EgRPL19-2 in both seasons—as well as in the basal immunity to adapted pathogens, as pointed out by the negative regulation of this gene and of two WAKs-like proteins belonging to a plant-specific subfamily of the receptor-like kinase family (IPR045274), are the initial basis for such a postulate. By doing this, it creates the possibility for opportunist microorganisms in the soil to infect the plant and promote this bud-rot type of disease. Whether a specific opportunistic pathogen is prevalent or not still needs further evaluation, although we also postulate that this might not be the case.

Why do we find asymptomatic plants surrounded by symptomatic ones after spending a decade in the same conditions? The variability in the expression profiles of those three genes—and several others among the 53 remaining for further characterization—within this plant species, but also in the American oil palm (*E. oleifera*) population, and inside the populations of inter-specific hybrids between these two species, can pave the way to answering this question and identify bio-markers for the selection of oil palm plants resistant to the Fatal Yellowing disease. Mapping the differences in the promoter sequence of such genes, as well as those between them and their orthologs in the American oil palm, might help developing gene editing strategies able to protect such genes from the cascade of events triggered by the abiotic stress, and maintain the safety barriers raised and strong.

Supplementary Materials: The following supporting information can be downloaded at: https://www.mdpi.com/article/10.3390/ijms241612918/s1.

Author Contributions: Conceptualization: A.d.H.N.M., B.F.Q., C.A.F.d.S. and M.T.S.J.; Methodology, investigation, data curation, and formal analysis: C.B.B., T.L.C.d.S., J.C.R.N., A.P.L. and J.A.d.A.R.; Funding acquisition and supervision: M.T.S.J.; Writing—original draft: C.B.B., A.d.H.N.M., B.F.Q., C.A.F.d.S. and M.T.S.J.; Writing—review and editing: M.T.S.J. All authors have read and agreed to the published version of the manuscript.

Funding: The grant (01.13.0315.00 DendêPalm Project) for this study was awarded by the Brazilian Ministry of Science, Technology, and Innovation (MCTI) via the Brazilian Innovation Agency FINEP. The authors confirm that the funder had no influence over the study design, the content of article, or selection of this journal.

Institutional Review Board Statement: Not applicable.

Informed Consent Statement: Not applicable.

Data Availability Statement: The datasets used and/or analyzed in the current study are available from the corresponding author on reasonable request.

Acknowledgments: The authors acknowledge scholarship to C.B.B. and T.L.C.S. by the Coordination for the Improvement of Higher Education Personnel (CAPES), and fellowship to J.C.R.N. by the National Council for Scientific and Technological Development (CNPq). The authors also acknowledge the support of Roberto Yokoyama, Denpasa—Dendê do Pará S/A company, who opened a Denpasa oil palm plantation for us to collect all soil and plant samples used in this study.

Conflicts of Interest: Authors A.P.L., J.A.d.A.R., A.d.H.N.M., C.A.F.d.S., B.F.Q. and M.T.S.J. were employed by company The Brazilian Agricultural Research Corporation—Embrapa. The remaining authors declare that the research was conducted in the absence of any commercial or financial relationships that could be construed as potential conflict of interest.

References

1. Statista. 2023. Available online: www.statista.com (accessed on 30 June 2023).
2. Murphy, D.J.; Goggin, K.; Paterson, R.R.M. Oil palm in the 2020s and beyond: Challenges and solutions. *CABI Agric. Biosci.* **2021**, *2*, 39. [CrossRef]
3. Ritchie, H.; Roser, M. Forests and Deforestation. Published Online at OurWorldInData.org. 2021. Available online: https://ourworldindata.org/forests-and-deforestation (accessed on 13 July 2023).

4. MAPA—Ministério da Agricultura, Pecuária e Abastecimento. Diagnóstico da Produção Sustentável da Palma de Óleo. 2018. Available online: http://www.abrapalma.org/pt/wp-content/uploads/2018/06/DIAGNOSTICO_PALMA1.pdf (accessed on 30 June 2023).
5. Bertone, M.V. A Importância do Programa de Produção Sustentável de Palma de Óleo: Produtividade e Sustentabilidade. 2011. Available online: https://issuu.com/embrapa/docs/revista_agroenergia_ed2 (accessed on 30 June 2023).
6. Bittencourt, C.B.; Lins, P.d.C.; Boari, A.d.J.; Quirino, B.F.; Teixeira, W.G.; Souza Junior, M.T. Oil Palm Fatal Yellowing (FY), a Disease with an Elusive Causal Agent. In *Elaeis Guineensis*; Kamyab, H., Ed.; IntechOpen: London, UK, 2022. [CrossRef]
7. Boari, A.d.J. Estudos Realizados Sobre o Amarelecimento Fatal do Dendezeiro (Elaeis Guineensis Jacq.) No Brasil. 2008. Available online: https://www.infoteca.cnptia.embrapa.br/infoteca/handle/doc/410160 (accessed on 30 June 2023).
8. Corley, R.H.V.; Tinker, P.B. *The Oil Palm*, 5th ed.; Wiley: Hoboken, NJ, USA, 2015. [CrossRef]
9. Laranjeira, F.F.; Amorin, L.; Bergamin Filho, A.; Berger, R.D.; Hau, B. Análise espacial do Amarelecimento Fatal do dendezeiro como ferramenta para elucidar sua etiologia. *Fitopatol. Bras.* **1998**, *23*, 397–403.
10. Silveira, R.I.; Veiga, A.S.; Ramos, E.J.A.; Parente, J.R. *Evolução da Sintomatologia do Amarelecimento Fatal a Adubações com Omissão de Macro e Micronutrientes*; Denpasa: Belém, PA, Brazil, 2000; p. 35.
11. Viégas, I.d.J.M.; Frazão, D.A.C.; Júnior, J.F.; Trindade, D.R.; Thomazl, M.A.A. Teores de Micronutrientes em Folhas de Dendezeiros Sadios e com Sintomas de Amarelecimento Fatal. XXV Reunião Brasileira de Fertilidade Do Solo e Nutrição de Plantas. Available online: https://ainfo.cnptia.embrapa.br/digital/bitstream/item/100995/1/4469.pdf (accessed on 30 June 2023).
12. Muniz, R.S. *Alterações do Fluxo Hídrico e Seus Efeitos na Dinâmica do Ferro e na Estrutura de um Latossolo Amarelo na Amazônia*; Universidade Federal do Rio de Janeiro: Rio de Janeiro, Brazil, 2017. Available online: https://pantheon.ufrj.br/handle/11422/9680 (accessed on 30 June 2023).
13. Costa, O.Y.d.A.; Tupinambá, D.D.; Bergmann, J.C.; Barreto, C.C.; Quirino, B.F. Fungal diversity in oil palm leaves showing symptoms of Fatal Yellowing disease. *PLoS ONE* **2018**, *13*, e0191884. [CrossRef]
14. Rodrigues-Neto, J.C.; Correia, M.V.; Souto, A.L.; Ribeiro, J.A.A.; Vieira, L.R.; Souza, M.T., Jr.; Rodrigues, C.M.; Abdelnur, P.V. Metabolic fingerprinting analysis of oil palm reveals a set of differentially expressed metabolites in fatal yellowing symptomatic and non-symptomatic plants. *Metabolomics Off. J. Metabolomic Soc.* **2018**, *14*, 142. [CrossRef] [PubMed]
15. Nascimento, S.V.D.; Magalhães, M.M.; Cunha, R.L.; Costa, P.H.O.; Alves, R.C.O.; Oliveira, G.C.; Valadares, R.B.D.S. Differential accumulation of proteins in oil palms affected by fatal yellowing disease. *PLoS ONE* **2018**, *13*, e0195538. [CrossRef] [PubMed]
16. Torres, G.A.; Sarria, G.A.; Varon, F.; Coffey, M.D.; Elliott, M.L.; Martinez, G. First Report of Bud Rot Caused by *Phytophthora palmivora* on African Oil Palm in Colombia. *Plant Dis.* **2010**, *94*, 1163. [CrossRef]
17. Torres, G.A.; Sarria, G.A.; Martinez, G.; Varon, F.; Drenth, A.; Guest, D.I. Bud Rot Caused by *Phytophthora palmivora*: A Destructive Emerging Disease of Oil Palm. *Phytopathology* **2016**, *106*, 320–329. [CrossRef]
18. Reddy, K.R.; Patrick, W.H. Effect of alternate aerobic and anaerobic conditions on redox potential, organic matter decomposition and nitrogen loss in a flooded soil. *Soil Biol. Biochem.* **1975**, *7*, 87–94. [CrossRef]
19. Favre, F.; Tessier, D.; Abdelmoula, M.; Génin, J.M.; Gates, W.P.; Boivin, P. Iron reduction and changes in cation exchange capacity in intermittently waterlogged soil. *Eur. J. Soil Sci.* **2002**, *53*, 175–183. [CrossRef]
20. Bittencourt, C.B.; Carvalho da Silva, T.L.; Rodrigues Neto, J.C.; Vieira, L.R.; Leão, A.P.; de Aquino Ribeiro, J.A.; Abdelnur, P.V.; de Sousa, C.A.F.; Souza, M.T., Jr. Insights from a Multi-Omics Integration (MOI) Study in Oil Palm (*Elaeis guineensis Jacq.*) Response to Abiotic Stresses: Part One-Salinity. *Plants* **2022**, *11*, 1755. [CrossRef]
21. Gertsman, I.; Barshop, B.A. Promises and pitfalls of untargeted metabolomics. *J. Inherit. Metab. Dis.* **2018**, *41*, 355–366. [CrossRef] [PubMed]
22. Wang, Z.; Gerstein, M.; Snyder, M. RNA-Seq: A revolutionary tool for transcriptomics. *Nat. Rev. Genet.* **2009**, *10*, 57–63. [CrossRef] [PubMed]
23. Sharma, M.; Sudheer, S.; Usmani, Z.; Rani, R.; Gupta, P. Deciphering the Omics of Plant-Microbe Interaction: Perspectives and New Insights. *Curr. Genom.* **2020**, *21*, 343–362. [CrossRef] [PubMed]
24. Dev Sareshma, S.; Subha, B. *Assessing Host-Pathogen Interaction Networks via RNA-Seq Profiling: A Systems Biology Approach*; IntechOpen: London, UK, 2021. [CrossRef]
25. Zheng, S.; Terauchi, R. Plant–Pathogen Interaction: New Era of Plant–Pathogen Interaction Studies: "Omics" Perspectives. In *Plant Omics: Advances in Big Data Biology*; CABI Biotechnology Series; CABI International: Wallingford, UK, 2022. [CrossRef]
26. Liu, Z.; Pan, Y.; Li, Y.; Ouellet, T.; Foroud, N.A. RNA-Seq Data Processing in Plant-Pathogen Interaction System: A Case Study. *Methods Mol. Biol.* **2023**, *2659*, 119–135. [CrossRef] [PubMed]
27. Gregory, B.; Rahman, N.; Bommakanti, A.; Shamsuzzaman, M.; Thapa, M.; Lescure, A.; Zengel, J.M.; Lindahl, L. The small and large ribosomal subunits depend on each other for stability and accumulation. *Life Sci. Alliance* **2019**, *2*, e201800150. [CrossRef] [PubMed]
28. Nagaraj, S.; Senthil-Kumar, M.; Ramu, V.S.; Wang, K.; Mysore, K.S. Plant Ribosomal Proteins, RPL12 and RPL19, Play a Role in Nonhost Disease Resistance against Bacterial Pathogens. *Front. Plant Sci.* **2016**, *6*, 1192. [CrossRef]
29. Ramu, V.S.; Dawane, A.; Lee, S.; Oh, S.; Lee, H.K.; Sun, L.; Senthil-Kumar, M.; Mysore, K.S. Ribosomal protein QM/RPL10 positively regulates defence and protein translation mechanisms during nonhost disease resistance. *Mol. Plant Pathol.* **2020**, *21*, 1481–1494. [CrossRef]

30. Ayliffe, M.; Sørensen, C.K. Plant nonhost resistance: Paradigms and new environments. *Curr. Opin. Plant Biol.* **2019**, *50*, 104–113. [CrossRef]
31. Panstruga, R.; Moscou, M.J. What is the Molecular Basis of Nonhost Resistance? *Mol. Plant Microbe Interact.* **2020**, *33*, 1253–1264. [CrossRef]
32. Wu, Y.; Sexton, W.; Yang, B.; Xiao, S. Genetic approaches to dissect plant nonhost resistance mechanisms. *Mol. Plant Pathol.* **2023**, *24*, 272–283. [CrossRef]
33. Semrad, K.; Green, R.; Schroeder, R. RNA chaperone activity of large ribosomal subunit proteins from *Escherichia coli*. *RNA* **2004**, *10*, 1855–1860. [CrossRef] [PubMed]
34. Kovacs, D.; Rakacs, M.; Agoston, B.; Lenkey, K.; Semrad, K.; Schroeder, R.; Tompa, P. Janus chaperones: Assistance of both RNA- and protein-folding by ribosomal proteins. *FEBS Lett.* **2009**, *583*, 88–92. [CrossRef] [PubMed]
35. Gorelova, V.; De Lepeleire, J.; Van Daele, J.; Pluim, D.; Meï, C.; Cuypers, A.; Leroux, O.; Rébeillé, F.; Schellens, J.H.M.; Blancquaert, D.; et al. Dihydrofolate Reductase/Thymidylate Synthase Fine-Tunes the Folate Status and Controls Redox Homeostasis in Plants. *Plant Cell* **2017**, *29*, 2831–2853. [CrossRef]
36. Singh, R.; Ong-Abdullah, M.; Low, E.T.; Manaf, M.A.; Rosli, R.; Nookiah, R.; Ooi, L.C.; Ooi, S.E.; Chan, K.L.; Halim, M.A.; et al. Oil palm genome sequence reveals divergence of interfertile species in Old and New worlds. *Nature* **2013**, *500*, 335–339. [CrossRef]
37. Paysan-Lafosse, T.; Blum, M.; Chuguransky, S.; Grego, T.; Pinto, B.L.; Salazar, G.A.; Bileschi, M.L.; Bork, P.; Bridge, A.; Colwell, L.; et al. InterPro in 2022. *Nucleic Acids Res.* **2023**, *51*, D418–D427. [CrossRef] [PubMed]
38. Carvalho da Silva, T.L.; The Brazilian Agricultural Research Corporation, Embrapa Agroenergy, Brasília, DF, Brazil; Grynberg, P.; The Brazilian Agricultural Research Corporation, Embrapa Agroenergy, Brasília, DF, Brazil; Togawa, R.C.; The Brazilian Agricultural Research Corporation, Embrapa Agroenergy, Brasília, DF, Brazil; Souza, M.T., Jr.; The Brazilian Agricultural Research Corporation, Embrapa Agroenergy, Brasília, DF, Brazil. *Unpublished work*, 2023.
39. McCoy, R.M.; Julian, R.; Kumar, S.R.V.; Ranjan, R.; Varala, K.; Li, Y. A Systems Biology Approach to Identify Essential Epigenetic Regulators for Specific Biological Processes in Plants. *Plants* **2021**, *10*, 364. [CrossRef]
40. Souza, M.T., Jr.; The Brazilian Agricultural Research Corporation, Embrapa Agroenergy, Brasília, DF, Brazil. *Unpublished work*, 2023.
41. Qi, H.; Zhu, X.; Guo, F.; Lv, L.; Zhang, Z. The Wall-Associated Receptor-Like Kinase TaWAK7D Is Required for Defense Responses to Rhizoctonia cerealis in Wheat. *Int. J. Mol. Sci.* **2021**, *22*, 5629. [CrossRef] [PubMed]
42. Li, M.; Ma, J.; Liu, H.; Ou, M.; Ye, H.; Zhao, P. Identification and Characterization of Wall-Associated Kinase (WAK) and WAK-like (WAKL) Gene Family in Juglans regia and Its Wild Related Species Juglans mandshurica. *Genes* **2022**, *13*, 134. [CrossRef]
43. Boutrot, F.; Zipfel, C. Function, Discovery, and Exploitation of Plant Pattern Recognition Receptors for Broad-Spectrum Disease Resistance. *Annu. Rev. Phytopathol.* **2017**, *55*, 257–286. [CrossRef]
44. Shingaki-Wells, R.; Millar, A.H.; Whelan, J.; Narsai, R. What happens to plant mitochondria under low oxygen? An omics review of the responses to low oxygen and reoxygenation. *Plant Cell Environ.* **2014**, *37*, 2260–2277. [CrossRef]
45. León, J.; Castillo, M.C.; Gayubas, B. The hypoxia-reoxygenation stress in plants. *J. Exp. Bot.* **2021**, *72*, 5841–5856. [CrossRef] [PubMed]
46. Sousa, C.A.F.; Sodek, L. The metabolic response of plants to oxygen deficiency. *Braz. J. Plant Physiol.* **2002**, *14*, 83–94. [CrossRef]
47. Fukao, T.; Bailey-Serres, J. Plant responses to hypoxia—Is survival a balancing act? *Trends Plant Sci.* **2004**, *9*, 449–456. [CrossRef]
48. Souza, R.; Veiga, A.; Ramos, E. *Amarelecimento Fatal do Dendezeiro: Identificação Prática*; Denpasa: Belém, PA, Brazil, 2000; p. 27.
49. OmicsBox—Bioinformatics Made Easy, BioBam Bioinformatics, 3 March 2019. Available online: https://www.biobam.com/omicsbox (accessed on 18 July 2023).
50. Andrews, S. FastQC: A Quality Control Tool for High throughput Sequence Data. 2010. Available online: https://www.bioinformatics.babraham.ac.uk/projects/fastqc/ (accessed on 18 July 2023).
51. Bolger, A.M.; Lohse, M.; Usadel, B. Trimmomatic: A flexible trimmer for Illumina sequence data. *Bioinformatics* **2014**, *30*, 2114–2120. [CrossRef] [PubMed]
52. Dobin, A.; Davis, C.A.; Schlesinger, F.; Drenkow, J.; Zaleski, C.; Jha, S.; Batut, P.; Chaisson, M.; Gingeras, T.R. STAR: Ultrafast universal RNA-seq aligner. *Bioinformatics* **2013**, *29*, 15–21. [CrossRef]
53. Anders, S.; Pyl, P.T.; Huber, W. HTSeq—A Python framework to work with high-throughput sequencing data. *Bioinformatics* **2015**, *31*, 166–169. [CrossRef]
54. Robinson, M.D.; McCarthy, D.J.; Smyth, G.K. edgeR: A Bioconductor package for differential expression analysis of digital gene expression data. *Bioinformatics* **2010**, *26*, 139–140. [CrossRef]
55. Vargas, L.H.G.; Neto, J.C.R.; de Aquino Ribeiro, J.A.; Ricci-Silva, M.E.; Souza, M.T., Jr.; Rodrigues, C.M.; de Oliveira, A.E.; Abdelnur, P.V. Metabolomics analysis of oil palm (*Elaeis guineensis*) leaf: Evaluation of sample preparation steps using, UHPLC–MS/MS. *Metabolomics* **2016**, *12*, 153. [CrossRef]
56. Neto, J.C.R.; Vieira, L.R.; de Aquino Ribeiro, J.A.; de Sousa, C.A.F.; Júnior, M.T.S.; Abdelnur, P.V. Metabolic effect of drought stress on the leaves of young oil palm (*Elaeis guineensis*) plants using UHPLC-MS and multivariate analysis. *Sci. Rep.* **2021**, *11*, 18271. [CrossRef]
57. Gowda, H.; Ivanisevic, J.; Johnson, C.H.; Kurczy, M.E.; Benton, H.P.; Rinehart, D.; Nguyen, T.; Ray, J.; Kuehl, J.; Arevalo, B.; et al. Interactive XCMS Online: Simplifying Advanced Metabolomic Data Processing and Subsequent Statistical Analyses. *Anal. Chem.* **2014**, *86*, 6931–6939. [CrossRef]

58. Tautenhahn, R.; Patti, G.J.; Rinehart, D.; Siuzdak, G. XCMS Online: A web-based platform to process untargeted metabolomic data. *Anal. Chem.* **2012**, *84*, 5035–5039. [CrossRef] [PubMed]
59. Pang, Z.; Chong, J.; Zhou, G.; de Lima Morais, D.A.; Chang, L.; Barrette, M.; Gauthier, C.; Jacques, P.É.; Li, S.; Xia, J. MetaboAnalyst 5.0: Narrowing the gap between raw spectra and functional insights. *Nucleic Acids Res.* **2021**, *49*, W388–W396. [CrossRef] [PubMed]
60. Eriksson, L.; Johansson, E.; Kettaneh-Wold, N.; Wold, S. *Introduction to Multi-and Megavariate Data Analysis Using Projection Methods (PCA & PLS)*; Umetrics: Umeå, Sweden, 1999.
61. Li, S.; Park, Y.; Duraisingham, S.; Strobel, F.H.; Khan, N.; Soltow, Q.A.; Jones, D.P.; Pulendran, B. Predicting network activity from high throughput metabolomics. *PLoS Comput. Biol.* **2013**, *9*, e1003123. [CrossRef] [PubMed]
62. Subramanian, A.; Tamayo, P.; Mootha, V.K.; Mukherjee, S.; Ebert, B.L.; Gillette, M.A.; Paulovich, A.; Pomeroy, S.L.; Golub, T.R.; Lander, E.S.; et al. Gene set enrichment analysis: A knowledge-based approach for interpreting genome-wide expression profiles. *Proc. Natl. Acad. Sci. USA* **2005**, *102*, 15545–15550. [CrossRef] [PubMed]
63. Kanehisa, M.; Sato, Y.; Morishima, K. BlastKOALA and GhostKOALA: KEGG Tools for Functional Characterization of Genome and Metagenome Sequences. *J. Mol. Biol.* **2016**, *428*, 726–731. [CrossRef]
64. Brink, B.G.; Seidel, A.; Kleinbölting, N.; Nattkemper, T.W.; Albaum, S.P. Omics Fusion—A Platform for Integrative Analysis of Omics Data. *J. Integr. Bioinform.* **2016**, *13*, 296. [CrossRef]

CAPÍTULO III – ARTIGO 2

Insights from a Multi-Omics Integration (MOI) Study in Oil Palm (*Elaeis guineensis* Jacq.) Response to Abiotic Stresses: Part One – Salinity

Autores: Cleiton Barroso Bittencourt, Thalliton Luiz Carvalho da Silva, Jorge Cândido Rodrigues Neto, Letícia Rios Vieira, André Pereira Leão, José Antônio de Aquino Ribeiro, Patrícia Verardi Abdelnur, Carlos Antônio Ferreira de Sousa, Manoel Teixeira Souza.

Publicado no Periódico *Plants*
https://www.mdpi.com/2223-7747/11/13/1755
Volume 11(13):1755. doi: 10.3390/plants11131755, Junho, 2022.

plants

MDPI

Article

Insights from a Multi-Omics Integration (MOI) Study in Oil Palm (*Elaeis guineensis* Jacq.) Response to Abiotic Stresses: Part One—Salinity

Cleiton Barroso Bittencourt [1], Thalliton Luiz Carvalho da Silva [1], Jorge Cândido Rodrigues Neto [2], Letícia Rios Vieira [1], André Pereira Leão [2], José Antônio de Aquino Ribeiro [2], Patrícia Verardi Abdelnur [2], Carlos Antônio Ferreira de Sousa [3] and Manoel Teixeira Souza, Jr. [1,2,*]

[1] Graduate Program of Plant Biotechnology, Federal University of Lavras, Lavras 37200-000, Brazil; cleiton_court@hotmail.com (C.B.B.); ThallitonS@gmail.com (T.L.C.d.S.); leticia_rios1518@hotmail.com (L.R.V.)
[2] Embrapa Agroenergia, Brasília 70770-901, Brazil; jorgecrn@hotmail.com (J.C.R.N.); andre.leao@embrapa.br (A.P.L.); jose.ribeiro@embrapa.br (J.A.d.A.R.); patricia.abdelnur@embrapa.br (P.V.A.)
[3] Embrapa Meio Norte, Teresina 64006-245, Brazil; carlos.antonio@embrapa.br
* Correspondence: manoel.souza@embrapa.br; Tel.: +55-61-3448-3210

Abstract: Oil palm (*Elaeis guineensis* Jacq.) is the number one source of consumed vegetable oil nowadays. It is cultivated in areas of tropical rainforest, where it meets its natural condition of high rainfall throughout the year. The palm oil industry faces criticism due to a series of practices that was considered not environmentally sustainable, and it finds itself under pressure to adopt new and innovative procedures to reverse this negative public perception. Cultivating this oilseed crop outside the rainforest zone is only possible using artificial irrigation. Close to 30% of the world's irrigated agricultural lands also face problems due to salinity stress. Consequently, the research community must consider drought and salinity together when studying to empower breeding programs in order to develop superior genotypes adapted to those potential new areas for oil palm cultivation. Multi-Omics Integration (MOI) offers a new window of opportunity for the non-trivial challenge of unraveling the mechanisms behind multigenic traits, such as drought and salinity tolerance. The current study carried out a comprehensive, large-scale, single-omics analysis (SOA), and MOI study on the leaves of young oil palm plants submitted to very high salinity stress. Taken together, a total of 1239 proteins were positively regulated, and 1660 were negatively regulated in transcriptomics and proteomics analyses. Meanwhile, the metabolomics analysis revealed 37 metabolites that were upregulated and 92 that were downregulated. After performing SOA, 436 differentially expressed (DE) full-length transcripts, 74 DE proteins, and 19 DE metabolites underwent MOI analysis, revealing several pathways affected by this stress, with at least one DE molecule in all three omics platforms used. The Cysteine and methionine metabolism (map00270) and Glycolysis/Gluconeogenesis (map00010) pathways were the most affected ones, each one with 20 DE molecules.

Keywords: transcriptomics; proteomics; metabolomics; integratomics; abiotic stress; African oil palm

Citation: Bittencourt, C.B.; Carvalho da Silva, T.L.; Rodrigues Neto, J.C.; Vieira, L.R.; Leão, A.P.; de Aquino Ribeiro, J.A.; Abdelnur, P.V.; de Sousa, C.A.F.; Souza, M.T., Jr. Insights from a Multi-Omics Integration (MOI) Study in Oil Palm (*Elaeis guineensis* Jacq.) Response to Abiotic Stresses: Part One—Salinity. *Plants* **2022**, *11*, 1755. https://doi.org/10.3390/plants11131755

Academic Editor: Hanna Bandurska

Received: 6 June 2022
Accepted: 27 June 2022
Published: 30 June 2022

1. Introduction

Oil palm (*Elaeis guineensis* Jacq.) has the highest productivity among the main oilseed crops, reaching 3–8 times more oil per area than any other crop [1]. In 2021/2022, approximately 82 million metric tons of palm oil and palm kernel oil was consumed worldwide, making oil palm the number one source of consumed vegetable oil in the world [2]. It is the raw source of a wide range of products used by many industries, such as the food and steel industries, the manufacture of cleaning products, the pharmaceutical and cosmetics industries, and the biofuels industry [3].

Several countries placed, in the equatorial belt, expanded oil palm plantations in tropical forests where this crop meets its natural condition of high rainfall throughout the

year [4]. Despite the significant economic gains, this movement imposes environmental stresses, such as biodiversity loss, greenhouse gas emissions, land degradation, and air and water pollution [1]. In Brazil, over 95% of the oil palm plantations are in the Amazon rainforest, where only 2.14% of the total area destined for commercial plantations is currently in use [5]. This under-utilization status is due to many constraints, such as environmental legal restrictions imposed by the Brazilian Government and logistical difficulties, which together hinder the production flow to the main industrial areas in the country and also the occurrence of pests and diseases [6,7].

Outside the Amazon rainforest, there is an extensive area in Brazil with favorable conditions for cultivating oil palm [8]. There are many logistic advantages to producing oil palm outside the Amazon region, offering a window of opportunity to increase the area with oil palm plantations and, consequently, the total national palm oil yield. However, these areas experience long periods of drought throughout the year when oil palm does not meet the physiological water requirement to maintain productivity [8–10]. Consequently, the oil palm grower needs to irrigate the crop and must do so with proper management to avoid soil salinization.

Approximately 30% of the world's irrigated agricultural lands are damaged by salinity, negatively affecting the productivity of traditional crops [11]. Most crop plants have evolved under very low soil salinity, and, under high salt, their development is highly inhibited, even leading to death at a concentration ranging between 100 and 200 mM NaCl [12]. Salinity stress affects plants by decreasing the osmotic potential of the soil solution, making it harder for the root to absorb water from the soil and consequently experiencing drought stress, and by accumulating sodium and chloride ions in the cytoplasm, leading to the inhibition of many enzyme reactions due to ion toxicity [13]. Salt stress tolerance in plants involves many morphophysiological and biochemical changes, such as stomatal closing, osmolyte accumulation, and increased Na^+/Cl^- antiporter, governed by multigenic traits [14].

Considering those circumstances, it is clear that any initiative to promote oil palm cultivation outside the Amazon Forest in Brazil needs to take drought and salinity together when researching for knowledge and technology to empower breeding programs to develop superior genotypes for those regions. The first challenge is understanding the morphophysiological, biochemical, and molecular responses of oil palm to these two abiotic stresses. In doing so, our group has studied the response of young oil palm plants from different angles, applying different omics platforms, alone or in combination [6,15,16]. Vieira and colleagues showed that young oil palm submitted to a high concentration of NaCl reduces the rates of CO_2 assimilation, stomatal conductance to water vapor, and transpiration [6]. Then, Ref. [15] confirmed a preponderant role of transcription factors in the early response of oil palm plants to salinity stress, and [16] identified the pathways and the metabolites most affected by drought stress.

The current study is a new step on our research activities characterizing the biochemical and molecular responses of *E. guineensis* to salinity stress, where we carried out a comprehensive, large-scale, single-omics analysis (SOA), and Multi-Omics Integration (MOI) analysis of the metabolome, transcriptome, and proteome profiles on the leaves of young oil palm plants submitted by Vieira and colleagues [6] with repsect to very high salinity stress.

2. Results

2.1. Oil Palm Transcriptome under Salinity Stress

When comparing salt-stressed against control plants, the pairwise differential expression analysis revealed 2728 differentially expressed (DE) proteins in the oil palm genome at False Discovery Rate (FDR) ≤ 0.05 in which 1138 were upregulated ($Log_2(FC) > 0$) and 1590 were downregulated ($Log_2(FC) < 0$) (Table 1, Supplementary Table S1).

Table 1. Differentially expressed (DE) peaks and features in the leaves of young oil palm plants submitted to salinity stress selected by means of three distinct omics platforms (transcriptomics, metabolomics, and proteomics).

Transcriptomics	**Number of Features**	**Up**	**Down**	**Non-DE**
WGS–Proteins	43,551	1138	1590	40,823
Metabolomics	**Number of Peaks**	**Up**	**Down**	**Non-DE**
Positive Polar	2843	18	34	2791
Negative Polar	1855	19	58	1778
Proteomics *	**Number of Features**	**Up**	**Down**	**Non-DE**
LC/MS	813	101	70	642

* Up = Proteins found exclusively in stressed samples + Proteins that attended to statistical criteria of PatternLab V software; Down = Proteins found exclusively in control samples + Proteins that attended to statistical criteria of PatternLab V software [17].

A total of 1165 proteins with 792 distinct K numbers were present among the 2728 DE ones, including 693 enzymes, from which 436 belonged to known pathways (Supplementary Table S1).

The set of 693 enzymes underwent gene ontology analyses, and only the ten most populated groups per GO term are shown in Figure 1. The biological process subgroups with the largest number of representatives were carbohydrate metabolic process, followed by protein phosphorylation and fatty acid biosynthesis process. For molecular function, the most populated subgroups were ATP binding, metal ion binding, and heme binding. Finally, for cellular component the integral component of membrane came in first, followed by cytoplasm and cytosol components.

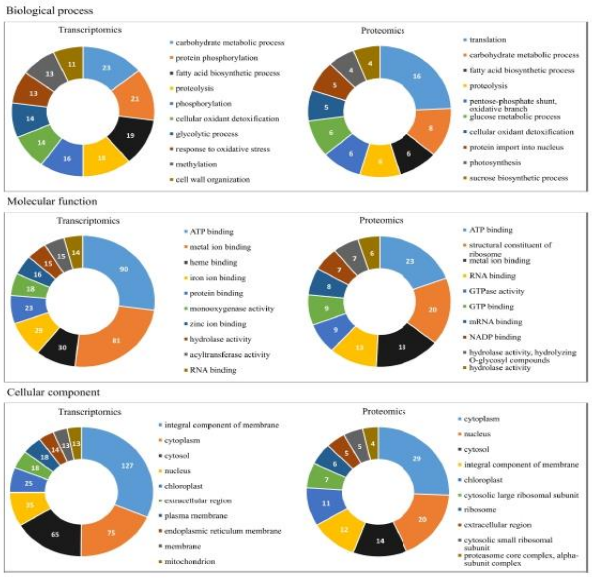

Figure 1. Gene Ontology (GO) annotation classification statistics graph from full-length transcriptome and proteome in the leaves of young oil palm plants under salinity stress; classified accordingly to biological process, cellular component, and molecular function. Only the ten most populated groups per GO term are shown. Numbers represent the amount of positive hits.

Furthermore, the DE enzymes were also classified according to the Enzyme Commission (EC) number, a numerical classification scheme for enzymes based on the chemical reaction. At a first level of classification that involves a general type of enzyme-catalyzed reaction that ranges from one to six, enzymes were dominated by oxidoreductases (EC 1), transferases (EC 2) and hydrolases (EC 3) classes (Figure 2a). In the subclasses of oxidoreductases class (EC 1), DE enzymes were represented mainly by those acting on paired donors, with the incorporation of or reduction in molecular oxygen (EC 1.14), followed by enzymes acting on the CH-OH group of donors (EC 1.1) and acting on the aldehyde or oxo group of donors (EC 1.1). The most representative subclass of transferases class (EC 2) included those with a function of transferring phosphorus-containing groups (EC 2.7), acyltransferases (EC 2.3) and glycosyltransferases (EC 2.4). Finally, the hydrolases (EC 3) had subclasses with compounds involved and acting on ester bonds (EC 3.1), glycosylases (EC 3.2), and acting on peptide bonds (peptidases) (EC 3.4) subclasses that were standing out.

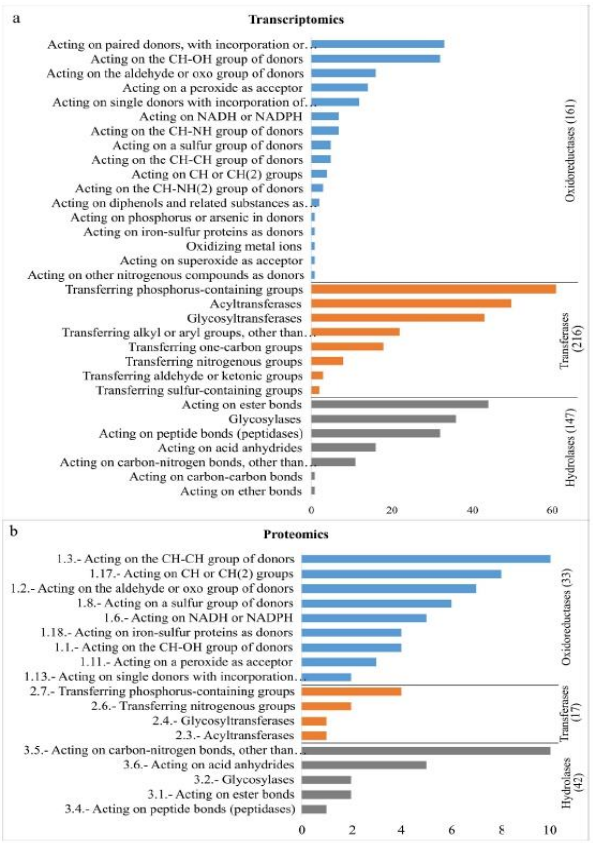

Figure 2. Gene Ontology (GO) annotation classification statistics graph from full-length transcriptome and proteome in the leaves of young oil palm plants under salinity stress; classified accordingly to chemical reactions by which proteins are classified according to E.C. Only the three prevalent classes are shown: oxireductases (EC 1), transferases (EC 2), and hydrolases (EC 3). (**a**)—Transcriptomics Single Analysis, and (**b**)—Proteomics Single Analysis.

2.2. Oil Palm Proteome under Salinity Stress

A global proteomics analysis led to the identification of 3234 and 2872 peptides with high confidence (FDR $\leq$ 0.01) in control and stressed samples, respectively, which infers up to 1809 protein entries from *E. guineensis* proteome (Uniprot) in both conditions—control and stressed (Table 2).

Table 2. Absolute numbers of all peptides and proteins identified via proteomics analysis in the leaves of young oil palm plants submitted to salinity stress.

	Control	Stressed	Total
Peptide Spectrum Match (PSM)	5419	5391	10,808
Total number of peptides	3234	2872	4254
Number of unique peptides	1805	1606	2426
Total number of proteins entries	1497	1436	1809
Total number of proteins using the maximum parsimony criterion	826	831	1019

Approximately 38% of proteins (688) were inferred from more than four peptides, and about 34% (622) had at least one proteotypic peptide observation. A list of all peptides and proteins confidently identified, as well as a simplified list of 1019 proteins according to the maximum parsimony criterion, is presented in Supplementary Tables S2–S4. Control and stressed conditions shared 662 protein identifications; 62 and 89 proteins were uniquely detected in control and stressed samples, respectively (Figure 3a, Supplementary Tables S5–S7).

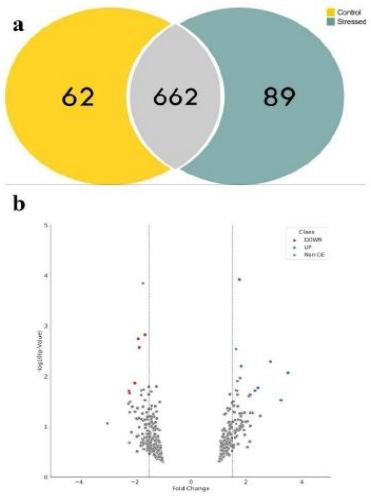

Figure 3. Summary of the proteomics analysis performed on the leaves of young oil palm plants under salinity stress using the PatternLab for Proteomics V software. (**a**) Control and stressed conditions shared 662 protein identifications; 62 and 89 proteins were uniquely detected in control and stressed samples, respectively; (**b**) volcano plot of the differentially abundant proteins reported by Pattern Lab's T Fold module, where 20 proteins showed statistically significant differences in their abundance—proteins in blue were significantly up-regulated while the ones in red were significantly down-regulated between stressed and control samples.

Twenty proteins showed statistically significant differences in their abundance between stressed and control samples (Table 3). As shown in Figure 3b, 12 proteins (in blue) were significantly up-regulated while eight (in red) were significantly down-regulated between stressed and control samples. A group of 642 proteins did not meet the statistical criteria and was not considered for further analysis (Table 1). Our differential abundance analysis considered proteins identified at least in two replicates in each condition. This filtering process decreased the list of 316 and 380 proteins uniquely identified in stressed and control to 89 and 62, respectively.

Table 3. List of the differentially expressed proteins detected in both biological conditions (Stressed and Control) with statistical significance (FDR $\leq$ 0.05).

Entry	Class	Fold Change	*p*-Value	Signal in Control	Signal in Stressed	Gene ID at NCBI	Description
A0A6I9RY35	UP	3.50631	0.00860	0.00027	0.00094	LOC105054572	probable inactive purple acid phosphatase 29
A0A6I9QVF6	UP	3.25426	0.02982	0.00104	0.00340	LOC105040203	GTP-binding nuclear protein
A0A6I9R375	UP	3.25426	0.02982	0.00085	0.00275	LOC105043116	GTP-binding nuclear protein
A0A6I9RFH3	UP	3.25426	0.02982	0.00104	0.00340	LOC105047773	GTP-binding nuclear protein
A0A6I9QCS1	UP	2.87620	0.00511	0.00059	0.00169	LOC105033701	Proteasome subunit alpha type
A0A6I9QQJ4	UP	2.43453	0.01697	0.00103	0.00251	LOC105039272	60S ribosomal protein L35a-1
B3TLX9	UP	2.43453	0.01697	0.00103	0.00251	LOC105037063	60S ribosomal protein L35a-1
A0A6I9QWA8	UP	2.33349	0.01927	0.00071	0.00165	LOC105039716	Succinate-semialdehyde dehydrogenase
A0A6I9RG83	UP	2.14817	0.02330	0.00062	0.00133	LOC105045986	uncharacterized protein LOC105045986
B3TLY5	UP	1.83395	0.00630	0.00105	0.00193	CAT2	Catalase
A0A6I9QQQ6	UP	1.76320	0.00012	0.00068	0.00119	LOC105039332	V-ATPase 69 kDa subunit
A0A6I9R4U7	UP	1.63284	0.00286	0.00276	0.00450	LOC105044322	Malate dehydrogenase
A0A6I9S1Z5	DOWN	−1.63290	0.00151	0.00166	0.00101	LOC105055575	ruBisCO large subunit-binding protein subunit alpha
A0A6I9QJN4	DOWN	−1.84374	0.00267	0.00177	0.00096	LOC105036569	CBBY-like protein
A0A6I9RPV6	DOWN	−1.84374	0.00267	0.00177	0.00096	LOC105051320	CBBY-like protein
A0A6J0PH47	DOWN	−1.88477	0.00179	0.00395	0.00210	LOC105044080	Ferredoxin—NADP reductase, chloroplastic
A0A6I9S9I9	DOWN	−2.00037	0.01375	0.00091	0.00045	LOC105058225	uncharacterized protein LOC105058225
A0A6I9RWU5	DOWN	−2.19127	0.02157	0.00284	0.00129	LOC105054048	actin-101
A0A6I9RC26	DOWN	−2.21145	0.01945	0.00172	0.00078	LOC105047077	sorbitol dehydrogenase isoform X2
A0A6I9RDE7	DOWN	−2.21145	0.01945	0.00172	0.00078	LOC105047077	sorbitol dehydrogenase isoform X1

This group of 171 DE protein sequences—including those found exclusively in control (62) and stressed (89) in at least two replicates and those 20 proteins that attended to the statistical criteria of PatternLab V software—was submitted to functional annotation and MOI analyses. The KEGG mapper reconstruction results revealed 131 proteins with 84 distinct K numbers, including 99 enzymes. Seventy-three enzymes belonged to known pathways and were used in the MOI analysis.

This set of 171 selected proteins was then submitted to gene ontology analyses, and again only the ten most populated groups per GO term are shown in Figure 1. The biological process subgroups with the largest number of proteins were translation, followed by carbohydrate metabolic process, fatty acid biosynthetic process, proteolysis, pentose-phosphate shunt, oxidative branch, and glucose metabolic process. For molecular function, the proteins were mainly distributed in the subgroups of ATP binding, structural constituent of ribosome, and metal ion binding. Finally, the cellular component of the cytoplasm came in first, followed by the nucleus and cytosol.

The prevalent chemical reactions by which proteins were classified according to EC were Oxireductases (EC 1), transferases (EC 2), and hydrolases (EC 3) classes (Figure 2b). In the subclasses of oxidoreductases, the main groups were acting on the CH-CH group of donors (EC 1.3), acting on Ch or CH(2) groups of donors (EC 1.17), and acting on the aldehyde or oxo group of donors (EC 1.2). The most representative subclasses of transferases class included those with a transferring phosphorus-containing groups (EC 2.7) and transferring nitrogenous groups (EC 2.6). For hydrolases, those acting on carbon–nitrogen bonds (EC 3.5) and acting on acid anhydrides (EC 3.6) came first.

2.3. Oil Palm Metabolome under Salinity Stress

Statistical analysis on Metaboanalyst returned 2843 and 1855 peaks, respectively, in the polar-positive and polar-negative fractions (Table 1). Fifty-two peaks were differentially expressed, and eighteen were up-regulated and thirty-four were down-regulated in the polar-positive while seventy-seven were differentially expressed in the polar-negative, in which nineteen were up-regulated and fifty-eight were down-regulated.

All 129 peaks differentially expressed were then submitted to functional interpretation via analysis in the MS Peaks to Pathway module, and the combined mummichog and GSEA pathway meta-analysis resulted in a list of 19 differentially expressed metabolites (DEMs), which was then submitted to the pathway topology analysis module (Table 4). The monobactam biosynthesis (map00261); arginine biosynthesis (map00220); beta-alanine metabolism (map00410); pentose phosphate pathway (map00030); carbon fixation in photosynthetic organisms (map00710); alanine, aspartate and glutamate metabolism (map00250); galactose metabolism (map00052); and glutathione metabolism (map00480) pathways came out as the one with a raw $p \leq 0.05$ (Figure 4).

Table 4. List of metabolites identified in the leaves of young oil palm plants submitted to salinity stress via metabolomics analysis, after submitting the differentially expressed (DE) peaks to the pathway topology analysis module in MetaboAnalyst 5.0. FDR: False Discovery Rate; and FC: Fold Change.

Query Mass	Matched Compound	Matched Form	Mass Difference	Compound Name	FDR	Log_2(FC)
145.01452	C00026	M-H[–]	2.69×10^{-4}	Oxoglutaric acid	0.0106	–0.4146
616.17640	C00032	M[1+]	8.96×10^{-4}	Heme	0.0039	2.8661
106.04953	C00049	M-CO+H[1+]	2.53×10^{-4}	L-Aspartic acid	0.0292	0.9617
306.07651	C00051	M-H[–]	2.27×10^{-5}	Glutathione	0.0204	1.5265
289.03241	C00117	M+CH3COO[–]	3.46×10^{-5}	D-Ribose 5-phosphate	0.0475	–0.9714
427.01748	C00224	M(C13)-H[–]	1.46×10^{-3}	Adenosine phosphosulfate	0.0172	–0.6544
172.98600	C00262	M+K-2H[–]	7.55×10^{-4}	Hypoxanthine	0.0004	–1.5351
203.22237	C00750	M+H[1+]	6.58×10^{-4}	Spermine	0.0036	2.4559
163.04033	C00811	M-H[–]	2.65×10^{-4}	4-Hydroxycinnamic acid	0.0065	–0.3818
162.02134	C01419	M-NH3+H[1+]	6.49×10^{-4}	Cysteinylglycine	0.0263	1.2145

Table 4. *Cont.*

Query Mass	Matched Compound	Matched Form	Mass Difference	Compound Name	FDR	Log_2(FC)
260.02535	C05345	M(C13)-H[–]	4.92×10^{-4}	Beta-D-Fructose 6-phosphate	0.0489	–1.0337
359.11946	C05399	M-H+O[–]	3.09×10^{-5}	Melibiitol	0.0103	–1.6922
254.09610	C05401	M(C13)-H[–]	1.95×10^{-4}	Galactosylglycerol	0.0410	–0.7515
326.09623	C05839	M(C13)-H[–]	6.61×10^{-5}	cis-beta-D-Glucosyl-2-hydroxycinnamate	0.0472	–1.4286
277.06946	C05911	M-CO+H[1+]	1.11×10^{-3}	Pentahydroxyflavanone	0.0143	–1.0759
337.05555	C10107	M+H2O+H[1+]	1.09×10^{-4}	Myricetin	0.0313	–2.4012
337.00976	C11453	M+CH3COO[–]	8.02×10^{-4}	2-C-Methyl-D-erythritol 2,4-cyclodiphosphate	0.0272	0.8232
259.02223	C17214	M+Cl37[–]	1.45×10^{-4}	2-(3′-Methylthio)propylmalic acid	0.0222	–0.9440
447.91027	G00005	M(C13)+2H [2+]	1.30×10^{-3}	(GlcNAc)2 (Man)3 (PP-Dol)1	0.0263	0.4044

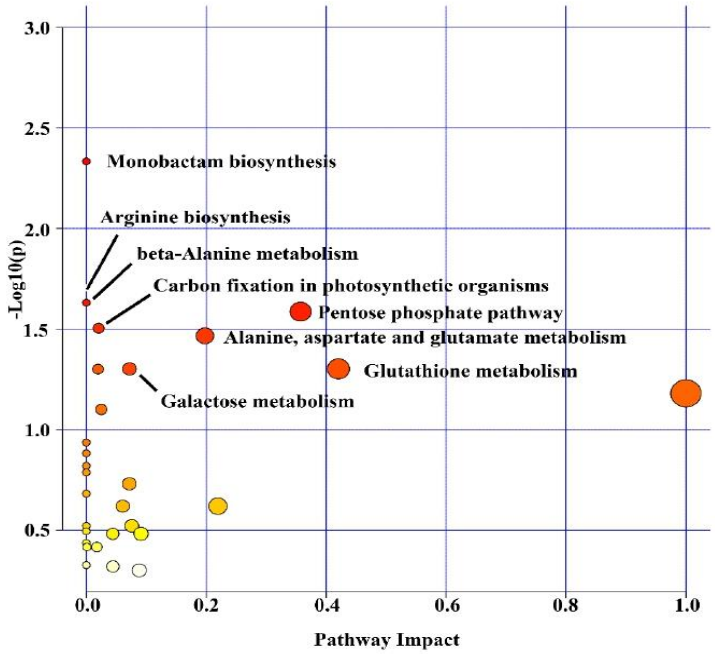

Figure 4. Summary of the pathway analysis in the leaves of young oil palm plants under salinity stress using the Pathway Topology Analysis modules of MetaboAnalyst 5.0. The metabolome view resulted from the analysis in the Pathway Topology Analysis module using the Hypergeometric test, the relative betweenness centrality node importance measure, and the latest KEGG version of the *Oryza sativa* pathway library. Pathway impact takes into account both node centrality parameters—betweenness centrality and degree centrality—and represents the importance of annotated compounds in a specific pathway.

2.4. Integrating Oil Palm Transcriptome, Proteome and Metabolome

A total of 510 enzymes (436 from transcriptomics analysis and 74 from proteomics analysis) (Supplementary Table S8) and 19 metabolites from metabolomics analysis (Table 3), all selected as differentially expressed in the leaves of young oil palm plants (stressed/control), were submitted to MOI analysis.

By applying the Omics Fusion platform to perform the MOI analysis, results revealed a group of eleven pathways affected by salinity stress, and with at least one molecule differentially expressed in each one of the three omics platforms used (Table 5). The Cysteine and methionine metabolism (map00270) and the Glycolysis/Gluconeogenesis (map00010) pathways came tied first in this list, each one with 20 unique molecules from the transcriptome/proteome/metabolome integrative analysis (Supplementary Table S9).

Table 5. List of top eleven pathways affected by salinity stress obtained via Multi-Omics Integration (MOI). Transcriptomics, proteomics, and metabolomics data from leaves of young oil palm plants after being under 0.0 (control) and 2.0 (stressed) g of NaCl/100 g of substrate for 12 days.

Pathway	Pathway ID	Occurrence of Transcripts	Occurrence of Proteins	Occurrence of Metabolites	Occurrence of Unique Molecule
Cysteine and methionine metabolism	270	15	5	2	20
Glycolysis/Gluconeogenesis	10	17	3	1	20
Glyoxylate and dicarboxylate metabolism	630	14	4	1	16
Carbon fixation in photosynthetic organisms	710	12	2	2	15
Glycine, serine and threonine metabolism	260	11	2	1	14
Pentose phosphate pathway	30	10	4	2	14
Glutathione metabolism	480	9	3	3	13
Amino sugar and nucleotide sugar metabolism	520	10	2	1	12
Carbon fixation pathways in prokaryotes	720	7	6	1	11
Citrate cycle (TCA cycle)	20	5	4	1	8
Butanoate metabolism	650	4	2	1	7

3. Discussion

Soil salinization reduces plant growth and productivity of most terrestrial crops with economic importance, including oil palm [13]. In the case of oil palm, Refs. [6,18,19] reported the development of salinization protocols, which are necessary to study the response of *E. guineensis* to this abiotic stress in the search for some intraspecific trait variability. Such protocols are also needed to select tolerant oil palm genotypes developed via genetic engineering or genome editing strategies. These two studies generated not only morphophysiological, biochemical, and molecular insights into the response of this species to this abiotic stress but also reported on the ionic imbalance in the substrate, roots, and leaves of young oil palm plants under salinity stress.

Salinity tolerance is a multigenic trait that governs physiological, biochemical, and molecular mechanisms to facilitate water retention and/or acquisition, protect chloroplast functions, and maintain ion homeostasis [13]. Datasets in genomics, transcriptomics, proteomics, metabolomics, epigenomics, ionomics, and phenomics are accumulating everywhere, intending to gain insights into the mechanisms behind plant interaction with abiotic stresses; however, due to the molecular complexity of such interaction, single-omics analyses (SOA) will have limited power in delivering a more systemic and accurate picture of those responses. Multi-Omics Integration (MOI) strategies [20] are a new window of opportunity facilitating hypothesis generation, leading to the non-trivial challenge of unraveling the mechanisms behind this multigenic trait.

In the present study, SOA showed that carbohydrate metabolism and translation were the most affected biological process subcategories for differentially expressed genes and proteins, respectively. In addition to being a substrate for energy production, carbohydrates

play a role in plant stress perception and signal transduction and can also mediate osmotic regulation and carbohydrate distribution [21].

From the translation point of view, the protein synthesis machinery is quite sensitive to salt since the production of new proteins is crucial for salinity tolerance [22]. Salinity-tolerant species have a more efficient system for regulating transcription, synthesis, and protein processing when compared to sensitive species [23]. Genes encoding the plastid translation machinery in *Arabidopsis thaliana* are salt responsive, indicating a possible role in supporting chloroplast functionality [23]. *Reaumuria soongarica* (Pall.) Maxim., a salt-tolerant species, showed a complex pattern of protein expression, mainly those involved in translation, ribosomal structure, and biogenesis [24].

The dominant molecular function for DE enzymes identified in this study was ATP-binding proteins. These enzymes use the energy of ATP hydrolysis to catalyze a series of chemical reactions [25]. Most ATP-binding proteins are intracellular and extracellular transmembrane proteins, participating in the movement of various molecules and, under stress conditions, in intracellular osmotic balance maintenance [26]. ABC transporters that constitute one of the most populated families of proteins driven by ATP hydrolysis revealed a complex expression pattern in *E. guineensis* under drought stress, pointing to their role in controlling the influx and efflux of chemical molecules while in water scarcity [27].

Integral membrane components, the most affected subcategory of cellular components, include, in this category, proteins incorporated into cell membranes. Salt stress causes damage to the cell membrane, altering its permeability, lipid composition, and enzyme activity [28]. Several factors cause changes in the structure of cell membrane components during salt stress; among them, the excessive production of reactive oxygen species (ROS) is highlighted, which causes conformational changes in membrane proteins and lipid peroxidation, reducing the efficiency of transport systems and increasing membrane permeability [29].

In salinity-tolerant cultivars, an increase in the antioxidant defense system occurs, reducing lipid peroxidation and maintaining adequate levels of membrane permeability. On the other hand, there is an increase in the leakage of electrolytes from the membranes, which indicates a loss of membrane integrity in the sensitive plants [29]. The increase in electrolyte leakage has already been evident in oil palm leaves, indicating possible damage caused by salinity, with direct consequences in photosynthetic capacity reduction and biomass accumulation [18].

In the present study, an attempt to integrate three distinct omics platforms—transcriptomics, proteomics, and metabolomics—was reported for the first time to gain further insights into the mechanisms behind the response of young oil palm plants to salinity stress. The MOI strategy used in the present study is a pathway-based approach for integrating omics datasets. Such integration was only possible due to the selection and characterization of salt-responsive genes coding for enzymes in the oil palm reference genome. Enzymes catalyzing reactions in a metabolic pathway are the bridges to connect transcriptomics, proteomics, and metabolomics datasets in such an integratomics study.

The present MOI study revealed eleven pathways affected by the salinity stress in the leaves of the young oil palm plant, with at least one molecule differentially expressed in all three platforms used. The Cysteine and methionine metabolism (map00270) and Glycolysis/Gluconeogenesis (map00010) pathways were the most affected ones. Even though this study identified other pathways, further discussion will concentrate only on these two.

Reactions that promote cysteine (Cys) biosynthesis are involved in the pathway of cysteine and methionine metabolism [30]. Cys acts as a sulfur donor for the biosynthesis of many essential bio-molecules, such as methionine, vitamins, co-factors, and Fe-S groups, and for the production of glutathione (GSH), considered the principal determinant of cellular redox homeostasis [30]. The enzymes serine O-acetyltransferase (EC 2.3.1.30) and cysteine synthase (EC 2.5.1.47) usually carry out the Cysteine biosynthesis in two

steps. These enzymes are highly conserved in plants and are responsible for maintaining homeostasis between cysteine consumption and sulfate reduction [31].

Among the enzymes integrated into the cysteine and methionine metabolism pathway, seven and twelve were up- and down-regulated in the leaves of young oil palm plants under salinity stress, respectively. Serine O-acetyltransferase experienced an approximately 11-fold increase in expression, while L-lactate dehydrogenase experienced a decrease of about 90% in its original expression level. As cysteine is the first organic compound in the primary metabolism of sulfate, the elevated transcription of serine O-acetyltransferase may indicate that sulfate entry into the pathway plays a role in the saline stress response in oil palm. In tobacco, plants over-expressing bacterial serine O-acetyltransferase conferred resistance to high levels of oxidative stress with a four-fold higher cysteine expression [32]. Recently, Ref. [33] demonstrated that the exogenous application of nitric oxide (NO), a compound that regulates the response to different stresses in plants, increased the content of enzymes synthesizing Cys, helping maintain the cellular homeostasis in plants under the osmotic tension.

Amino acid methionine has nutritional value for plants, participating in the initiation of translation, in addition to being a precursor of S-Adenosyl methionine (SAM), the donor of the methyl group that regulates different essential cellular processes, such as cell division, synthesis cell wall, chlorophyll synthesis, and membrane synthesis [34]. SAM is synthesized from adenosine triphosphate (ATP) and methionine by the enzyme S-adenosylmethionine synthetase—SAMS (EC 2.5.1.6). The present study showed that this enzyme had a 2.6 fold increase in expression under salinity stress. Overexpression of the SsSAMS2 gene from the halophyte plant of *Suaeda salsa* L. in transgenic tobacco plants enhanced salt tolerance, as indicated by maintaining a higher photosynthetic rate and accumulation of more biomass [35].

GSH is a low molecular weight thiol crucial for maintaining the regulation of cellular redox homeostasis [30]. Two ATP-dependent enzymes, glutamate-cysteine ligase (EC:6.3.2.2) and GSH synthetase (EC:6.3.2.3), catalyze GSH synthesis from cysteine, glutamate, and glycine [36]. In the present study, the metabolite glutathione (C00051) upregulated 2.9 fold while the enzyme glutathione synthase downregulated to 70% of its original levels in the leaves of young oil palm plants under salinity stress. Meanwhile, all versions of glutamate–cysteine ligase found in the reference genome of oil palm [37,38] were non-DE. The exogenous application of GSH reversed the effects of salt stress on seedlings of tomatoes, as well as the expression and activities of enzymes related to the synthesis and metabolism of GSH, including gamma-glutamylcysteine synthetase (γ-ECS) and glutathione synthetase (GS), among others [39].

The glycolysis pathway directly supplies energy to plant cells from reactions that oxidize hexoses to produce ATP and pyruvate, the latter acting as a substrate for entry into the citric acid cycle (TCA). Conversely, the gluconeogenesis pathway synthesizes hexoses using low molecular weight compounds to meet energy needs under the conditions of reduced glucose supply [40]. The ATP-dependent 6-phosphofructokinase 2 (PKF) and pyruvate kinase (PK) enzymes from the glycolytic pathway did downregulate in the leaves of young oil palm plants under saline stress. Those two enzymes, together with hexokinase, are regulators of glycolysis, as they participate in irreversible reactions [40]. The energy production via glycolysis plays a role in the saline stress response in plants as it provides ATP to support the stress condition [41].

That was evident in the study by [41], where salt stress inhibited the growth of *Cucumis sativus* L. with a significant reduction in ATP production rates [41] and applied exogenous putrescine (Put), reversing the saline stress with positive modulation in the PFK and PK levels. In halophyte species *Bruguiera sexangular*, both PFK and PK enzymes increased expression in response to long-term salinity [42]. This suggests that increased PFK and PK activity increases the activity of the glycolytic pathway to maintain normal physiological metabolism under saline stress conditions in halophyte species. Salinity stress possibly

promoted a reduction in ATP production as it negatively affected enzymes in the flow of glycolysis and TCA in oil palm.

Fructose-1,6-bisphosphatase (FBPase) and phosphate dikinase (PPDK), enzymes of the gluconeogenesis pathway, were negatively regulated in oil palm under salt stress. Under saline stress conditions, the active synthesis of sugars by this route contributes to mitigating the osmotic stress effect resulting from the submission of plants to a saline environment. In maize (*Zea mays* L.), the photosynthesis rate was similar between control plants and plants under neutral salt stress, suggesting that gluconeogenesis acted on the active synthesis of sugars and the maintenance of osmotic balance [43].

The overexpression of TaFBA-10 in *A. thaliana* (L.) Heynh increased FAB activity with positive effects on scavenging ROS under cold stress, whereas chlorophyll content was severely affected [44]. The PPDK enzyme, in turn, is an enzyme involved in the regulation of the C4 pathway in plants. PPDK enzyme activity increases in salinity tolerant accessions of *Miscanthus sinensis* Andersson [45]. In this manner, the activity of this enzyme compensates for the suppression of the Calvin Cycle by saline stress.

Another enzyme that participates in energy production is L-lactate dehydrogenase type B (LDH). This enzyme did downregulate in young oil palm plants under salinity stress. Lactate dehydrogenase (LDH) converts pyruvate to lactate that regenerates NAD + to maintain cellular respiration under anaerobic conditions. Under flood stress conditions, the initiation of fermentation responds to keeping energy supply in hypoxia conditions [46]. The downregulation of the LDH enzyme in palm oil at 12 DAT indicates a deficiency in response to salinity stress and may indicate a possible anaerobic condition caused by it.

Vieira and colleagues showed that young oil palm plants are sensitive to high concentrations of NaCl [6]. The present MOI study, which used datasets generated from leaf tissue collected by Vieira and colleagues, showed that enzymes competing for energy production in the glycolysis and gluconeogenesis pathways were negatively affected by salinity stress in the leaves of young oil palm plants. Concomitantly, gluconeogenesis, which involves the synthesis of glucose from non-carbohydrate substances, apparently does not represent an immediate response to reduced glucose supply in this oilseed crop under such stress.

The samples for transcriptome, metabolome, and proteome analyses were collected at once, exactly 12 days after the onset of the stress, using a split sample study design. In terms of data integration, accordingly to [47], the ideal situation is to have samples originating from the same biological source material and obtained at the same time—a piece of tissue may be cut into several sections and one used for a specific omics platform analysis, whilst the other is used to another one. In such design, the samples are more similar in that they all are assumed to produce data without batch effects between the different omics data sets [47].

It is clear that the small number of DE metabolites was the main limitation of the pathway-based MOI approach used in this study. The biggest number of DE metabolites in the eleven most affected pathways identified in the MOI analysis was three, while there were up to six proteins and 17 transcripts. The possible main reason to the fact that only 19 metabolites were differentially expressed in the leaves of young oil palm plants submitted to salinity stress was the mmetabolomics approach used. The untargeted metabolomics is an exciting technology for searching for novel metabolic perturbations in various biological systems, allowing the profile of many hundreds or thousands peaks with varying chemical properties at once; however, there are still various obstacles, such as the limited capability to identify novel compounds of interest and the need for advanced and more robust databases [48]. In the present study, we used the latest KEGG version of the *O. sativa* pathway library.

4. Materials and Methods

4.1. Plant Material, Experimental Design and Saline Stress

The oil palm plants used in this study were clones regenerated out of embryogenic calluses obtained from the leaves of an adult plant—genotype AM33, a Deli × Ghana from

ASD Costa Rica, as previously reported by [6]. Before starting the experiments, plants were standardized accordingly to the developmental stage, size, and number of leaves. They were in the growth stage known as bifid saplings, and the experiment was performed in March 2018 in a greenhouse at Embrapa Agroenergy in Brasília, DF, Brazil (S-15.732°, W-47.900°). The main environmental variables (temperature, humidity, and radiation) fluctuated according to the weather conditions and underwent monitoring throughout the entire experimental period using the data collected at a nearby meteorological station (S-15.789°, W-47.925°).

The experiment consisted of five salinity levels (0.0, 0.5, 1.0, 1.5, and 2.0 g of NaCl per 100 g of substrate (a mixture of vermiculite, soil, and the Bioplant commercial substrate (Bioplant Agrícola Ltda, Nova Ponte, MG, Brazil), in a 1:1:1 ratio, on a dry basis), with four replicates in a completely randomized design (for additional details, see [6]). The substrate mixture was fertilized using 2.5 g L^{-1} of the N-P2O5-K2O formula (20-20-20). For the omics (transcriptomics, metabolomics, and proteomics) analysis described in the present study, we collected the apical leaves from control and stressed plants (0.0 and 2.0 g of NaCl per 100 g of substrate) 12 days after imposition of the treatments (DAT).

4.2. Transcriptomics Data Analysis

Leaves harvested from control and stressed plants were immediately immersed in liquid nitrogen and stored at −80 °C until RNA extraction; three plants for treatments. Details regarding total RNA extraction and quality analysis, library preparation, and sequencing are in [15,19]. RNA-Seq raw sequence data are in the Sequence Read Archive (SRA) database of the National Center for Biotechnology Information (NCBI) under BioProject number PRJNA573093.

All the transcriptomics analysis was performed with OmicsBox platform—version 2.0.36 [49], as previously described by [15,17]. The oil palm genome [19,20]—downloaded from NCBI (BioProject PRJNA268357; BioSample SAMN02981535) in September 2021—was the reference genome for RNA-Seq data alignment. The pairwise differential expression analysis between experimental conditions (Stressed Plants—12 DAT X Control—12 DAT) was performed through edgeR software version 3.28.0 [50], applying a simple design and an exact statistical test without the use of a filter for low counts genes.

4.3. Proteomics Data Analysis

Leaves samples for proteomics analysis were harvested, immediately immersed in liquid nitrogen, and then stored at −80 °C until protein extraction; three plants for control and three from stressed plants. Approximately 5.0 g of ground tissue—with 0.02 g/g of PVP (polyvinylpolypyrrolidone) added to it—was weighed and mixed with 3.0 mL of buffer (50 mM Tris HCl + 14 mM β-mercaptoethanol, pH 7.5) and 30 µL of protease inhibitor. After gently stirring the suspension on ice for 10 min, it was centrifuged at 10.000 G at 4.0 °C for 15 min. Then, 1.0 mL of the supernatant was transferred to 2.0 mL microtubes, mixed with 1.0 mL of 10% TCA (trichloroacetic acid) solution in acetone, kept at −20 °C for 2 h for protein precipitation, and then centrifuged at 10,000 G at 4.0 °C for 15 min. The protein pellet underwent wash with ice-cold 80% acetone, followed by centrifugation under the same conditions as above. After washing twice, we stored it at −80 °C until protein quantification [51] and visualization in an SDS-PAGE Gel.

After protein quantification, all samples went to the GenOne company (Rio de Janeiro, RJ, Brazil) fort protein preparation and LC-MS/MS analysis. After undergoing treatment with 10 mM DTT at 56 °C for 30 min, followed by 40 mM iodoacetamide (IDA) at room temperature in the dark and also for 30 min. Then, samples were incubated for 20 h at 37 °C with trypsin (1:50) in a thermomixer at 800 rpm. At last, after adding 50 µL of 95% acetonitrile and 5% TFA, samples were stirred three times at 1000 rpm for 15 min for tryptic peptides extraction, vacuum dried, and dissolved in 20 µL of 0.1% formic acid in water.

For a global proteomics analysis, we adopted a label-free quantitation approach using spectral counting by LC-MS/MS passing the samples through a nano-high performance

liquid chromatography (EASY 1000; Thermo Fisher, Waltham, MA, USA) coupled to Orbitrap Q Exactive Plus (Thermo Scientific, Waltham, MA, USA) mass spectrometer. An MS scan spectra ranging from 375 to 2000 m/z were acquired using a resolution of 70,000 in the Orbitrap. We used the Xcalibur software (version 2.0.7) (Thermo Scientific, Waltham, MA, USA) to obtain the data in biological triplicates.

The PatternLab for Proteomics V software [23] was used to process the raw files. We used the Comet algorithm [52], the *E. guineensis* Uniprot reference database (30,667 entries), and 123 common contaminant proteins (Proteome ID: UP000504607) to perform peptide sequence matching (PSM) and employed a target-reverse strategy to increase confidence in protein identifications [53]. The search considered semi-specific candidates and allowed a maximum of two missed cleavages. Fixed cysteine carbamidomethylation and variable methionine oxidation were applied; the Comet search engine used a precursor mass tolerance of 40 ppm and a fragment compartment tolerance of 0.02.

We employed the SEPro—Search Engine Processor—module of PatternLab [54] to validate the peptide spectrum matches and, subsequently, grouped identifications by enzymatic specificity (semi-specific), resulting in two distinct subgroups. Then, we applied XCorr, DeltaCN, Spectral Counting Score, and Peaks Matched values to generate a Bayesian discriminator. SEPro automatically establishes a cutoff score to accept a 1% false discovery rate (FDR) based on the number of decoys performed independently on each subset of data, resulting in a false positive rate independent of the triptych status. We chose a minimum sequence length of six amino acid residues and discarded similar proteins that represent an identical sequence and consist of a fragment of another one. At last, a final list of mapped proteins was composed only of PSMs with less than five ppm.

4.4. Metabolomics Data Analysis

Leaves harvested from control and stressed plants were immediately immersed in liquid nitrogen and stored at −80 °C until metabolite extraction: four plants for treatments. Before solvent extraction, all samples underwent grounding in liquid nitrogen. The solvents used were methanol grade UHPLC, acetonitrile grade LC-MS, formic acid grade LC-MS, sodium hydroxide ACS grade LC-MS, all from Sigma-Aldrich, and water treated in a Milli-Q system from Millipore. We employed a well-established protocol [16,55,56] to extract the metabolites in three phases (polar, non-polar, and protein pellet). Aliquots of 50 mg of ground sample were transferred to 2 mL microtubes, and then 1 mL of a mixture of 1:3 (*v:v*) methanol/methyl tert-butyl ether (MTBE) at −20 °C was added. Homogenization on an orbital shaker at 4.0 °C and ultrasound treatment in an ice bath were each performed for 10 min. As the next step, we added 500 µL of a mixture of 1:3 (*v:v*) methanol/water to each microtube. After centrifugation (15,300× g at 4.0 °C for 5 min), an upper non-polar (green) and a lower polar (brown) phase and a protein pellet remained in each microtube. After transferring both fractions separately to 1.5 mL microtubes, they were submitted to a Speed vac system (Centrivap, Labconco) to be vacuum dried. Finally, the dry-fraction, resuspended in 500 µL of 1:3 (*v:v*) methanol and water mixture and transferred to vials, were now ready for analysis.

Analytical method UHPLC–MS/MS (ultra-high performance liquid chromatography and tandem mass spectrometry) was used in this study. The UHPLC system (Nexera X2, Shimadzu Corporation, Kyoto, Japan) was equipped with a reverse-phase column from Waters Technologies (Acquity UPLC HSS T3, 1.8 µm, 2.1 by 150 mm at 35 °C). Solvent A was 0.1% (*v:v*) formic acid in water and solvent B was 0.1% (*v:v*) formic acid in acetonitrile/methanol (70:30, *v:v*). The gradient elution used, with a flow rate of 0.4 mL min^{-1}, was as follows: 0–1 min isocratic, 0% B; 1–3 min, 5% B; 3–10 min, 50% B; 10–13 min, 100% B; 13–15 min isocratic, 100% B; then, 5 min rebalancing was conducted to the initial conditions. The rate of acquisition spectra was 3.00 Hz, mass range *m/z* 70–1200 for the polar fraction analysis and *m/z* 300–1600 for the lipidic fraction.

High-resolution mass spectrometry was used for detection (MaXis 4G Q-TOF MS, Bruker Daltonics) equipped with an electrospray source in positive (ESI-(+)-MS) and

negative (ESI-(−)-MS) modes. The settings of the mass spectrometer were as follows: capillary voltage, 3800 V; dry gas flow, 9 L min^{-1}; dry temperature, 200 °C; nebulizer pressure, 4 bar; final plate offset, 500 V. For the external calibration of the equipment, we used a sodium formate solution (10 mM HCOONa solution in 50:50 *v:v* isopropanol and water containing 0.2% formic acid) injected through a six-way valve at the beginning of each chromatographic run. Ampicillin ([M+H] + *m/z* 350.1186729 and [M-H]- *m/z* 348.1028826) was the internal standard for later peak normalization on data analysis.

DataAnalysis 4.2 software (Bruker Daltonics, Bremen, Germany) was the first used to analyze the raw data from UHPLC-MS, as mzMXL files. Pre-processing of data was performed using XCMS Online [57,58], including peak detection, retention time correction, and alignment of the metabolites. CentWave was used for peak detection ($\Delta m/z$ = 10 ppm; minimum peak width, 5 s; maximum peak width, 20 s). For the alignment of retention times, the parameters were as follows: mzwid = 0.015; minfrac = 0.5; bw = 5. The unpaired parametric *t*-test (Welch t-test) was used for the statistical analysis at the pre-processing stage. Then, a data set was created from control (0.0 g) and stressed plants subjected to NaCl/100 g of the fresh substrate at 12 DAT. All with four biological repeats.

The pre-processed data (csv file) underwent analysis in the Statistical Analysis module of the MetaboAnalyst 5.0 [59,60]. The scaling used was the Pareto method [61]. Afterward, the differentially expressed peaks (DEPs) selected were those passing the criteria of false rate discovery (FDR) ≤ 0.05 and Log_2 (fold change (FC)) $\neq 1$. When using the MS Peaks to Pathway module to analyze the selected DEPs, we employed the following parameters: molecular weight tolerance of 5 ppm; mixed ion mode; joint analysis using both the mummichog [62] and Gene Set Enrichment Analysis—GSEA [63] algorithms; the latest KEGG version of the *O. sativa* pathway library. The *p*-value cutoff from the mummichog algorithm was at 1.0×10^{-5}.

When two or more matched forms were observed as DEP (in the case of isotopes), the mass error was the criteria for the feature selection for the comparison with metabolite databases, keeping the smallest [56]. The mass error was also the criteria in the case of a single matched compound relative to two or more DEPs. The mass spectra of all DEPs underwent analysis for more information about the adduct forms obtained from the database comparison. Subsequently, we performed the putative annotation of the metabolites of interest by applying the filtered exact mass data to the molecular formula from KEGG.

Finally, the KEGG IDs of the matched compounds were submitted to the pathway analysis module for visualization through integrating enrichment and pathway topology analysis [64]. Parameter sets were as follows: the hypergeometric test and the latest KEGG version of the *O. sativa* pathway library.

4.5. Functional Annotation and Itegratomics Analysis

The results obtained using OmicsBox and PatternLab V underwent a functional classification. Distinct multiFASTA files generated were submitted to the functional classification in the BlastKOALA platform [64].

The approach used to integrate the three omics was pathway mapping, and the analysis was performed using the Omics Fusion platform [65]. Previously to the integration of multi-omics data, the NCBI accession of transcripts related to enzymes was converted to UniProt ID. Thus, the input data used were the IDs of each omics, which include UniProt Accession for transcriptomics and proteomics, and KEGG ID for metabolomics. Firstly, the data were enriched through several databases (EMBL, KEGG, NCBI, and UniProt), and then the module "KEGG feature distribution" was used to map these omics data in known pathways.

5. Conclusions

Previously, in addition to showing that young oil palm submitted to a high concentration of NaCl reduces the rates of CO_2 assimilation, stomatal conductance to water vapor,

and transpiration, our group also confirmed a preponderant role of transcription factors in the early response of oil palm plants to salinity stress [6,15]. Data from ionomics, phenomics, and transcriptomics (mRNA and miRNA) were employed to show that. Currently, two new omics platforms joined this list—metabolomics and proteomics—and a first MOI study was performed. For phenomics–morphophysiological characterization, data came from two salinity stress experiments carried out in November 2017 and March 2018, and all the transcriptome, metabolome, and proteome data came from one of the experiments at once, 12 days after the onset of the stress, using a split-sample study design. Extensive leaf necrosis was already visible when the samples from the stressed treatment (electrical conductivity of ~40 dS m^{-1}) were collected, and one must consider that when analyzing these omics data sets.

The SOA and MOI studies here reported generated new insights on the response the early response of oil palm plants to salinity stress, pointing out genes, proteins, metabolites, and pathways directly affected by this stress. The eleven pathways identified by MOI analysis definitely appear at the top of the list as priorities for further studies. However, it is clear that two factors limited the accomplishments of the MOI study—the small number of differentially expressed metabolites identified via an untargeted metabolomics approach and the lack of data regarding the Log_2(FC) from the proteins found exclusively in the control and stressed treatments when using the global proteomics analysis. No Log_2(FC) from most of the DE proteins was identified, and only 19 DE metabolites limited the use of correlation studies.

Supplementary Materials: The following supporting information can be downloaded at: https://www.mdpi.com/article/10.3390/plants11131755/s1, Table S1: Proteins from the oil palm genome differentially expressed (FDR $\leq$ 0.05) in the leaves of young oil palm plants under salinity stress. FC—Fold Change; CPM—Count Per Million; FDR—False Discovery Rate; Kegg Orthology number; E.C. number; Table S2: a—List of all peptides confidently identified in oil palm conditions; b—list of all proteins confidently identified in oil palm conditions; c—all proteins confidently identified in oil palm conditions with maximum parsimony criterion; Table S3: a—list of the proteins detected only in control biological condition; b—list of the proteins detected only in stressed biological condition; c—list of all differentially expressed proteins detected in both biological conditions (Stressed and Control) with statistical significance (FDR $\leq$ 0.05); Table S4: a—list of 510 differentially expressed enzymes (436 from transcriptomics and 74 from proteomics) prospected in the transcriptome and proteome of young oil palm plants under salinity stress and submitted to integrative analysis; b—The top two pathways with the largest number of components and its description, obtained from transcriptomics, proteomics, and metabolomics integrative analysis using the Omics Fusion platform. Table S5: List of the proteins detected only in control biological condition; Table S6: List of the proteins detected only in stressed biological condition; Table S7: List of all proteins detected in both biological conditions (Stressed and Control) with statistical significance (FDR $\leq$ 0.05); Table S8: List of 510 differentially expressed enzymes (436 from transcriptomics and 74 from proteomics) prospected in the transcriptome and proteome of young oil palm plants under salinity stress and submitted to integrative analysis; Table S9: The top two pathways with the largest number of components and its description, obtained from transcriptomics, proteomics, and metabolomics integrative analysis using the Omics Fusion platform.

Author Contributions: Conceptualization: C.A.F.d.S., P.V.A. and M.T.S.J.; methodology, investigation, data curation, and formal analysis: C.B.B., T.L.C.d.S., J.C.R.N., L.R.V., A.P.L. and J.A.d.A.R.; funding acquisition and supervision: M.T.S.J.; writing—original draft: C.B.B., T.L.C.d.S. and J.C.R.N.; writing—review and editing: C.A.F.d.S. and M.T.S.J. All authors have read and agreed to the published version of the manuscript.

Funding: This work was funded by the Brazilian Innovation Agency—FINEP (01.13.0315.00 DendêPalm Project)—and the Coordination for the Improvement of Higher Education Personnel–CAPES (Scholarships for C.B.B., T.L.C.d.S., and L.R.V.). The funding bodies covered all student and project costs but were not involved in the design, collection, analysis and interpretation of the data or the preparation of the manuscript.

Data Availability Statement: The data sets used and/or analyzed during the current study are available from the corresponding author upon reasonable request.

Conflicts of Interest: The authors declare no conflict of interest.

References

1. Qaim, M.; Sibhatu, K.T.; Siregar, H.; Grass, I. Environmental, Economic, and Social Consequences of the Oil Palm Boom. *Annu. Rev. Resour. Econ.* **2020**, *12*, 321–344. [CrossRef]
2. Shahbandeh, M. Production Volume of Palm Oil Worldwide from 2012/13 to 2021/22. Available online: https://www.statista.com/statistics/613471/palm-oil-production-volume-worldwide/ (accessed on 21 February 2022).
3. Ahmad, F.B.; Zhang, Z.; Doherty, W.O.S.; O'Hara, I.M. The Outlook of the Production of Advanced Fuels and Chemicals from Integrated Oil Palm Biomass Biorefinery. *Renew. Sustain. Energy Rev.* **2019**, *109*, 386–411. [CrossRef]
4. Furumo, P.R.; Aide, T.M. Characterizing Commercial Oil Palm Expansion in Latin America: Land Use Change and Trade. *Environ. Res. Lett.* **2017**, *12*, 024008. [CrossRef]
5. Bentes, E.d.S.; Homma, A.K.O. *Importação e Exportação de Óleo e Palmiste de Dendezeiro no Brasil (2010–2015)*; Embrapa Amazônia Oriental: Belém, Brazil, 2016.
6. Vieira, L.R.; Silva, V.N.B.; Casari, R.A.d.C.N.; Carmona, P.A.O.; Sousa, C.A.F.d.; Souza Júnior, M.T. Morphophysiological Responses of Young Oil Palm Plants to Salinity Stress. *Pesqui. Agropecuária Bras.* **2020**, *55*, e01835. [CrossRef]
7. Bittencourt, C.B.; Lins, P.d.C.; Boari, A.d.J.; Quirino, B.F.; Teixeira, W.G.; Souza Júnior, M.T. Oil Palm Fatal Yellowing (FY), a Disease with an Elusive Causal Agent. In *Elaeis Guineensis*; IntechOpen: London, UK, 2022.
8. Costa, S.J.d.; Erasmo, E.A.L.; Tavares, T.C.d.O.; Silva, J. Respostas Fisiológicas de Dendê Submetidas ao Estresse Hídrico em Condições do Cerrado. *Rev. Bras. Agropecuária Sustentável* **2018**, *8*. [CrossRef]
9. Azevedo, J.A.d.; Junqueira, N.T.V.; Braga, M.F.; de Sá, M.A.C. *Parâmetros de Irrigação Durante o Período Seco em Plantas Jovens de Dendê Cultivadas no Cerrado*; Comunicado Técnico; Embrapa Cerrados: Brasília, Brazil, 2008.
10. Antonini, A.J.C.d.A.; Oliveira, A.D.d. *Potencial de Cultivo da Palma de Óleo Irrigada nas Condições do Cerrado*; Documentos/Embrapa Cerrados; Empresa Brasileira de Pesquisa Agropecuária: Brasília, Brazil, 2021.
11. Shahid, S.A.; Zaman, M.; Heng, L. Soil Salinity: Historical Perspectives and a World Overview of the Problem. In *Guideline for Salinity Assessment, Mitigation and Adaptation Using Nuclear and Related Techniques*; Springer International Publishing: Cham, Switzerland, 2018; pp. 43–53.
12. Carillo, P.; Grazia, M.; Pontecorvo, G.; Fuggi, A.; Woodrow, P. Salinity Stress and Salt Tolerance. In *Abiotic Stress in Plants-Mechanisms and Adaptations*; InTech: Rijeka, Croatia, 2011; pp. 21–38.
13. Isayenkov, S.V.; Maathuis, F.J.M. Plant Salinity Stress: Many Unanswered Questions Remain. *Front. Plant Sci.* **2019**, *10*, 80. [CrossRef]
14. Liang, W.; Ma, X.; Wan, P.; Liu, L. Plant Salt-Tolerance Mechanism: A Review. *Biochem. Biophys. Res. Commun.* **2018**, *495*, 286–291. [CrossRef]
15. Salgado, F.F.; Vieira, L.R.; Silva, V.N.B.; Leão, A.P.; Grynberg, P.; do Carmo Costa, M.M.; Togawa, R.C.; de Sousa, C.A.F.; Júnior, M.T.S. Expression Analysis of MiRNAs and Their Putative Target Genes Confirm a Preponderant Role of Transcription Factors in the Early Response of Oil Palm Plants to Salinity Stress. *BMC Plant Biol.* **2021**, *21*, 518. [CrossRef]
16. Rodrigues-Neto, J.C.R.; Vieira, L.R.; de Aquino Ribeiro, J.A.; de Sousa, C.A.F.; Júnior, M.T.S.; Abdelnur, P.V. Metabolic Effect of Drought Stress on the Leaves of Young Oil Palm (*Elaeis guineensis*) Plants Using UHPLC–MS and Multivariate Analysis. *Sci. Rep.* **2021**, *11*, 18271. [CrossRef]
17. Santos, M.D.M.; Lima, D.B.; Fischer, J.S.G.; Clasen, M.A.; Kurt, L.U.; Camillo-Andrade, A.C.; Monteiro, L.C.; de Aquino, P.F.; Neves-Ferreira, A.G.C.; Valente, R.H.; et al. Simple, Efficient and Thorough Shotgun Proteomic Analysis with PatternLab V. *Nat. Protoc.* **2022**, 17. [CrossRef]
18. Cha-Um, S.; Takabe, T.; Kirdmanee, C. Ion Contents, Relative Electrolyte Leakage, Proline Accumulation, Photosynthetic Abilities and Growth Characters of Oil Palm Seedlings in Response to Salt Stress. *Pak. J. Bot.* **2010**, *42*, 2191–2200.
19. Ferreira, T.M.M.; Leão, A.P.; Sousa, C.A.F.d.; Souza Júnior, M.T. Genes Highly Overexpressed in Salt-Stressed Young Oil Palm (*Elaeis guineensis*) Plants. *Rev. Bras. Eng. Agrícola Ambient.* **2021**, *25*, 813–818. [CrossRef]
20. Jamil, I.N.; Remali, J.; Azizan, K.A.; Nor Muhammad, N.A.; Arita, M.; Goh, H.-H.; Aizat, W.M. Systematic Multi-Omics Integration (MOI) Approach in Plant Systems Biology. *Front. Plant Sci.* **2020**, *11*, 944. [CrossRef]
21. Jiao, Y.; Zhang, J.; Pan, C. Integrated Physiological, Proteomic, and Metabolomic Analyses of Pecan Cultivar 'Pawnee' Adaptation to Salt Stress. *Sci. Rep.* **2022**, *12*, 1841. [CrossRef]
22. Mostek, A.; Börner, A.; Badowiec, A.; Weidner, S. Alterations in Root Proteome of Salt-Sensitive and Tolerant Barley Lines under Salt Stress Conditions. *J. Plant Physiol.* **2015**, *174*, 166–176. [CrossRef]
23. Omidbakhshfard, M.A.; Omranian, N.; Ahmadi, F.S.; Nikoloski, Z.; Mueller-Roeber, B. Effect of Salt Stress on Genes Encoding Translation-Associated Proteins in *Arabidopsis thaliana*. *Plant Signal. Behav.* **2012**, *7*, 1095–1102. [CrossRef]
24. Yan, S.; Chong, P.; Zhao, M.; Liu, H. Physiological Response and Proteomics Analysis of *Reaumuria soongorica* under Salt Stress. *Sci. Rep.* **2022**, *12*, 2539. [CrossRef]

25. Chauhan, J.S.; Mishra, N.K.; Raghava, G.P. Identification of ATP Binding Residues of a Protein from Its Primary Sequence. *BMC Bioinform.* **2009**, *10*, 434. [CrossRef]
26. Dahuja, A.; Kumar, R.R.; Sakhare, A.; Watts, A.; Singh, B.; Goswami, S.; Sachdev, A.; Praveen, S. Role of ATP-binding Cassette Transporters in Maintaining Plant Homeostasis under Abiotic and Biotic Stresses. *Physiol. Plant.* **2021**, *171*, 785–801. [CrossRef]
27. Wang, L.; Lee, M.; Ye, B.; Yue, G.H. Genes, Pathways and Networks Responding to Drought Stress in Oil Palm Roots. *Sci. Rep.* **2020**, *10*, 21303. [CrossRef]
28. Guo, Q.; Liu, L.; Barkla, B.J. Membrane Lipid Remodeling in Response to Salinity. *Int. J. Mol. Sci.* **2019**, *20*, 4264. [CrossRef]
29. Mansour, M.M.F. Plasma Membrane Permeability as an Indicator of Salt Tolerance in Plants. *Biol. Plant* **2013**, *57*, 1–10. [CrossRef]
30. Couturier, J.; Chibani, K.; Jacquot, J.-P.; Rouhier, N. Cysteine–Based Redox Regulation and Signaling in Plants. *Front. Plant Sci.* **2013**, *4*, 105. [CrossRef]
31. Hell, R.; Wirtz, M. Metabolism of Cysteine in Plants and Phototrophic Bacteria. In *Sulfur Metabolism in Phototrophic Organisms*; Springer: Berlin/Heidelberg, Germany, 2008; Volume 27, pp. 59–91.
32. Blaszczyk, A.; Brodzik, R.; Sirko, A. Increased Resistance to Oxidative Stress in Transgenic Tobacco Plants Overexpressing Bacterial Serine Acetyltransferase. *Plant J.* **1999**, *20*, 237–243. [CrossRef]
33. Khan, M.N.; Mobin, M.; Abbas, Z.K.; Siddiqui, M.H. Nitric Oxide-Induced Synthesis of Hydrogen Sulfide Alleviates Osmotic Stress in Wheat Seedlings through Sustaining Antioxidant Enzymes, Osmolyte Accumulation and Cysteine Homeostasis. *Nitric Oxide* **2017**, *68*, 91–102. [CrossRef]
34. Amir, R.; Hacham, Y. Methionine Metabolism in Plants. In *Sulfur: A Missing Link between Soils, Crops, and Nutrition*; American Society of Agronomy, Inc.: Madison, WI, USA, 2008; Volume 50, pp. 251–279.
35. Qi, Y.-C.; Wang, F.-F.; Zhang, H.; Liu, W.-Q. Overexpression of *Suadea salsa* S-Adenosylmethionine Synthetase Gene Promotes Salt Tolerance in Transgenic Tobacco. *Acta Physiol. Plant.* **2010**, *32*, 263–269. [CrossRef]
36. Noctor, G.; Mhamdi, A.; Chaouch, S.; Han, Y.; Neukermans, J.; Marquez-Garcia, B.; Queval, G.; Foyer, C.H. Glutathione in Plants: An Integrated Overview. *Plant Cell Environ.* **2012**, *35*, 454–484. [CrossRef]
37. Ong, A.-L.; Teh, C.-K.; Mayes, S.; Massawe, F.; Appleton, D.R.; Kulaveerasingam, H. An Improved Oil Palm Genome Assembly as a Valuable Resource for Crop Improvement and Comparative Genomics in the Arecoideae Subfamily. *Plants* **2020**, *9*, 1476. [CrossRef]
38. Singh, R.; Ong-Abdullah, M.; Low, E.-T.L.; Manaf, M.A.A.; Rosli, R.; Nookiah, R.; Ooi, L.C.-L.; Ooi, S.; Chan, K.-L.; Halim, M.A.; et al. Oil Palm Genome Sequence Reveals Divergence of Interfertile Species in Old and New Worlds. *Nature* **2013**, *500*, 335–339. [CrossRef]
39. Zhou, Y.; Wen, Z.; Zhang, J.; Chen, X.; Cui, J.; Xu, W.; Liu, H. Exogenous Glutathione Alleviates Salt-Induced Oxidative Stress in Tomato Seedlings by Regulating Glutathione Metabolism, Redox Status, and the Antioxidant System. *Sci. Hortic.* **2017**, *220*, 90–101. [CrossRef]
40. Walker, R.P.; Chen, Z.-H.; Famiani, F. Gluconeogenesis in Plants: A Key Interface between Organic Acid/Amino Acid/Lipid and Sugar Metabolism. *Molecules* **2021**, *26*, 5129. [CrossRef] [PubMed]
41. Zhong, M.; Yuan, Y.; Shu, S.; Sun, J.; Guo, S.; Yuan, R.; Tang, Y. Effects of Exogenous Putrescine on Glycolysis and Krebs Cycle Metabolism in Cucumber Leaves Subjected to Salt Stress. *Plant Growth Regul.* **2016**, *79*, 319–330. [CrossRef]
42. Suzuki, M.; Hashioka, A.; Mimura, T.; Ashihara, H. Salt Stress and Glycolytic Regulation in Suspension-Cultured Cells of the Mangrove Tree, *Bruguiera sexangula*. *Physiol. Plant.* **2005**, *123*, 246–253. [CrossRef]
43. Guo, R.; Shi, L.; Yan, C.; Zhong, X.; Gu, F.; Liu, Q.; Xia, X.; Li, H. Ionomic and Metabolic Responses to Neutral Salt or Alkaline Salt Stresses in Maize (*Zea mays* L.) Seedlings. *BMC Plant Biol.* **2017**, *17*, 41. [CrossRef] [PubMed]
44. Peng, K.; Tian, Y.; Cang, J.; Yu, J.; Wang, D.; He, F.; Jiao, H.; Tan, Y. Overexpression of TaFBA-A10 from Winter Wheat Enhances Freezing Tolerance in *Arabidopsis thaliana*. *J. Plant Growth Regul.* **2022**, *41*, 314–326. [CrossRef]
45. Sun, Q.; Yamada, T.; Han, Y.; Takano, T. Influence of Salt Stress on C4 Photosynthesis in *Miscanthus sinensis* Anderss. *Plant Biol.* **2021**, *23*, 44–56. [CrossRef] [PubMed]
46. Xu, B.; Cheng, Y.; Zou, X.; Zhang, X. Ethanol Content in Plants of *Brassica Napus* L. Correlated with Waterlogging Tolerance Index and Regulated by Lactate Dehydrogenase and Citrate Synthase. *Acta Physiol. Plant.* **2016**, *38*, 81. [CrossRef]
47. Cavill, R.; Jennen, D.; Kleinjans, J.; Briedé, J.J. Transcriptomic and Metabolomic Data Integration. *Brief. Bioinform.* **2016**, *17*, 891–901. [CrossRef]
48. Gertsman, I.; Barshop, B.A. Promises and Pitfalls of Untargeted Metabolomics. *J. Inherit. Metab. Dis.* **2018**, *41*, 355–366. [CrossRef]
49. Götz, S.; Garcia-Gomez, J.M.; Terol, J.; Williams, T.D.; Nagaraj, S.H.; Nueda, M.J.; Robles, M.; Talon, M.; Dopazo, J.; Conesa, A. High-throughput functional annotation and data mining with the Blast2GO suite. *Nucleic Acids Res.* **2008**, *36*, 3420–3435. [CrossRef]
50. Robinson, M.D.; McCarthy, D.J.; Smyth, G.K. EdgeR: A Bioconductor Package for Differential Expression Analysis of Digital Gene Expression Data. *Bioinformatics* **2010**, *26*, 139–140. [CrossRef] [PubMed]
51. Bradford, M.M. A Rapid and Sensitive Method for the Quantitation of Microgram Quantities of Protein Utilizing the Principle of Protein-Dye Binding. *Anal. Biochem.* **1976**, *72*, 248–254. [CrossRef]
52. Eng, J.K.; Jahan, T.A.; Hoopmann, M.R. Comet: An Open-Source MS/MS Sequence Database Search Tool. *Proteomics* **2013**, *13*, 22–24. [CrossRef] [PubMed]

53. Elias, J.E.; Gygi, S.P. Target-Decoy Search Strategy for Increased Confidence in Large-Scale Protein Identifications by Mass Spectrometry. *Nat. Methods* **2007**, *4*, 207–214. [CrossRef]
54. Carvalho, P.C.; Fischer, J.S.G.; Xu, T.; Cociorva, D.; Balbuena, T.S.; Valente, R.H.; Perales, J.; Yates, J.R.; Barbosa, V.C. Search Engine Processor: Filtering and Organizing Peptide Spectrum Matches. *Proteomics* **2012**, *12*, 944–949. [CrossRef]
55. Vargas, L.H.G.; Neto, J.C.R.; de Aquino Ribeiro, J.A.; Ricci-Silva, M.E.; Souza Júnior, M.T.; Rodrigues, C.M.; de Oliveira, A.E.; Abdelnur, P.V. Metabolomics Analysis of Oil Palm (*Elaeis guineensis*) Leaf: Evaluation of Sample Preparation Steps Using UHPLC–MS/MS. *Metabolomics* **2016**, *12*, 153. [CrossRef]
56. Carvalho da Silva, T.L.; Belo Silva, V.N.; Braga, Í.d.O.; Rodrigues Neto, J.C.; Leão, A.P.; Ribeiro, J.A.d.A.; Valadares, L.F.; Abdelnur, P.V.; Sousa, C.A.F.; Souza Júnior, M.T. Integration of Metabolomics and Transcriptomics Data to Further Characterize Gliricidia sepium (Jacq.) Kunth under High Salinity Stress. *Plant Genome* **2022**, *15*, e20182. [CrossRef]
57. Gowda, H.; Ivanisevic, J.; Johnson, C.H.; Kurczy, M.E.; Benton, H.P.; Rinehart, D.; Nguyen, T.; Ray, J.; Kuehl, J.; Arevalo, B.; et al. Interactive XCMS Online: Simplifying Advanced Metabolomic Data Processing and Subsequent Statistical Analyses. *Anal. Chem.* **2014**, *86*, 6931–6939. [CrossRef]
58. Tautenhahn, R.; Patti, G.J.; Rinehart, D.; Siuzdak, G. XCMS Online: A Web-Based Platform to Process Untargeted Metabolomic Data. *Anal. Chem.* **2012**, *84*, 5035–5039. [CrossRef]
59. Chong, J.; Xia, J. Using MetaboAnalyst 4.0 for Metabolomics Data Analysis, Interpretation, and Integration with Other Omics Data. In *Computational Methods and Data Analysis for Metabolomics*; Li, S., Ed.; Methods in Molecular Biology; Humana: New York, NY, USA, 2020; Volume 2104, pp. 337–360.
60. Chong, J.; Wishart, D.S.; Xia, J. Using MetaboAnalyst 4.0 for Comprehensive and Integrative Metabolomics Data Analysis. *Curr. Protoc. Bioinform.* **2019**, *68*, e86. [CrossRef]
61. Eriksson, L.; Johansson, E.; Kettaneh-Wold, N.; Wold, S. *Introduction to Multi-and Megavariate Data Analysis Using Projection Methods (PCA & PLS)*; Umetrics AB: Umeå, Sweden, 1999.
62. Li, S.; Park, Y.; Duraisingham, S.; Strobel, F.H.; Khan, N.; Soltow, Q.A.; Jones, D.P.; Pulendran, B. Predicting Network Activity from High Throughput Metabolomics. *PLoS Comput. Biol.* **2013**, *9*, e1003123. [CrossRef]
63. Subramanian, A.; Tamayo, P.; Mootha, V.K.; Mukherjee, S.; Ebert, B.L.; Gillette, M.A.; Paulovich, A.; Pomeroy, S.L.; Golub, T.R.; Lander, E.S.; et al. Gene Set Enrichment Analysis: A Knowledge-Based Approach for Interpreting Genome-Wide Expression Profiles. *Proc. Natl. Acad. Sci. USA* **2005**, *102*, 15545–15550. [CrossRef]
64. Kanehisa, M.; Sato, Y.; Morishima, K. BlastKOALA and GhostKOALA: KEGG Tools for Functional Characterization of Genome and Metagenome Sequences. *J. Mol. Biol.* **2016**, *428*, 726–731. [CrossRef]
65. Brink, B.G.; Seidel, A.; Kleinbölting, N.; Nattkemper, T.W.; Albaum, S.P. Omics Fusion—A Platform for Integrative Analysis of Omics Data. *J. Integr. Bioinform.* **2016**, *13*, 43–46. [CrossRef]

CAPÍTULO IV – ARTIGO 3

Insights from a Multi-Omics Integration (MOI) Study in Oil Palm (*Elaeis guineensis* Jacq.) Response to Abiotic Stresses: Part Two—Drought

André Pereira Leão, Cleiton Barroso Bittencourt, Thalliton Luiz Carvalho da Silva, Jorge Cândido Rodrigues Neto, Ítalo de Oliveira Braga, Letícia Rios Vieira, José Antônio de Aquino Ribeiro, Patrícia Verardi Abdelnur, Carlos Antônio Ferreira de Sousa, Manoel Teixeira Souza Júnior.

Publicado no Periódico *Plants*
https://www.mdpi.com/2223-7747/11/20/2786
Volume 11(20): 1755. doi:10.3390/plants11131755

plants

MDPI

Article

Insights from a Multi-Omics Integration (MOI) Study in Oil Palm (*Elaeis guineensis* Jacq.) Response to Abiotic Stresses: Part Two—Drought

André Pereira Leão [1], Cleiton Barroso Bittencourt [2], Thalliton Luiz Carvalho da Silva [2], Jorge Cândido Rodrigues Neto [1], Ítalo de Oliveira Braga [2], Letícia Rios Vieira [2], José Antônio de Aquino Ribeiro [1], Patrícia Verardi Abdelnur [1], Carlos Antônio Ferreira de Sousa [3] and Manoel Teixeira Souza Júnior [1,2,*]

[1] Embrapa Agroenergia, Brasília 70770-901, DF, Brazil
[2] Graduate Program of Plant Biotechnology, Federal University of Lavras, Lavras 37200-000, MG, Brazil
[3] Embrapa Meio Norte, Teresina 64006-245, PI, Brazil
* Correspondence: manoel.souza@embrapa.br; Tel.: +55-61-3448-3210

Abstract: Drought and salinity are two of the most severe abiotic stresses affecting agriculture worldwide and bear some similarities regarding the responses of plants to them. The first is also known as osmotic stress and shows similarities mainly with the osmotic effect, the first phase of salinity stress. Multi-Omics Integration (MOI) offers a new opportunity for the non-trivial challenge of unraveling the mechanisms behind multigenic traits, such as drought and salinity resistance. The current study carried out a comprehensive, large-scale, single-omics analysis (SOA) and MOI studies on the leaves of young oil palm plants submitted to water deprivation. After performing SOA, 1955 DE enzymes from transcriptomics analysis, 131 DE enzymes from proteomics analysis, and 269 DE metabolites underwent MOI analysis, revealing several pathways affected by this stress, with at least one DE molecule in all three omics platforms used. Moreover, the similarities and dissimilarities in the molecular response of those plants to those two abiotic stresses underwent mapping. Cysteine and methionine metabolism (map00270) was the most affected pathway in all scenarios evaluated. The correlation analysis revealed that 91.55% of those enzymes expressed under both stresses had similar qualitative profiles, corroborating the already known fact that plant responses to drought and salinity show several similarities. At last, the results shed light on some candidate genes for engineering crop species resilient to both abiotic stresses.

Keywords: transcriptomics; proteomics; metabolomics; integratomics; abiotic stress; African oil palm

Citation: Leão, A.P.; Bittencourt, C.B.; Carvalho da Silva, T.L.; Rodrigues Neto, J.C.; Braga, Í.d.O.; Vieira, L.R.; de Aquino Ribeiro, J.A.; Abdelnur, P.V.; de Sousa, C.A.F.; Souza Júnior, M.T. Insights from a Multi-Omics Integration (MOI) Study in Oil Palm (*Elaeis guineensis* Jacq.) Response to Abiotic Stresses: Part Two—Drought. *Plants* **2022**, *11*, 2786. https://doi.org/10.3390/plants11202786

Academic Editor: Hanna Bandurska

Received: 5 September 2022
Accepted: 28 September 2022
Published: 20 October 2022

1. Introduction

The palm oil industry established itself in places around the world where the oil palm (*Elaeis guineensis* Jacq.), the number one source of vegetable oil consumed today, exists in its natural environment of high rainfall throughout the year. Those places are in an area of 5° latitude from the Equator line, and as one moves further north or south in the tropical belt, one experiences long periods of drought throughout the year when oil palm does not receive the physiological water level required to maintain productivity. Consequently, the oil palm grower must embrace artificial irrigation, together with the production cost linked to it, not to mention the risk of facing problems of soil salinization.

A recent report by the UN Convention to Combat Desertification, entitled Drought in Numbers 2022—Restoration to Readiness and Resilience, brings to light the dimension of the damages caused by this abiotic stress on the planet and shows to some extent what is needed to overcome this problem and sustainably ensure food security [1]. Drought stress is one of the most severe environmental stresses affecting agriculture worldwide. The efficient and effective use of genetics and biotechnology is among the most proactive interventions necessary to mitigate the effects of water deprivation on plant productivity [2].

Plant response to drought is a complex biological system that needs investigation via an integrative approach that must involve both drought-tolerant and intolerant genotypes. Resistance to drought in plants results from the dynamic interaction of various parts of this system that need deep understanding in order to enable the design of approaches for the effective vertical or horizontal transfer of such traits to drought intolerant genotypes [2,3]. A Multi-Omics Integration (MOI) study [4–6], made viable due to the recent massive generation of genomics, transcriptomics, proteomics, and metabolomics datasets, is helping the non-trivial challenge of unraveling the mechanisms behind this multigenic trait, and mapping not only resistance genes but also their hot spots for precision genome editing [7].

Plant responses to drought and salinity stresses show several similarities, especially in the first phase of the latter, the osmotic effect [8–10]. Distinct studies showed the existence of genes able to promote resistance to more than one abiotic stress at once. For instance, Brini et al. [11] showed that the transgenic *Arabidopsis thaliana* plants overexpressing two distinct genes from wheat were much more resistant to both stresses than the isogenic wild-type plants. The same was true for Feng et al. [12], who overexpressed a gene from pepper in *A. thaliana* and showed that this gene positively regulates heat, salt, and drought resistance in pepper. In another example, Zhang et al. [13] overexpressed three genes from sweet potato in sweet potato and obtained genetically modified plants tolerant to salt and drought stresses.

Jha et al. [14], Zargar et al. [15], Muthuramalingam et al. [16], and Bittencourt et al. [17] are a few examples of recent reports dealing with the use of MOI approaches toward understanding plant responses to these abiotic stresses. The current study is a step forward in our research activities on characterizing the biochemical and molecular response of oil palm to abiotic stress. After carrying out a comprehensive, large-scale, single-omics analysis (SOA) and an MOI analysis of the metabolome, transcriptome, and proteome profiles on the leaves of young oil palm plants submitted to salinity stress [17], we here report a similar study characterizing the response of this oilseed crop to water deprivation. Furthermore, the differentially expressed (DE) molecules responsive to both drought (from this study) and salt (from [17]) underwent additional MOI analysis and correlation study to identify the commonalities and differences in the response of such plants to both stresses.

2. Results

2.1. Oil Palm Transcriptome under Drought Stress

When comparing drought-stressed plants against the control ones, the pairwise differential expression analysis revealed that out of the 43,551 proteins from the oil palm genome [18,19], 8421 (19.34%) were differentially expressed (DE) at False Discovery Rate (FDR) ≤ 0.05; being 4262 upregulated ($Log_2(FC) > 0$) and 4159 downregulated ($Log_2(FC) < 0$) (Supplementary Table S1).

This group of 8421 DE protein sequences was submitted to analysis in the BlastKOALA annotation tool for the K number assignment, revealing 4133 DE proteins with K number and 1955 with Enzyme Commission (EC) numbers. This set of 1955 DE enzymes underwent gene ontology analyses to classify them accordingly to biological process (BP), molecular function (MF), and cellular component (CC).

The BP subgroups with more representatives were protein phosphorylation, followed by carbohydrate metabolic process, phosphorylation, proteolysis, and cellular oxidant detoxification. For MF, the most populated subgroups were ATP binding, metal ion binding, iron ion binding, and heme binding. Finally, for the CC subgroup, the integral component of the membrane came in first, followed by the cytoplasm, nucleus, and cytosol components (Figure 1a).

Furthermore, the DE enzymes underwent classification according to the EC number, a numerical classification scheme for enzymes based on the chemical reaction. The first classification level involves a general type of enzyme-catalyzed reaction that ranges from one to six, and the oxidoreductases (EC 1), transferases (EC 2), and hydrolases (EC 3) classes dominated. Enzymes acting on paired donors, with the incorporation or reduction

in molecular oxygen (EC 1.14) was the most populated group among the subclasses of oxidoreductases, with 86 hits. The most representative subclass of transferases included those with a function of transferring phosphorus-containing groups, glycosyltransferases, and acyltransferases, with 218, 123, and 86 hits, respectively. Finally, the hydrolases had the following subclasses standing out with over 50 hits: compounds involved and acting on ester bonds, acting on peptide bonds (peptidases), glycosylases, and acting on acid anhydrides (Figure 1b).

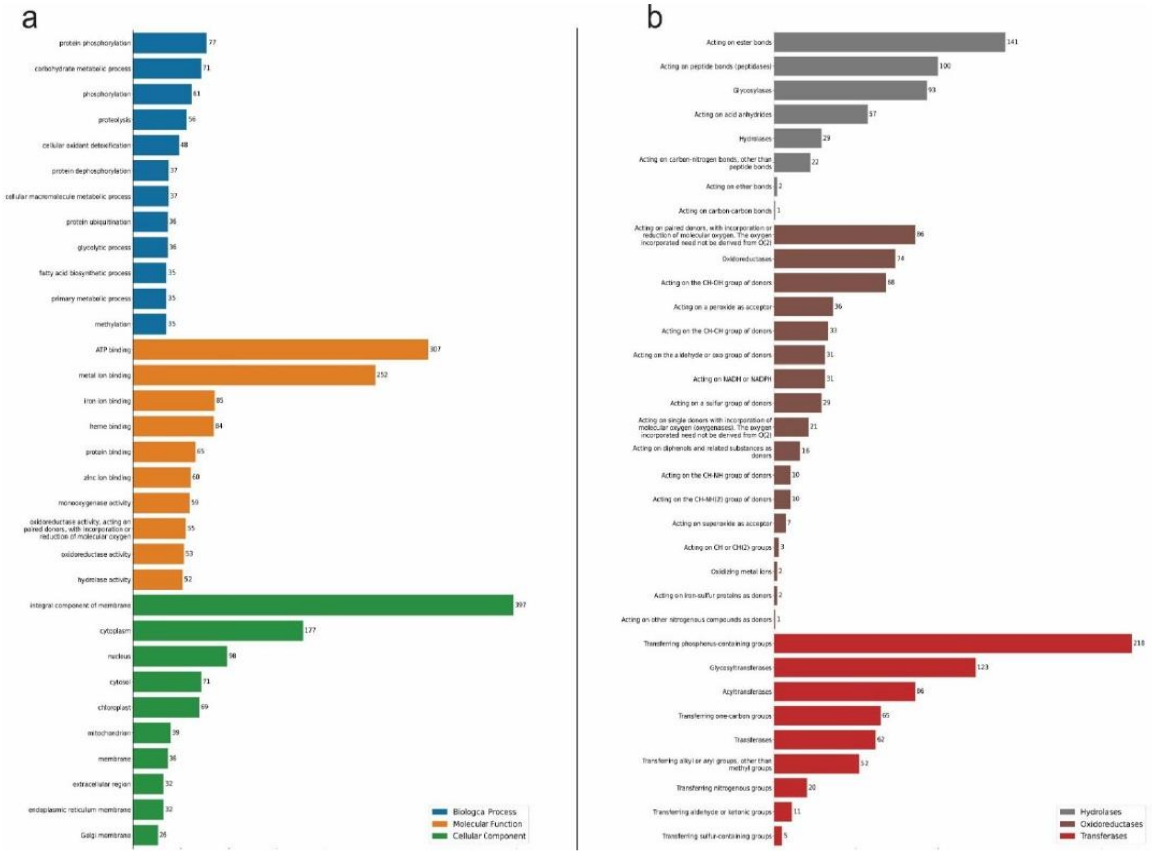

Figure 1. Gene Ontology (GO) annotation classification statistics graph from full-length transcriptome in the leaves of young oil palm plants under drought stress. Classified accordingly to biological process, cellular component, and molecular function (**a**); and to chemical reactions by which proteins are classified according to EC (**b**). Only the most populated groups per GO term, and only the three prevalent classes of enzymes are shown. Numbers represent the amount of positive hits.

2.2. Oil Palm Proteome under Drought Stress

It was possible to identify with high confidence (FDR $\leq$ 0.01) a total of 3659 and 3824 peptides in control and stressed samples, respectively, which infers up to 1859 protein entries from *E. guineensis* proteome (Uniprot) in both conditions (Table 1).

Seven hundred and seventy-nine proteins were inferred from more than four peptides and five hundred and ten had at least one proteotypic peptide observation. All peptides and proteins identified and the list of 1085 proteins according to the maximum parsimony

criterion are presented in Supplementary Tables S2–S4. The control and salt-stressed treatments shared 706 protein identifications, while 76 and 152 proteins were uniquely detected in control and stressed samples, respectively (Supplementary Tables S5 and S6). Fifty-six proteins showed statistically significant differences in their abundance between stressed and control samples; among them, there were thirty-five proteins upregulated and twenty-one downregulated (Supplementary Table S7). Our differential abundance analysis considered proteins identified at least in two replicates in each condition.

Table 1. Absolute numbers of all peptides and proteins identified via proteomics analysis in the leaves of young oil palm plants submitted to drought stress.

	Control	Stressed	Total
Peptide Spectrum Match (PSM)	6733	6495	13,065
Total number of peptides	3659	3824	5182
Number of unique peptides	2098	2088	3068
Total number of proteins entries	1353	1617	1859
Total number of proteins using the maximum parsimony criterion	762	934	1085

A group of 284 proteins that attended to the statistical criteria of PatternLab V software underwent functional annotation and MOI analyses, being 76 found exclusively in the control plants, 152 found only in the drought-stressed plants, and 56 showed statistically significant differences in their abundance between the two treatments used. Those 284 DE proteins underwent analysis in the BlastKOALA annotation tool, revealing 215 DE proteins with K numbers and 131 with EC numbers.

This set of 131 DE enzymes underwent gene ontology analyses to classify them accordingly to biological process (BP), molecular function (MF), and cellular component (CC). The BP top subgroups were carbohydrate metabolic processes, followed by cellular oxidant detoxification and glycolytic process, with 13, 10, and 10 hits, respectively. For MF, the proteins were mainly from subgroups of ATP binding, metal ion binding, magnesium ion binding, and pyridoxal phosphate binding, all with over ten hits. Finally, the CC of the cytoplasm came in first, followed by the cytosol, integral component of membrane, and mitochondrion, all with over ten hits (Figure 2a).

The prevalent chemical reactions according to EC were Oxireductases (EC 1), transferases (EC 2), and hydrolases (EC 3) classes. In the subclasses of oxidoreductases, the top group was acting on a peroxide as an acceptor, followed by acting on the CH-OH group of donors and acting on the aldehyde or oxo group of donors. The most representative subclass of transferases class was the one with transferring phosphorus-containing groups (Figure 2b).

The results from transcriptome and proteome single-omics analysis (SOA), when comparing drought-stressed young oil palm plants against the control ones, show that the ATP binding came as the number one BP affected by the stress, followed by the metal ion binding process. Meanwhile, transferring phosphorus-containing groups, glycosyltransferases, and acyltransferases were subclasses of prevalent chemical reactions in both SOA (Figures 1 and 2).

2.3. Oil Palm Metabolome under Drought Stress

The statistical analysis performed on the MetaboAnalyst has returned 3363 and 2538 peaks in the positive and negative polar fractions, respectively. Ninety-six were up- and seventy-one downregulated in the polar-positive. Two hundred ninety-one were up- and nine downregulated, in the polar-negative.

All 467 differentially expressed peaks (DEPs) were then submitted to functional interpretation via analysis in the MS Peaks to Pathway module, and the combined mummichog and GSEA pathway meta-analysis produced a list of 269 differentially expressed metabolites (DEMs), which underwent analysis in the pathway topology analysis module (Supplementary Table S8). The tyrosine metabolism (map00350); phenylpropanoid biosyn-

thesis (map00940); arginine biosynthesis (map00220); isoquinoline alkaloid biosynthesis (map00950); pyrimidine metabolism (map00240); arginine and proline metabolism (map00330); betalain biosynthesis (map00965); monobactam biosynthesis (map00261); valine, leucine and isoleucine biosynthesis (map00290); pentose phosphate pathway (map00030); aminoacyl-tRNA biosynthesis (map00970); flavonoid biosynthesis (map00941); histidine metabolism (map00340); stilbenoid, diarylheptanoid and gingerol biosynthesis (map00945); riboflavin metabolism (map00740); phenylalanine, tyrosine and tryptophan biosynthesis (map00400); and one carbon pool by folate (map00670) pathways were the most affected pathways with a raw $p \leq 0.05$; in this order, from top to bottom.

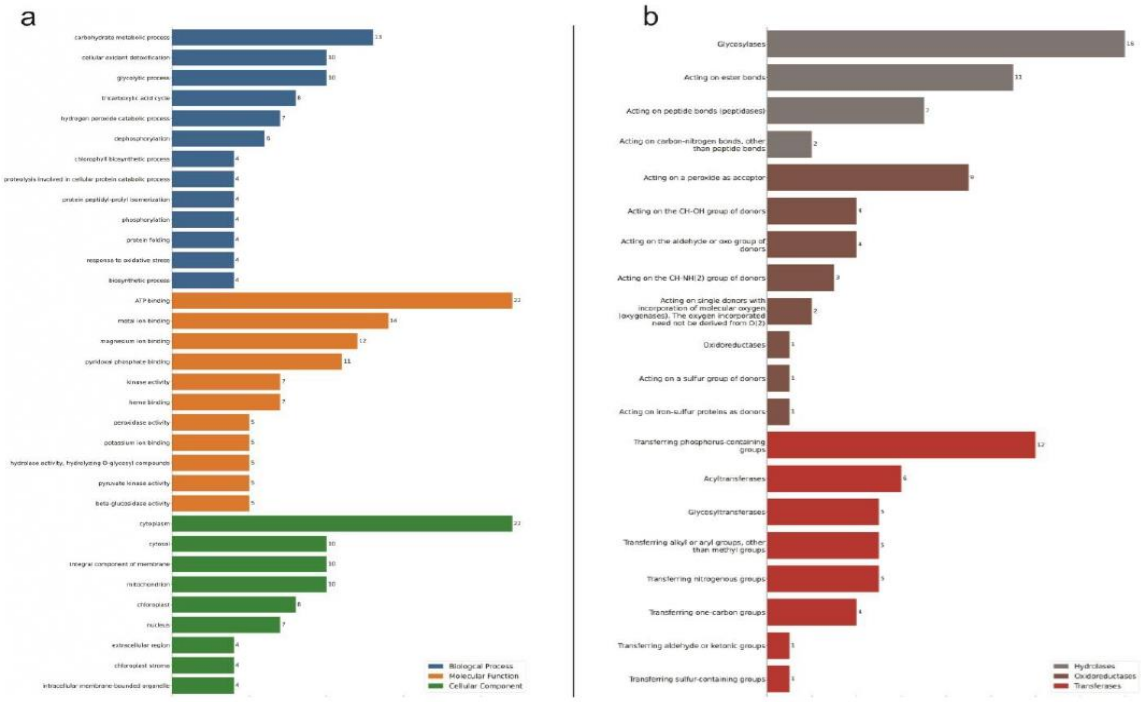

Figure 2. Gene Ontology (GO) annotation classification statistics graph from proteome in the leaves of young oil palm plants under drought stress. Classified accordingly to biological process, cellular component, and molecular function (**a**); and to chemical reactions by which proteins are classified according to EC. Only the most populated groups per GO term, and only the three prevalent classes of enzymes are shown (**b**). Numbers represent the amount of positive hits.

2.4. Integrating Oil Palm Transcriptome, Proteome and Metabolome under Drought Stress

The approach used to integrate the datasets from the three omics platforms was a pathway-based mapping approach, similar to that previously used by Bittencourt et al. [17] (Figure 3).

All enzymes (from SOA analysis—transcriptomics or proteomics) and metabolites (from metabolomics SOA analysis), selected as differentially expressed in the leaves of young oil palm plants (stressed/control), underwent MOI analysis.

When applying the Omics Fusion platform to perform the MOI analysis, a group of 56 pathways appeared as affected by drought stress, with at least one molecule differentially expressed in each of the three omics platforms used. Those pathways with ≥20 unique molecules differentially expressed are shown in Table 2. The Cysteine and

methionine metabolism (map00270) pathway came first, with 47 molecules from the transcriptome/proteome/metabolome integrative analysis (Figure 4).

2.5. Commonalities and Dissimilarity in the Transcriptome, Proteome, and Metabolome Profiles of Young Oil Palm Plants Separately Submitted to Drought and Salinity Stresses

To generate the data regarding the commonalities and dissimilarity in the response of young oil palm plants separately submitted to drought and salinity stresses, all datasets generated in this present study underwent a comparison analysis with the equivalent datasets that had been previously generated and used in Bittencourt et al. [17].

In the transcriptomics analysis, there is a positive correlation between the behavior of the 554 enzymes differentially expressed under drought and salinity stresses (Supplementary Table S9) when 91.15% of the enzymes had the same qualitative profile (upregulated or downregulated), independently of the stress condition (Figure 5). This result is a strong amount of evidence that there are several commonalities regarding gene expression—molecular dynamics—in young oil palm plants submitted separately to these two abiotic stresses. It is also a valuable source of information to further study the osmotic effect. However, 8.85% of those enzymes had different qualitative profiles (Figure 5), where 29 enzymes were downregulated under salt stress and upregulated under drought (Figure 6a), and 20 had the opposite behavior (Figure 6b).

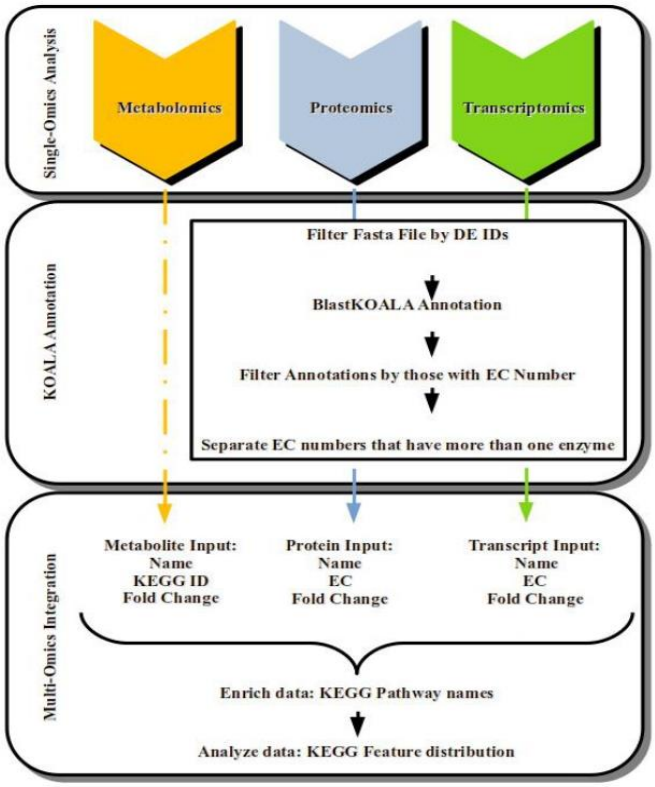

Figure 3. Summarized workflow used to Single-Omics Analysis (SOA), KOALA Annotation, and Multi-Omics Integration (MOI) applied to characterize the transcriptomics, proteomics, and metabolomics datasets generated from the leaves of young oil palm plants submitted to abiotic stress.

In the case of the proteomics analysis, a group of enzymes were also differentially expressed under both abiotic stresses (Table 3). Most of them had the same qualitative profile independently of the stress condition and a minority had different ones. For instance, enzymes A0A6J0PP21 and A0A6I9S451, two isoforms coded by the same gene (LOC105053549) in the oil palm genome and described as L-ascorbate peroxidases in the KEGG database, were upregulated under drought stress and downregulated almost to no detection under salt stress.

In the case of the metabolomics analysis, a group of 13 metabolites was also differentially expressed in both scenarios. Among them, eight had the same qualitative profile, independently of the stress and five had different ones (Figure 7). The metabolite Melibiitol (C05399) was the one that showed the highest quantitative difference in expression, with a Log_2(FC) of −4.698 (or 3.85% of the initial expression level in the control treatment) under salinity stress and of 1.53 (or 190% on the top of the initial expression level) under drought stress.

At last, when applying the Omics Fusion platform to perform the MOI analysis using only the proteins and metabolites DE in both scenarios, Cysteine and methionine metabolism came first in the list of most affected pathways, with 15 full-length transcripts coding for enzymes, two enzymes (from the proteomics analysis), and two metabolites (Table 4).

Table 2. List of the pathways most affected by drought stress—number of unique molecules—obtained via Multi-Omics Integration (MOI). Transcriptomics, proteomics, and metabolomics data from leaves of young oil palm plants 14 days after imposition of the treatments (control and water deprivation).

Pathway Name	Pathway ID	Occurrence of			Unique Molecules
		Transcripts	Proteins	Metabolites	
Cysteine and methionine metabolism	270	30	8	14	47
Purine metabolism	230	25	3	17	42
Porphyrin and chlorophyll metabolism	860	24	4	12	37
Amino sugar and nucleotide sugar metabolism	520	25	4	9	35
Glycine, serine, and threonine metabolism	260	24	7	9	34
Pyrimidine metabolism	240	17	1	16	33
Glycolysis/Gluconeogenesis	10	26	9	4	30
Phenylpropanoid biosynthesis	940	12	3	18	30
Pentose phosphate pathway	30	17	8	11	29
Arginine and proline metabolism	330	16	1	13	29
Aminoacyl-tRNA biosynthesis	970	13	1	15	29
Glyoxylate and dicarboxylate metabolism	630	17	8	8	28
Pyruvate metabolism	620	20	6	5	26
Starch and sucrose metabolism	500	22	5	3	26
Tyrosine metabolism	350	13	2	12	25
Phenylalanine, tyrosine, and tryptophan biosynthesis	400	17	1	8	25
Methane metabolism	680	16	5	8	24
Alanine, aspartate, and glutamate metabolism	250	18	5	6	24
Lysine degradation	310	14	3	9	24
Tryptophan metabolism	380	15	4	7	23
Terpenoid backbone biosynthesis	900	17	4	5	23
Carbon fixation in photosynthetic organisms	710	19	6	3	22
Citrate cycle (TCA cycle)	20	16	8	5	21
Arginine biosynthesis	220	9	3	11	21
Galactose metabolism	52	12	3	8	21
Valine, leucine, and isoleucine degradation	280	15	2	5	21
Carbon fixation pathways in prokaryotes	720	13	4	6	20
Glutathione metabolism	480	13	3	7	20
Glycerolipid metabolism	561	15	2	4	20
Ascorbate and aldarate metabolism	53	13	1	7	20

Table 3. Enzymes differentially expressed in the leaf of young oil palm plants under both drought and salinity stresses.

Protein ID	Gene ID *	KO Number	EC	Source		Profile		Fold Change		Description_KEGG
				Salt	Drought	Salt	Drought	Salt	Drought	
A0A6J0PH47	LOC105044080	K02641	1.18.1.2	Common	Common	Down	Down	−1.885	−3.730	ferredoxin-NADP+ reductase
B3TLY5	CAT2	K03781	1.11.1.6	Common	Common	Up	Up	1.834	3.177	catalase
B3TM49	LOC105035746	K08967	1.13.11.53 1.13.11.54 1.13.11.53 1.13.11.54	Only Control	Common	Down	Up	NA	3.277	1,2-dihydroxy-3-keto-5-methylthiopentene dioxygenase
A0A6I9QHS4						Down	Up	NA	2.463	
A0A6J0PS13	LOC105039298	K15918	2.7.1.31	Only Control	Only Control	Down	Down	NA	NA	D-glycerate 3-kinase
A0A6I9RVC5	LOC105053135	K05396	4.4.1.15	Only Control	Only Control	Down	Down	NA	NA	D-cysteine desulfhydrase
A0A6J0PP21 A0A6I9S451	LOC105053549	K00434	1.11.1.11	Only Control	Only Stressed	Down	Up	NA	NA	L-ascorbate peroxidase
A0A6I9RWM2	LOC105053973	K00344	1.6.5.5	Only Control	Only Stressed	Down	Up	NA	NA	NADPH: quinone reductase
A0A6I9QWL2	LOC105040656	K03405	6.6.1.1	Only Stressed	Only Stressed	Up	Up	NA	NA	magnesium chelatase subunit I
A0A6I9QXL0	LOC105041662	K10525	5.3.99.6	Only Stressed	Only Stressed	Up	Up	NA	NA	allene oxide cyclase
A0A6J0PKN5	LOC105048171	K03405	6.6.1.1	Only Stressed	Only Stressed	Up	Up	NA	NA	magnesium chelatase subunit I
A0A6I9QUV8	LOC105040597	K00430	1.11.1.7	Only Stressed	Only Stressed	Up	Up	NA	NA	peroxidase
M1H922	LOC105057156	K13379	2.4.1.- 5.4.99.30	Only Stressed	Only Stressed	Up	Up	NA	NA	reversibly glycosylated polypeptide/UDP-arabinopyranose mutase
A0A6I9R7V0	LOC105045344									
A0A6I9R784	LOC105045348									
A0A6I9QEA6	LOC105033962	K25108	3.2.1.73	Only Stressed	Only Stressed	Up	Up	NA	NA	licheninase
A0A6I9R7N0	LOC105045343									
A0A6I9QD17	LOC105033964									

* Gene ID—In *Elaeis guineensis* genome at NCBI; KO—KEGG Orthology; EC—Enzyme Commission Number; Common—Present in both control and stressed; NA—Not Applicable; Up—Upregulated; Down—Downregulated.

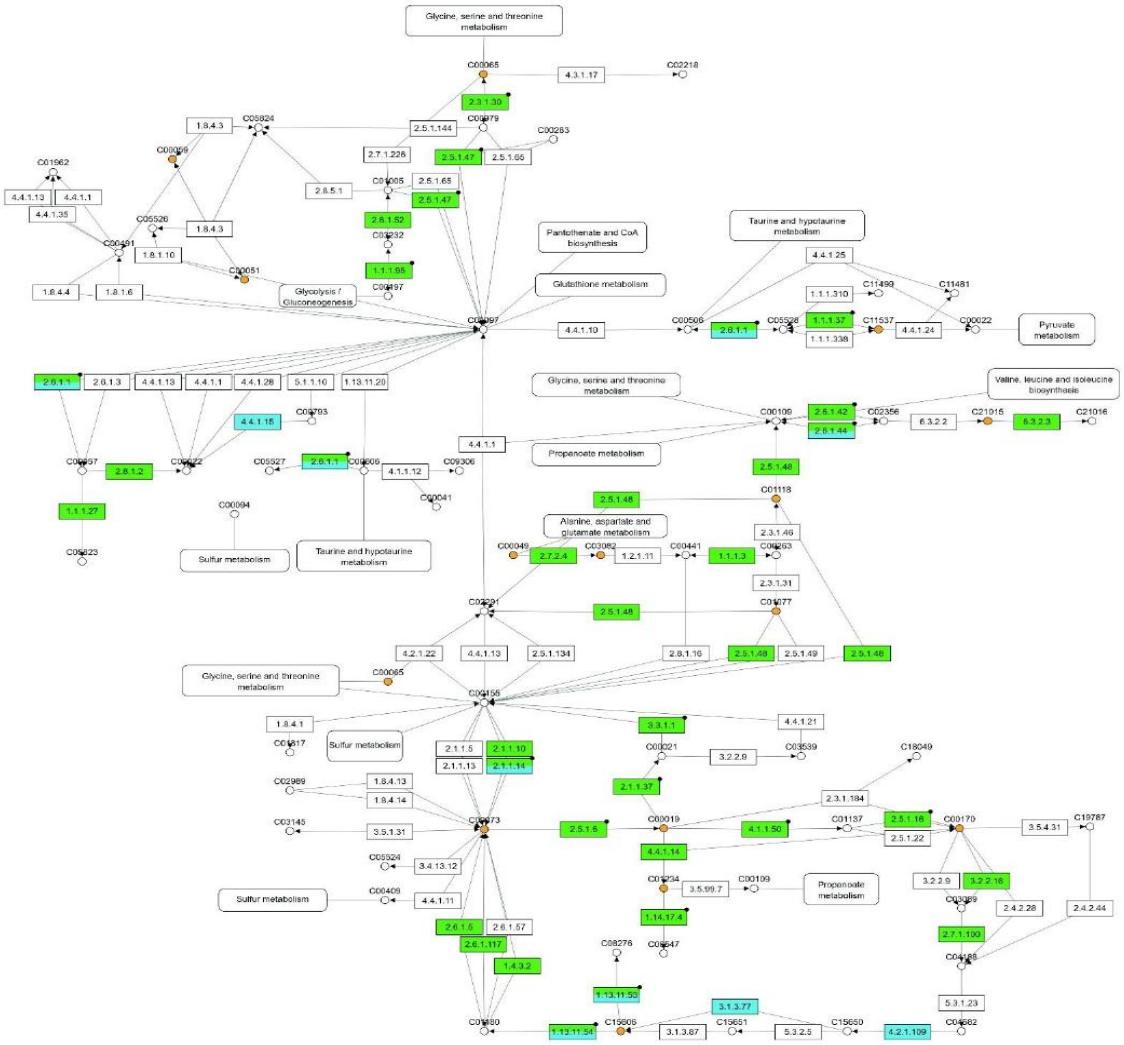

Figure 4. Enzymes (EC number) and metabolites (KEGG Compound number) from the Cysteine and methionine metabolism (map00270) pathway differentially expressed in the apical leaf of young oil palm plants submitted to drought stress. Metabolites differentially expressed are shown as orange circles, metabolites non-differentially expressed are shown as white circles, and enzymes non-differentially expressed are shown as white, and those differentially expressed are shown as green (from transcriptomics), as blue (from proteomics), and green/blue rectangles (from transcriptomics and proteomics).

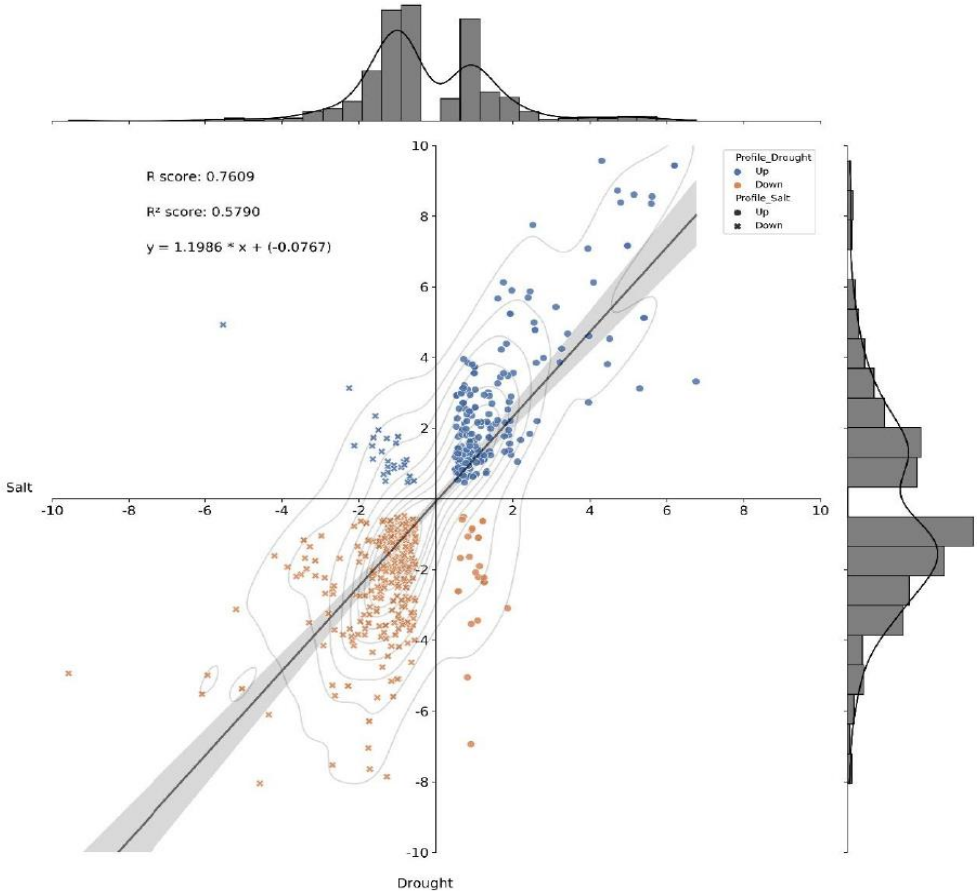

Figure 5. Histogram and correlation analysis of the Log_2(FC) of differentially expressed enzymes by pairwise comparison of two scenarios—drought and salinity stress. FC—fold change. Dots represent enzymes positively regulated under salt stress, x's represent enzymes negatively regulated under salt stress. Blue dots and x's represent enzymes positively regulated under drought-stress, and orange dots and x's represent enzymes negatively regulated under drought-stress.

Table 4. Molecules (full-length transcripts, metabolites, and proteins) from the Cysteine and methionine metabolism (map00270) pathway differentially expressed in the apical leaf of young oil palm plants under both drought and salinity stresses.

Name	Type	EC	KO	Salinity			Drought			Description
				logFC	Profile	Source	logFC	Profile	Source	
XP_010905665.1	TRNS	2.3.1.30	K00640	3.4	Up	NA	4.7	Up	NA	cysE; serine O-acetyltransferase
XP_010914049.1	TRNS	4.1.1.50	K01611	0.7	Up	NA	2.1	Up	NA	speD, AMD1; S-adenosylmethionine decarboxylase
XP_010915297.1	TRNS	2.5.1.47	K01738	0.9	Up	NA	2.5	Up	NA	cysK; cysteine synthase
XP_010920378.1	TRNS	2.6.1.1	K14454	1.0	Up	NA	3.8	Up	NA	GOT1; aspartate aminotransferase, cytoplasmic
XP_010921340.1	TRNS	2.5.1.6	K00789	1.4	Up	NA	2.4	Up	NA	metK, MAT; S-adenosylmethionine synthetase

Table 4. *Cont.*

Name	Type	EC	KO	Salinity			Drought			Description
				logFC	Profile	Source	logFC	Profile	Source	
XP_010924485.1	TRNS	2.3.1.30	K00640	−0.9	Down	NA	−0.7	Down	NA	cysE; serine O-acetyltransferase
XP_010927510.1	TRNS	1.1.1.95	K00058	−0.8	Down	NA	−1.2	Down	NA	serA, PHGDH; D-3-phosphoglycerate dehydrogenase/2-oxoglutarate reductase
XP_010928399.1	TRNS	2.7.1.100	K00899	−1.0	Down	NA	−2.5	Down	NA	mtnK; 5-methylthioribose kinase
XP_010931932.1	TRNS	6.3.2.3	K21456	−0.5	Down	NA	−1.1	Down	NA	GSS; glutathione synthase
XP_010938608.1	TRNS	2.6.1.44	K00830	−0.6	Down	NA	−3.2	Down	NA	AGXT; alanine-glyoxylate transaminase/serine-glyoxylate transaminase/serine-pyruvate transaminase
XP_010939394.1	TRNS	2.6.1.117	K23977	−0.5	Down	NA	−0.7	Down	NA	GTK; L-glutamine—4-(methylsulfanyl)-2-oxobutanoate aminotransferase
XP_010941130.1	TRNS	1.1.1.27	K00016	−3.4	Down	NA	−1.7	Down	NA	LDH, ldh; L-lactate dehydrogenase
XP_010942212.1	TRNS	2.5.1.16	K00797	−0.7	Down	NA	0.5	Up	NA	speE, SRM, SPE3; spermidine synthase
XP_010943220.1	TRNS	1.1.1.37	K00026	−0.6	Down	NA	−1.9	Down	NA	MDH2; malate dehydrogenase
XP_019711215.1	TRNS	2.6.1.5	K00815	0.8	Up	NA	1.0	Up	NA	TAT; tyrosine aminotransferase
C00051	METB	-	NA	0.3	Up	NA	0.9	Up	NA	Glutathione
C00049	METB	-	NA	1.1	Up	NA	4.6	Up	NA	L-Aspartate
A0A6I9QHS4	PROT	1.13.11.53 1.13.11.54	K08967	NA	NA	OC	1.3	Up	COM	1,2-dihydroxy-3-keto-5-methylthiopentene dioxygenase
A0A6I9RVC5	PROT	4.4.1.15	K05396	NA	NA	OC	NA	NA	OC	D-cysteine desulfhydrase
B3TM49	PROT	1.13.11.53 1.13.11.54	K08967	NA	NA	OC	1.7	Up	COM	1,2-dihydroxy-3-keto-5-methylthiopentene dioxygenase

NA—Not Applicable; OC—Only Control; COM—Common, present in the control as well as the stressed treatments.

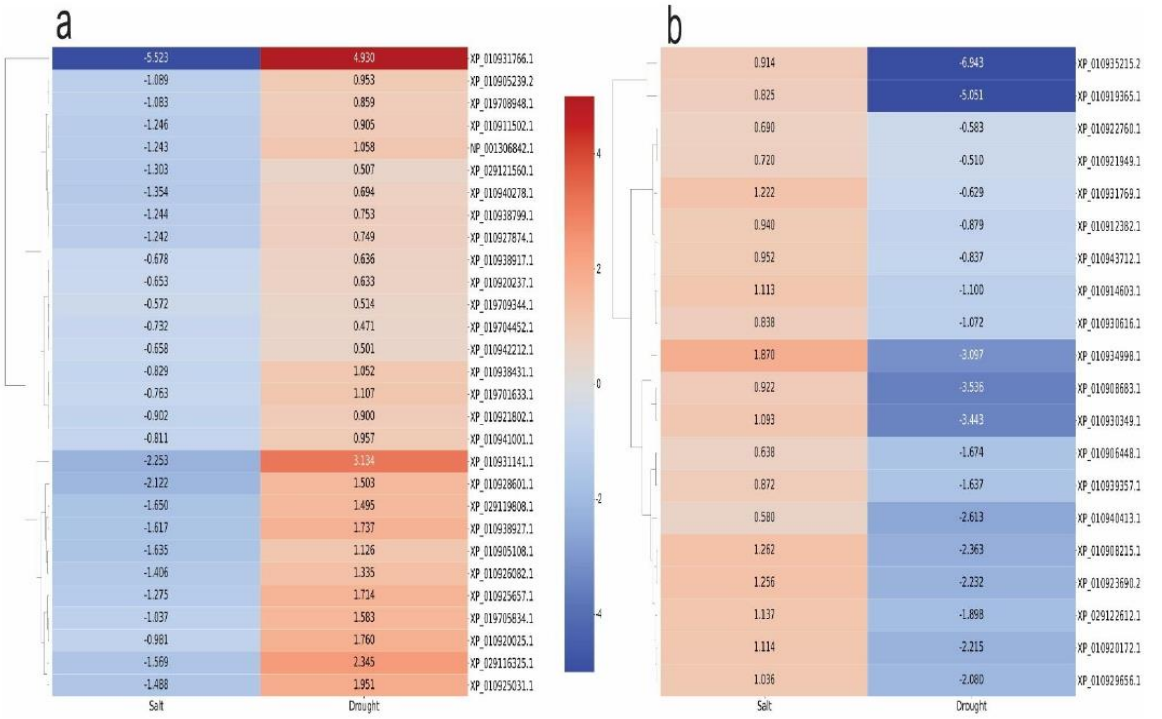

Figure 6. Heatmap of the differentially expressed enzymes from transcriptomics analysis that showed different qualitative profiles in the two scenarios studied—drought and salinity stresses. (**a**)—downregulated in salt and upregulated in drought stress; and (**b**)—upregulated in salt and downregulated in drought stress.

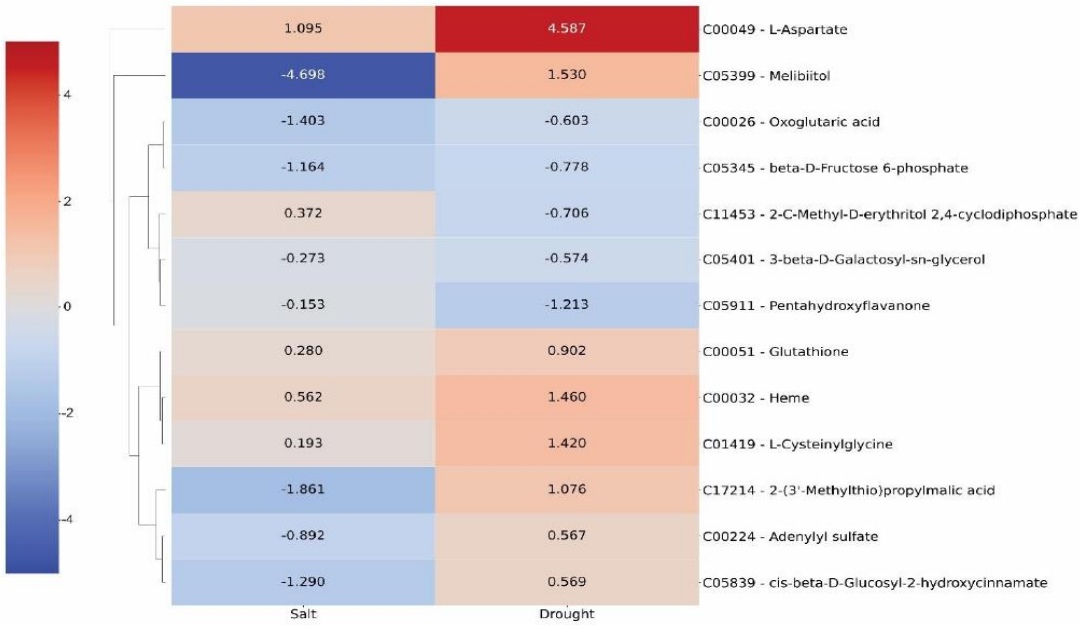

Figure 7. Heatmap of the 13 differentially expressed metabolites that were found in the two scenarios studied—drought and salinity stresses.

3. Discussion

Plant response to water deprivation shows several similarities with the first phase of salinity stress, the osmotic effect [8–10]. The current study is a step further in a study in our lab that applies different omics platforms to characterize the morphophysiological and molecular responses of young oil palms to two abiotic stresses—salinity and drought [17,20–23].

The young oil palm plants used in the study by Bittencourt et al. [17] and the ones used in the present study are clones of a specific plant—genotype AM33, a Deli x Ghana from ASD Costa Rica. Moreover, they were of almost similar age, cultivated under the same main environmental variables—as they were submitted to stress almost at the same time in the same greenhouse, and the stresses lasted 12 days in the case of salinity and 14 days in the case of drought, or almost the same time. Consequently, one can say that it is a unique opportunity to use all omics datasets—transcriptomics, proteomics, and metabolomics—from either one of the studies to map the similarities and dissimilarities in the response of those plants to those abiotic stresses. It is important to state that, in the case of salinity stress, plants were under field conditions throughout the entire experiment to ensure that the osmotic effect was due to the excess of salt in the soil and not otherwise [20].

In the present study, single-omics analyses showed that the most affected biological process subcategories in the transcriptome were protein phosphorylation, carbohydrate metabolic, and phosphorylation processes; meanwhile, in the proteome, the most affected ones were carbohydrate metabolism, cellular oxidant detoxification, and glycolytic processes. The transcriptomics and proteomics results, whether under salinity [17] or drought stress (present study), show that the most affected biological process subcategories in the transcriptome and proteome profiles are very much the same in the apical leaf of young oil palm plants.

Stress mitigation results from the action of several distinct proteins, allowing plants to survive under unfavorable conditions, including water deprivation. Post-translation

modifications, such as protein phosphorylation, promote changes in those proteins that already existed in the cells before the onset of the stress and play roles important in plant resistance to abiotic stresses [24,25]. Carbohydrate metabolism also plays a role in plant stress perception and signal transduction, besides being a substrate for energy production and a mediator of osmotic regulation and carbohydrate distribution [26].

The number one molecular function affected by drought or salinity stress in the apical leaf of young oil palm plants, revealed by both the transcriptome and proteome profiles obtained here and by Bittencourt et al. [17], was ATP binding. ATP binding proteins (ABPs) have a binding site that allows adenosine-5′-triphosphate (ATP) molecules to interact, and they have roles important in membrane transport and the regulation of various metabolic processes. The ATP-binding cassette (ABC) transporters belong to a large protein family and are present in the membranes of chloroplasts, mitochondria, peroxisomes, and vacuoles. They participate in several biological processes of regulation in plants, including resistance to drought and salinity stresses, and are considered reliable targets for developing stress-tolerant crop plants in the future [27]. Consequently, it was no surprise that the number one cellular component affected by the two abiotic stresses in question, either under drought or salinity stress, was an integral component of a membrane in the transcriptome profile and cytoplasm in the proteome profile.

The oxidoreductases, transferases, and hydrolases classes of enzymes had the highest number of positive hits, similar to what we saw in Bittencourt et al. [17]. Within those classes, one can find several subclasses equally affected by drought and salinity stress. Several successful cases of resistance to abiotic stresses achieved by the overexpression of genes coding for oxidoreductases, transferases, or hydrolases enzymes are available in the scientific literature [28–30], showing that here also resides reliable targets to generate stress-tolerant crop plants.

The integration of transcriptomics, proteomics, and metabolomics datasets to gain further insights into the mechanism behind the response of young oil palm plants to drought stress used a much larger number of differentially expressed molecules compared to the MOI study carried out previously by Bittencourt et al. [17], when a total of 510 enzymes and 19 metabolites, differentially expressed under salinity stress, were used. Here, 1955 DE enzymes from transcriptomics analysis, 131 DE enzymes from proteomics analysis, and 269 differentially expressed metabolites (DEMs) underwent MOI analysis. The consequent result was a significant increase in the number of unique DE molecules in the most affected pathways.

The present MOI study showed that the Cysteine and methionine metabolism was the most affected pathway in the apical leaf of young oil palm plants under drought stress, with 47 unique DE molecules. In Bittencourt et al. [17], this pathway was the number one in the rank of affected ones, tied together with Glycolysis/Gluconeogenesis pathway (map00010), both with 20 unique DE molecules. The latter turned out to be the seventh most affected pathway in the list of the most affected ones in young oil palm plants under drought stress, with 30 unique DE molecules. Glycine, serine, and threonine metabolism (map00260) and Amino sugar and nucleotide sugar metabolism (map00520) were present in both lists of most affected pathways, with 34 and 35 unique DE molecules, respectively, in plants under drought stress, and 14 and 12 DE molecules, respectively, under salinity stress [17]. At last, in the present study, when performing the MOI analysis only with the molecules (proteins and metabolites) differentially expressed in both scenarios—drought and salinity stresses—the Cysteine and methionine metabolism pathway again turned out to be the most affected.

Even though this study identified other pathways, further discussion will concentrate only on cysteine and methionine metabolism. Cysteine and methionine are sulfur-containing amino acids. Besides being the metabolic sulfide donor for all cellular components containing reduced sulfur, cysteine is also a precursor of methionine, glutathione, phytochelatins, iron-sulfur clusters, vitamin cofactors, and multiple secondary metabolites, and the incorporation of sulfide into cysteine takes place in chloroplasts, mitochondria, and

the cytoplasm [31]. Our results show that L-serine O-acetyltransferase, the first enzyme in cysteine biosynthesis, which catalyzes the synthesis of O-acetylserine (OAS) from acetyl-CoA (AcCoA) and L-serine (L-Ser), is upregulated in the apical leaf of young oil palm plants under saline (Log_2(FC) = 3.4) as well as drought stress (Log_2(FC) = 4.7). The same is true for the cysteine synthase, which catalyzes the synthesis of L-cysteine and acetate from OAS and hydrogen sulfide and showed a ~2-fold and ~6-fold increase, respectively, under saline and drought stresses.

Several enzymes from the omnipresent methionine salvage pathway (MSP), which uses dioxygen to regenerate methionine, associated with a ratchet-like step that prevents methionine back degradation [32], were differentially expressed in the apical leaf of young oil palm plants under saline and drought stresses. Enzymes from this pathway, such as S-adenosylmethionine synthetase, S-adenosylmethionine decarboxylase, and tyrosine aminotransferase, were positively regulated under both abiotic stresses. Meanwhile, 5-methylthioribose kinase and L-glutamine-4-(methylsulfanyl)-2-oxobutanoate aminotransferase were both downregulated. Resistance to salt and oxidative stress was achieved in Arabidopsis plants by the overexpression of a S-adenosylmethionine synthetase gene from salt-resistance sugar beet [33]. Barley stripe mosaic virus-based virus-induced gene silencing (BSMV-VIGS) of a S-adenosylmethionine synthetase gene in the Tibetan wild barley genotypes XZ5 severely compromised its resistance to both drought and salinity stress [34].

Besides mapping the commonalities in the molecular response of young oil palm plants to drought and salinity stresses, the present study also reported the molecules that displayed the opposite behavior when submitted separately to those two stresses. Stachyose synthetase (XP_010931766.1) is the enzyme that showed to most opposite behavior, downregulated under salt stress (Log_2(FC) = −5.5) and upregulated in drought (Log_2(FC) = 4.9). This enzyme catalyzes the reaction that produces myo-inositol plus stachyose from alpha-D-Galactosyl-(1->3)-1D-myo-inositol and Raffinose and was regulated positively in the drought-tolerant conifer *Larix olgensis* A. Henry under PEG-simulated drought stress [35]. According to Okemo et al. [36], the shoots of *Tripogon loliiformis*—an Australian resurrection plant—accumulated stachyose synthase transcripts and stachyose during drought stress. Stachyose triggers the formation of the hallmarks of plant apoptotic-like cell death in the desiccation-sensitive *Nicotiana benthamiana* but not the resilient *T. loliiformis*. Because of that, the stachyose synthase gene from this species is a potential candidate for improving stress resistance.

The present study, and the one by Bittencourt et al. [17], used transcriptome datasets from the apical leaf of young oil palm plants already showing extensive necrosis [20,23]. The reason stachyose synthase gene in *E. guineensis* increased approximately 32-fold under drought but decreased by almost 100% under saline stress, and considering that the transcriptome profiles used came from leaves with extensive necrosis, this is a question that needs further study to be answered.

The enzyme that showed to second most opposite behavior, downregulated under salt stress (Log_2(FC) = −2.3) and upregulated in drought (Log_2(FC) = 3.1), is a Topoisomerase II (XP_010931766.1). John et al. [37] over-expressed a topoisomerase II gene from tobacco in *Nicotiana tabaccum* and observed an increase in the resistance to salt stress.

The enzyme (XP_010934998.1) that showed the most opposite behavior, upregulated under salt stress (Log_2(FC) = 1.9) and downregulated in drought (Log_2(FC) = −3.1), is a member of the Cytochrome P450, E-class, group IV (IPR002403), protein family. Cytochrome P450s (CYPs) act as versatile catalysts and play a crucial role in the biosynthesis of secondary metabolites, antioxidants, and phytohormones in higher plants. The expression of several CYP genes is regulated in response to environmental stresses, with a role important in the crosstalk between abiotic and biotic stress responses, which make them candidate genes for engineering crop species resilient to biotic and abiotic stresses [38].

4. Materials and Methods

4.1. Plant Material, Growth Conditions, Experimental Design, and Drought Stress

The oil palm plants used in this study are clones of the ones used in the Bittencourt et al. [17] study. All plants—from both studies—came from the same embryogenic calluses. The young oil palm plants used in both studies were clones regenerated out of embryogenic calluses obtained from the leaves of an adult plant—genotype AM33, a Deli x Ghana from ASD Costa Rica; and were subjected to treatments when they were in the growth stage known as "bifid" saplings. Before starting the experiments, plants were standardized according to their developmental stage, size, and the number of leaves.

The experiment consisted of two water availability levels (field capacity—control and water deprivation—stressed), with four replicates in a completely randomized design. For the omics (transcriptomics, metabolomics, and proteomics) analysis described in the present study, we collected the apical leaves from control and stressed plants 14 days after imposing the treatments (DAT). See Rodrigues-Neto et al. [21] and Salgado et al. [23] for additional details regarding growth conditions, experimental design, drought stress, and the morphophysiological response of the oil palm plants.

4.2. Single-Omics Data Analysis, Functional Annotation, and Integratomics Analysis

Samples harvested from control and stressed plants were immediately immersed in liquid nitrogen and stored at −80 °C until RNA/Protein/Metabolite extraction; three replicates (plants) per treatment for RNA and protein extraction and four for the extraction of metabolites.

See Salgado et al. [22] for additional details on total RNA extraction, quality analysis, library preparation, and sequencing. The RNA-Seq raw sequence data are in the Sequence Read Archive (SRA) database of the National Center for Biotechnology Information (NCBI) under the BioProject number PRJNA573093. The transcriptomics analysis was performed using the OmicsBox platform—version 2.0.36 [39], as previously described [22]. The oil palm genome [18,19]—downloaded from NCBI (BioProject PRJNA268357; BioSample SAMN02981535) in September 2021—was the reference genome for RNA-Seq data alignment. The pairwise differential expression analysis between experimental conditions (Stressed Plants X Control) was performed as described [17].

The protein extraction protocol used here was the same used before [17]. The same happened for protein preparation and LC-MS/MS analysis at the GenOne company (Rio de Janeiro, RJ, Brazil). Data were acquired in biological triplicates using the the Xcalibur software (version 2.0.7) (Thermo Scientific, Waltham, MA, USA). Raw files were processed using the PatternLab for Proteomics V software [40], also as described by [17].

The metabolite extraction protocol used here was the same used by [17]. The DataAnalysis 4.2 software (Bruker Daltonics, Bremen, Germany) was the first used to analyze the raw data from UHPLC-MS as mzMXL files, and the pre-processing of data, peak detection, alignment of retention times and the statistical analysis at the pre-processing stage was similarly used by [17]. Then, a dataset was created from control and stressed plants. The pre-processed data (csv file) underwent analysis in the Statistical Analysis, MS Peaks to Pathway, and pathway analysis modules of the MetaboAnalyst 5.0 [41,42], exactly as previously described [17]. The differentially expressed peaks (DEPs) selected were those passing the criteria of false rate discovery (FDR) ≤ 0.05 and Log_2 (fold change [FC]) $\neq 1$.

The differentially expressed (DE) full-length ORFs and proteins identified in the OmicsBox and PatternLab V analysis underwent KOALA annotation before MOI analysis (Figure 1). The approach used to integrate the three omics was pathway-based mapping, performed using the Omics Fusion platform [43], as shown in Figure 1 and previously described [17].

4.3. Correlation Analysis of Differentially Expressed Molecules under Two Distinct Scenarios—Salinity and Drought Stresses

To perform a correlation analysis of differentially expressed (DE) full-length RNAs, proteins, and metabolites under two distinct scenarios, we used sets of data with the DE molecules from this present study and re-used the respective ones from [17]. First, to check the data distribution, we used the Data Overview module of Omics Fusion [43], the web platform for integrative analysis of Omics data, and then the Scatter Plot one for the correlation analysis between the sets of data—a pairwise combination of the different molecules and scenarios evaluated. The input data was the Log_2(FC) from the DE molecules obtained from the single-omics analysis.

5. Conclusions

The SOA and MOI studies here reported generated new insights on the early response of young oil palm plants to drought stress, pointing out genes, proteins, metabolites, and pathways directly affected by this stress.

The MOI study performed using the molecules differentially expressed under drought (from this study) and salinity stress (from [14]) gave a unique opportunity to map the similarities and dissimilarities in the molecular response of those plants to those abiotic stresses of very high importance.

All MOI studies showed that cysteine and methionine metabolism was the most affected pathway, independent of the abiotic stress applied. This was also the case when only those molecules differently expressed under both abiotic stresses were considered.

The correlation analysis revealed that only 8.85% of those enzymes which were differently expressed under both stresses had different qualitative profiles, corroborating the already known fact that plant responses to drought and salinity show several similarities, with emphasis on the osmotic effect.

Finally, besides allowing us to map the pathways most affected by two abiotic stresses in the leaves of young oil palm plants, this study also generated a list of genes, proteins, and metabolites responsive to those stresses. This list can be used as valuable information to help those interested in the prospection and validation of candidate genes to promote resistance to both abiotic stresses once overexpressed in oil palm or other plant species.

Supplementary Materials: The following supporting information can be downloaded at: https://www.mdpi.com/article/10.3390/plants11202786/s1, Table S1: Proteins from the oil palm genome differentially expressed (FDR $\leq$ 0.05) in the leaves of young oil palm plants under drought stress. FC—Fold Change, CPM—Count Per Million, FDR—False Discovery Rate, Kegg Orthology number, and E.C. number; Table S2: List of all peptides confidently identified in oil palm conditions; Table S3: List of all proteins confidently identified in oil palm conditions; Table S4: All proteins confidently identified in oil palm conditions with maximum parsimony criterion; Table S5: List of the proteins detected only in control biological condition; Table S6: List of the proteins detected only in stressed biological condition; Table S7: List of all differentially expressed proteins detected in both biological conditions (Stressed and Control) with statistical significance (FDR $\leq$ 0.05); Table S8: List of metabolites identified in the leaves of young oil palm plants submitted to drought stress via metabolomics analysis, after submitting the differentially expressed (DE) peaks to the pathway topology analysis module in MetaboAnalyst 5.0; Table S9: group of 554 enzymes differentially expressed under both abiotic stresses—drought and salinity.

Author Contributions: Conceptualization: C.A.F.d.S., P.V.A. and M.T.S.J. Methodology, investigation, data curation, and formal analysis: A.P.L., C.B.B., T.L.C.d.S., J.C.R.N., Í.d.O.B., L.R.V. and J.A.d.A.R. Funding acquisition and supervision: M.T.S.J. Writing—original draft: A.P.L., C.B.B., T.L.C.d.S., J.C.R.N. and Í.d.O.B. Writing—review and editing: C.A.F.d.S. and M.T.S.J. All authors have read and agreed to the published version of the manuscript.

Funding: This work was funded by the Brazilian Innovation Agency (Financiadora de Estudos e Projetos-FINEP-DendêPalm Project-01.13.0315.00) and the Coordination for the Improvement of Higher Education Personnel—CAPES (Scholarships for C.B.B., T.L.C.d.S., Í.d.O.B. and L.R.V.). The funding bodies covered all student and project costs but were not involved in the design, collection, analysis and interpretation of the data or the preparation of the manuscript.

Data Availability Statement: The datasets used and/or analyzed in the current study are available from the corresponding author on reasonable request.

Conflicts of Interest: The authors declare no conflict of interest.

References

1. UNCCD. UN Convention to Combat Desertification. Drought in Numbers 2022-Restoration to Readiness and Resilience. 2022. Available online: www.unccd.int/sites/default/files/2022-06/Drought%20in%20Numbers%20%28English%29.pdf (accessed on 31 August 2022).
2. Yang, X.; Cushman, J.C.; Borland, A.M.; Liu, Q. Editorial: Systems Biology and Synthetic Biology in Relation to Drought Tolerance or Avoidance in Plants. *Front. Plant Sci.* **2020**, *11*, 394. [CrossRef] [PubMed]
3. Shinwari, Z.K.; Jan, S.A.; Nakashima, K.; Yamaguchi-Shinozaki, K. Genetic engineering approaches to understanding drought tolerance in plants. *Plant Biotechnol. Rep.* **2020**, *14*, 151–162. [CrossRef]
4. Cavill, R.; Jennen, D.; Kleinjans, J.; Briedé, J.J. Transcriptomic and Metabolomic Data Integration. *Brief. Bioinform.* **2016**, *17*, 891–901. [CrossRef] [PubMed]
5. Jamil, I.N.; Remali, J.; Azizan, K.A.; Nor Muhammad, N.A.; Arita, M.; Goh, H.-H.; Aizat, W.M. Systematic Multi-Omics Integration (MOI) Approach in Plant Systems Biology. *Front. Plant Sci.* **2020**, *11*, 944. [CrossRef] [PubMed]
6. Scossa, F.; Alseekh, S.; Fernie, A.R. Integrating multi-omics data for crop improvement. *J. Plant Physiol.* **2021**, *257*, 153352. [CrossRef] [PubMed]
7. Wada, N.; Ueta, R.; Osakabe, Y. Precision genome editing in plants: State-of-the-art in CRISPR/Cas9-based genome engineering. *BMC Plant Biol.* **2020**, *20*, 234. [CrossRef] [PubMed]
8. Uddin, M.N.; Hossain, M.A.; Burritt, D.J. Salinity and drought stress: Similarities and differences in oxidative responses and cellular redox regulation. In *Water Stress and Crop Plants: A Sustainable Approach*; Ahmad, P., Ed.; Wiley: Chichester, UK, 2016; Volume 1, pp. 86–101.
9. Forni, C.; Duca, D.; Glick, B.R. Mechanisms of plant response to salt and drought stress and their alteration by rhizobacteria. *Plant Soil* **2017**, *410*, 335–356. [CrossRef]
10. Ma, Y.; Dias, M.C.; Freitas, H. Drought and Salinity Stress Responses and Microbe-Induced Tolerance in Plants. *Front. Plant Sci.* **2020**, *11*, 591911. [CrossRef]
11. Brini, F.; Hanin, M.; Mezghani, I.; Berkowitz, G.A.; Masmoudi, K. Overexpression of wheat Na+/H+ antiporter TNHX1 and H+-pyrophosphatase TVP1 improve salt- and drought-stress tolerance in *Arabidopsis thaliana* plants. *J. Exp. Bot.* **2007**, *58*, 301–308. [CrossRef]
12. Zhang, H.; Wang, Z.; Li, X.; Gao, X.; Dai, Z.; Cui, Y.; Zhi, Y.; Liu, Q.; Zhai, H.; Gao, S.; et al. The IbBBX24-IbTOE3-IbPRX17 module enhances abiotic stress tolerance by scavenging reactive oxygen species in sweet potato. *New Phytol.* **2022**, *233*, 1133–1152. [CrossRef]
13. Feng, X.H.; Zhang, H.X.; Ali, M.; Gai, W.X.; Cheng, G.X.; Yu, Q.H.; Yang, S.B.; Li, X.X.; Gong, Z.H. A small heat shock protein CaHsp25.9 positively regulates heat, salt, and drought stress tolerance in pepper (*Capsicum annuum* L.). *Plant Physiol. Biochem.* **2019**, *142*, 151–162. [CrossRef] [PubMed]
14. Jha, U.C.; Bohra, A.; Nayyar, H. Advances in "omics" approaches to tackle drought stress in grain legumes. *Plant Breed.* **2020**, *139*, 1–27. [CrossRef]
15. Zargar, S.M.; Mir, R.A.; Ebinezer, L.B.; Masi, A.; Hami, A.; Manzoor, M.; Salgotra, R.K.; Sofi, N.R.; Mushtaq, R.; Rohila, J.S.; et al. Physiological and Multi-Omics Approaches for Explaining Drought Stress Tolerance and Supporting Sustainable Production of Rice. *Front. Plant Sci.* **2022**, *12*, 803603. [CrossRef] [PubMed]
16. Muthuramalingam, P.; Jeyasri, R.; Rakkammal, K.; Satish, L.; Shamili, S.; Karthikeyan, A.; Valliammai, A.; Priya, A.; Selvaraj, A.; Gowri, P.; et al. Multi-Omics and Integrative Approach towards Understanding Salinity Tolerance in Rice: A Review. *Biology* **2022**, *11*, 1022. [CrossRef] [PubMed]
17. Bittencourt, C.B.; Carvalho da Silva, T.L.; Rodrigues Neto, J.C.; Vieira, L.R.; Leão, A.P.; de Aquino Ribeiro, J.A.; Abdelnur, P.V.; de Sousa, C.A.F.; Souza, M.T., Jr. Insights from a Multi-Omics Integration (MOI) Study in Oil Palm (*Elaeis guineensis* Jacq.) Response to Abiotic Stresses: Part One—Salinity. *Plants* **2022**, *11*, 1755. [CrossRef]
18. Singh, R.; Ong-Abdullah, M.; Low, E.-T.L.; Manaf, M.A.A.; Rosli, R.; Nookiah, R.; Ooi, L.C.-L.; Ooi, S.; Chan, K.-L.; Halim, M.A.; et al. Oil Palm Genome Sequence Reveals Divergence of Interfertile Species in Old and New Worlds. *Nature* **2013**, *500*, 335–339. [CrossRef]
19. Ong, A.-L.; Teh, C.-K.; Mayes, S.; Massawe, F.; Appleton, D.R.; Kulaveerasingam, H. An Improved Oil Palm Genome Assembly as a Valuable Resource for Crop Improvement and Comparative Genomics in the Arecoideae Subfamily. *Plants* **2020**, *9*, 1476. [CrossRef]

20. Vieira, L.R.; Silva, V.N.B.; Casari, R.A.D.C.N.; Carmona, P.A.O.; Sousa, C.A.F.D.; Souza Júnior, M.T. Morphophysiological Responses of Young Oil Palm Plants to Salinity Stress. *Pesq. Agropec. Bras.* **2020**, *55*, 1835. [CrossRef]
21. Rodrigues-Neto, J.C.R.; Vieira, L.R.; de Aquino Ribeiro, J.A.; de Sousa, C.A.F.; Júnior, M.T.S.; Abdelnur, P.V. Metabolic Effect of Drought Stress on the Leaves of Young Oil Palm (*Elaeis guineensis*) Plants Using UHPLC–MS and Multivariate Analysis. *Sci. Rep.* **2021**, *11*, 18271. [CrossRef]
22. Salgado, F.F.; Vieira, L.R.; Silva, V.N.B.; Leão, A.P.; Grynberg, P.; do Carmo Costa, M.M.; Togawa, R.C.; de Sousa, C.A.F.; Júnior, M.T.S. Expression Analysis of MiRNAs and Their Putative Target Genes Confirm a Preponderant Role of Transcription Factors in the Early Response of Oil Palm Plants to Salinity Stress. *BMC Plant Biol.* **2021**, *21*, 518. [CrossRef]
23. Salgado, F.F.; Carvalho da Silva, T.L.; Vieira, L.R.; Silva, V.N.B.; Leão, A.P.; do Carmo Costa, M.M.; Togawa, R.C.; de Sousa, C.A.F.; Grynberg, P.; Júnior, M.T.S. The early response of oil palm (*Elaeis guineensis* Jacq.) plants to water deprivation: Expression analysis of miRNAs and their putative target genes, and similarities with the response to salinity stress. *Front. Plant Sci.* 2022; *in press*.
24. Luo, F.; Deng, X.; Liu, Y.; Yan, Y. Identification of phosphorylation proteins in response to water deficit during wheat flag leaf and grain development. *Bot. Stud.* **2018**, *59*, 28. [CrossRef] [PubMed]
25. Damaris, R.N.; Yang, P. Protein Phosphorylation Response to Abiotic Stress in Plants. *Methods Mol. Biol.* **2021**, *2358*, 17–43. [CrossRef] [PubMed]
26. Jiao, Y.; Zhang, J.; Pan, C. Integrated Physiological, Proteomic, and Metabolomic Analyses of Pecan Cultivar 'Pawnee' Adaptation to Salt Stress. *Sci. Rep.* **2022**, *12*, 1841. [CrossRef] [PubMed]
27. Dahuja, A.; Kumar, R.R.; Sakhare, A.; Watts, A.; Singh, B.; Goswami, S.; Sachdev, A.; Praveen, S. Role of ATP-binding Cassette Transporters in Maintaining Plant Homeostasis under Abiotic and Biotic Stresses. *Physiol. Plant.* **2021**, *171*, 785–801. [CrossRef] [PubMed]
28. Liu, D.; Wang, L.; Zhai, H.; Song, X.; He, S.; Liu, Q. A novel α/β-hydrolase gene IbMas enhances salt tolerance in transgenic sweetpotato. *PLoS ONE* **2014**, *9*, e115128. [CrossRef] [PubMed]
29. Song, X.; Fang, J.; Han, X.; He, X.; Liu, M.; Hu, J.; Zhuo, R. Overexpression of quinone reductase from Salix matsudana Koidz enhances salt tolerance in transgenic *Arabidopsis thaliana*. *Gene* **2016**, *576*, 520–527. [CrossRef] [PubMed]
30. Stavridou, E.; Voulgari, G.; Michailidis, M.; Kostas, S.; Chronopoulou, E.G.; Labrou, N.E.; Madesis, P.; Nianiou-Obeidat, I. Overexpression of A Biotic Stress-Inducible *Pvgstu* Gene Activates Early Protective Responses in Tobacco under Combined Heat and Drought. *Int. J. Mol. Sci.* **2021**, *22*, 2352. [CrossRef]
31. Bonner, E.R.; Cahoon, R.E.; Knapke, S.M.; Jez, J.M. Molecular basis of cysteine biosynthesis in plants: Structural and functional analysis of O-acetylserine sulfhydrylase from *Arabidopsis thaliana*. *J. Biol. Chem.* **2005**, *280*, 38803–38813. [CrossRef]
32. Sekowska, A.; Ashida, H.; Danchin, A. Revisiting the methionine salvage pathway and its paralogues. *Microb. Biotechnol.* **2019**, *12*, 77–97. [CrossRef]
33. Ma, C.; Wang, Y.; Gu, D.; Nan, J.; Chen, S.; Li, H. Overexpression of S-Adenosyl-l-Methionine Synthetase 2 from Sugar Beet M14 Increased Arabidopsis Tolerance to Salt and Oxidative Stress. *Int. J. Mol. Sci.* **2017**, *18*, 847. [CrossRef]
34. Ahmed, I.M.; Nadira, U.A.; Qiu, C.W.; Cao, F.; Chen, Z.H.; Vincze, E.; Wu, F. The Barley S-Adenosylmethionine Synthetase 3 Gene HvSAMS3 Positively Regulates the Tolerance to Combined Drought and Salinity Stress in Tibetan Wild Barley. *Cells* **2020**, *9*, 1530. [CrossRef] [PubMed]
35. Zhang, L.; Yan, S.; Zhang, S.; Yan, P.; Wang, J.; Zhang, H. Glutathione, carbohydrate and other metabolites of Larix olgensis A. Henry reponse to polyethylene glycol-simulated drought stress. *PLoS ONE* **2021**, *16*, e0253780. [CrossRef] [PubMed]
36. Okemo, P.; Long, H.; Cheng, Y.; Mundree, S.; Williams, B. Stachyose triggers apoptotic like cell death in drought sensitive but not resilient plants. *Sci. Rep.* **2021**, *11*, 7099. [CrossRef] [PubMed]
37. John, R.; Ganeshan, U.; Singh, B.N.; Kaul, T.; Reddy, M.K.; Sopory, S.K.; Rajam, M.V. Over-expression of Topoisomerase II Enhances Salt Stress Tolerance in Tobacco. *Front. Plant Sci.* **2016**, *7*, 1280. [CrossRef] [PubMed]
38. Pandian, B.A.; Sathishraj, R.; Djanaguiraman, M.; Prasad, P.; Jugulam, M. Role of Cytochrome P450 Enzymes in Plant Stress Response. *Antioxidants* **2020**, *9*, 454. [CrossRef]
39. Götz, S.; García-Gómez, J.M.; Terol, J.; Williams, T.D.; Nagaraj, S.H.; Nueda, M.J.; Robles, M.; Talón, M.; Dopazo, J.; Conesa, A. High-throughput functional annotation and data mining with the Blast2GO suite. *Nucl. Acids Res.* **2008**, *36*, 3420–3435. [CrossRef]
40. Carvalho, P.C.; Fischer, J.S.G.; Xu, T.; Cociorva, D.; Balbuena, T.S.; Valente, R.H.; Perales, J.; Yates, J.R.; Barbosa, V.C. Search Engine Processor: Filtering and Organizing Peptide Spectrum Matches. *Proteomics* **2012**, *12*, 944–949. [CrossRef]
41. Chong, J.; Wishart, D.S.; Xia, J. Using MetaboAnalyst 4.0 for Comprehensive and Integrative Metabolomics Data Analysis. *Curr. Protoc. Bioinform.* **2019**, *68*, 1002. [CrossRef]
42. Chong, J.; Xia, J. Using MetaboAnalyst 4.0 for Metabolomics Data Analysis, Interpretation, and Integration with Other Omics Data. In *Computational Methods and Data Analysis for Metabolomics. Methods in Molecular Biology*; Li, S., Ed.; Humana: New York, NY, USA, 2020; Volume 2104, pp. 337–360.
43. Brink, B.G.; Seidel, A.; Kleinbölting, N.; Nattkemper, T.W.; Albaum, S.P. Omics Fusion–A Platform for Integrative Analysis of Omics Data. *J. Integr. Bioinform.* **2016**, *13*, 43–46. [CrossRef]

2. CONSIDERAÇÕES FINAIS

A palma de óleo africana (*Elaeis guineensis*) tem grande potencial de suprir parte considerável da demanda global por óleos vegetais. O plantio da palma de óleo fora das áreas tradicionais de cultivo, em florestas tropicais úmidas, é visto como uma oportunidade de expandir a zona de produção, promover o desenvolvimento econômico de outras regiões e reduzir a pressão sobre a biodiversidade.

As mudanças climáticas e a ampliação da zona de cultivo devem impor à palma de óleo, no futuro, desafios que podem impactar negativamente sua produtividade. Destacadamente, dentre os estresses abióticos que afetam as culturas, a disponibilidade hídrica e o estresse salino estão entre os mais preocupantes. No mesmo contexto, o Amarelecimento Fatal (AF) é visto com um dos principais obstáculos a produção da palma de óleo africana na América.

Os estudos de SOA (*Singular Omics Analysis*) e MOI (*Multi-Omics Integration*) realizados neste trabalho forneceram uma compreensão mais aprofundada sobre a resposta de plantas jovens da palma de óleo ao estresse de salinidade e seca, e ao amarelecimento fatal. Os resultados oferecem uma visão abrangente dos mecanismos moleculares envolvidos na resposta da palma de óleo, fornecendo uma base de conhecimento para pesquisas futuras e o desenvolvimento de estratégias para o melhoramento genético no contexto apresentado e, no âmbito do AF, um direcionamento para a melhor compressão do efeito do alagamento como um fator importante para o surgimento da doença.

Nossos resultados destacaram o metabolismo de cisteína e metionina como a via mais afetada no estresse à seca e a salinidade a partir da integração de enzimas e metabólitos. Destacamos em nosso estudo a similaridade entre as enzimas diferencialmente expressas nos dois cenários, com a maioria delas apresentando comportamento semelhante. Desta forma, a lista de genes, proteínas, e metabólitos responsivos aos estresses abióticos seca e salinidade encontrados, em uma avaliação de integração dentro de vias, representam um conjunto de componentes valiosos para trabalhos que pretendem prospectar e validar genes para promover resistência a ambos os estresses abióticos em palma de óleo ou outras espécies de plantas.

Em nossa abordagem sobre o AF, utilizando os dados de perfis físico-químicos dos solos, não conseguimos estabelecer uma correlação entre a composição do solo e das folhas com os fenótipos sintomático e assintomático. Embora esses resultados sejam consistentes com diversos estudos, destacamos ser de grande importância que estudos futuros verifiquem

as condições do solo, uma vez que a hipótese de o AF ser uma doença ligada a fatores do solo, mas sem influência primária da falta ou excesso de macro e micronutrientes.

Para SOA e MOI no âmbito do AF, nossas descobertas abrem caminho para estudos futuros com o intuito de aprofundar a compreensão do AF. Observamos evidências dentro dos 56 genes/proteínas diferencialmente expressos, comparando-se plantas sintomáticas e assintomáticas, independente do período, que fatores ligados a quebra de resistência contra patógenos não adaptados e a imunidade basal, ligado as condições anaeróbicas no período chuvoso, sejam os fatores cruciais para o aparecimento do AF. Postulamos essa hipótese com base na regulação negativa de EgRPL19-2 em ambas as estações e de duas proteínas semelhantes a WAKs de uma subfamília específica das plantas da família de quinases semelhantes a receptores (IPR045274).

Dessa maneira, os resultados apresentados fornecem uma base para o desenvolvimento de biomarcadores, com o propósito de selecionar plantas resistentes à doença. Isso é especialmente relevante devido à presença de indivíduos, como os assintomáticos selecionados para o presente estudo, que nunca manifestaram sintomas de AF, mesmo em regiões com severa incidência da doença. Além disso, a comparação molecular com *Elaeis oleífera*, a espécie resistente à doença, permitirá direcionar estratégias de edição genética, visando criar genótipos capazes de tolerar as condições de solo propícias ao surgimento do AF.

Por fim, apresentamos a integração dados gerados pelas diferentes tecnológicas ômicas, como transcriptômica, metabolômica e proteômica, como uma estratégia promissora para o estudo da resposta das plantas às doenças e a condições ambientais adversas, gerando subsídios para programas de melhoramento genético da palma de óleo e de outros recursos vegetais.